VIBRATION ANALYSIS OF PLATES, SHELLS AND BLADED RIMMED DISCS USING THE TRANSFER MATRIX-FINITE ELEMENT METHOD

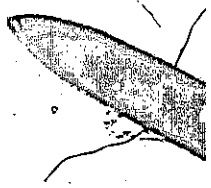

VIBRATION ANALYSIS OF PLATES, SHELLS AND BLADED RIMMED DISCS USING THE TRANSFER MATRIX-FINITE ELEMENT METHOD

by

MOHAMMED ADEL ALI MOHAMMED, M.Eng.

A Thesis

Submitted to the School of Graduate Studies

in Partial Fulfillment of the requirements

for the degree

Doctor of Philosophy

McMaster University

December 1972

DOCTOR OF PHILOSOPHY (1972)
(Mechanical Engineering)

McMASTER UNIVERSITY
Hamilton, Ontario.

TITLE: Vibration Analysis of Plates, Shells and Bladed Rimmed Discs using the Transfer Matrix-Finite Element Method.

AUTHOR: Mohammed Adel Ali Mohammed, B.Sc. (Eng.)
(Cairo University)
M.Eng.
(McMaster University)

SUPERVISOR: Dr. M. A. Dokainish.

NUMBER OF PAGES: x, 197

In recent years, the vibration problems associated with turbine blades have become of increasing importance. Blades in a gas turbine can fail if they are subjected to alternating forces having certain frequencies. Thus a need has arisen for accurate determination of these dangerous frequencies, so that the possibility of failure occuring during running can be avoided.

This thesis presents a numerical method to predict the frequencies which must be avoided in the design of gas turbines. The accuracy of the method is tested by using it to solve some vibration problems for which analytical or experimental results are available.

ACKNOWLEDGEMENTS

The author is pleased to record his gratitude to Dr. M. A. Dokainish for suggesting the problem for investigation and for his guidance and encouragement at every stage of the work.

The author is grateful to Dr. J. J. Emery, Dr. A. C. Hiedebrecht and Dr. B. Latto for their valuable suggestions.

Thanks are also due to my wife for her continuous help and for typing the manuscript.

The scholarship awarded by McMaster University, Mechanical Engineering Departement, is gratefully acknowledged.

ABSTRACT

The development of an in-plane annular sector finite element is presented. The accuracy of the element is tested by two numerical examples, and it gave satisfactory results.

Also, two modified cylindrical shell elements are developed. The first element has 20 degrees of freedom and the second has 28 degrees of freedom. It is found that the use of the 28 degrees of freedom element resulted in quite rapid convergence.

The accuracy of the transfer matrix - finite element method is tested by solving several vibration problems of plates and shells, for which analytical or experimental results are available. This method has the main advantage of requiring a small computer without reducing the number of degrees of freedom of the system.

Finally, the transfer matrix - finite element method is used to calculate the first few natural frequencies of nonrotating low aspect ratio turbomachinery blades mounted on a rimmed disc. The bladed rimmed disc is considered as an assembly of annular sector finite elements, cylindrical shell elements, and flat plates triangular elements. It is found that the natural frequencies obtained are lower than these obtained for cantilever blades. It is found also that instead of sharp natural frequencies, there are bands of frequencies, with the width of each band decreasing with increasing stiffness of the disc.

TABLE OF CONTENTS

LIST OF SYMBOLS

E	Young's Modulus
t	Thickness
ν	Poisson's ratio
ρ	Mass per unit volume
D	Flexural Rigidity $= Et^3/12(1-\nu^2)$
r	Radial co-Ordinate
θ	Azimuthal co-ordinate
ω	Circular frequency
β	Included angle
Ω	Nondimensional frequency
$\{\alpha\}$	Column vector of polynomial coefficients
L	Length of the plate
$[T]$	Transformation matrix
x', y', z'	Local co-ordinate axes for a triangular element
x, y, z	Co-ordinate axes for a blade
X, Y, Z	Global co-ordinate axes
u, v	In-plane displacements
w	Transverse displacement
$\theta_x, \theta_y, \theta_z$	Rotational displacements
$\{\delta\}$	Column vector of displacements
$\{F\}$	Column vector of forces
$[K]$	Stiffness matrix
$[M]$	Mass Matrix

R_i	Inner radius
R_o	Outer radius
R	Shell radius of curvature
$\{\sigma\}$	Column vector of stresses
$\{\varepsilon\}$	Column vector of strains
f	Frequency of vibration = $\omega/2\pi$
N_s	Rotational speed
$\{Z\}_i$	State vector at point i
$[T]_i$	Transfer matrix
w_r, w_θ	$\partial w/\partial r$, $\partial w/\partial \theta$, respectively
$\hat{u}$	Nondimensional displacement
σ_i	Internal applied stress
$\hat{\sigma}$	Nondimensional stress at a point
σ_θ	Tangential stress
σ_r	Radial stress
w_ξ, w_η, $w_{\xi\eta}$	$\partial w/\partial \xi$, $\partial w/\partial \eta$, $\partial^2 w/\partial \xi \partial \pi$, respectively
M_x, M_y, N_x, N_y	Moments and membrane forces
W	Width of fan blade
a,b	Length and width of cylindrical shell element
Vol	Volume of element

Superscripts

'	The quantity referred to local axes (x',y',z')
..	Second derivative with respect to time
-1	Inverse of matrix
T	Transpose of matrix

*	Virtual displacement along local axes
^	Nondimensional quantity

Subscripts

i	Strip i of a structure
R	Right edge
L	Left edge
A	Part A of a plate
B	Part B of a plate
p	In-plane matrix
b	Bending matrix
root	Root edge of a blade
free	Free edge of a blade
f	Free edge of a plate
θ_1	Edge of a structure where θ is θ_1
eq	Equivalent nodal forces corresponding to distributed loads

CHAPTER 1

INTRODUCTION

The design of modern gas turbines continues to emphasize the development of higher power and longer life for lighter weight. Unfortunately the resulting flexible structures also continue to exhibit the undesirable tendency to vibrate in any of its many natural modes. A major limitation in the path towards light weight and long life is the vibration causing metal fatigue. Thus a need has arisen for accurate determination of the vibration characteristics of turbine blades.

In the last twenty years, a large number of technical papers have appeared, giving various approaches to the vibration analysis of turbomachinary blades. The blades are generally idealized as cantilever beams. This beam type of analysis, although good enough for long blades, cannot be expected to give accurate results for low aspect ratio blades. Such blades ought to be treated as shells. For a complex structure like twisted tapered blade of aerofoil cross-section, the exact analysis based on shallow shell theory is rather a formidable task. However, recent advances utilizing the finite element method make such an analysis feasible.

In most of the work done on the vibration analysis of

turbine blades, the disc on which the blades are mounted is considered absolutely rigid. Hence, the blade can be treated as a separate unit for vibration analysis. However, the disc has some elasticity, and hence the blades and the disc should be considered as an assembly.

While the finite element method has proved to be a convenient and powerful technique for the approximate analysis of structures, it is known that the application of the finite element method for investigating the vibration analysis of a bladed disc requires a huge computer size, to obtain a reasonable accuracy. To overcome this difficulty, a method based on a combination of finite element technique and transfer matrix method is used.

In the present analysis the disc is assumed to be clamped at its inner edge, and it has a cylindrical rim on which the blades are mounted. The blades are fixed at their roots and there is no damping in the system and the effect of rotation is not considered.

The first objective of the present investigation is to review the significant work done on:

(a) the vibration analysis of turbomachinery blades, taking into account the effect of the elasticity of the disc.

(b) the numerical methods dealing with dynamic problems requiring computer size greater than the sizes available.

For the vibration analysis of the disc, we need an in-plane annular sector finite element. Hence the second objective is the derivation of such element. Since the finite element method introduces several approximations, it is therefore necessary to test the accuracy of this annular element. This is achieved by using it to obtain the solution for some problems for which the analytical solutions are available.

The best suitable existing cylindrical shell element assumes that the thickness of the shell is very small with respect to its radius. So the third objective of this analysis is to derive a modified cylindrical shell finite element without neglecting any term in the derivation. The application of this element is checked by using it to obtain the solution of some vibration problems for which experimental solutions are available.

The fourth objective is to test the accuracy of the method based on a combination of the finite element technique and the transfer matrix method, and also to show the reduction in computing size achieved by this method. The method is applied to study the vibration of: (a) a square cantilever plate, (b) a square simply supported plate, (c) annular cantilever plates , (d) a rectangular plate with irregular boundaries, (e) a cantilever fan blade and (f) clamped-ring stiffened circular cylindrical shells.

The last objective of the present analysis is to carry out the numerical computations in order to get the first few natural frequencies of a bladed rimmed disc when the blades are: (a) square flat plates, (b) twisted plates, and to see the effect of reducing the ratio of the outer to the inner radii of the disc.

CHAPTER 2

LITERATURE SURVEY

2.1 Introduction

The blades have an aerofoil cross-section and possess, in addition to camber and longitudinal taper, a pretwist to allow for the variation in tangential velocity along the length. The method of mounting the blades on the disc varies considerably for different types of engines. The elasticity of the disc and the shroud couples the vibratory motion of the blades of the same row. A certain amount of damping is also inherent in the system, arising from material inelasticity, friction at the root, aerodynamic forces, etc. An accurate determination of the vibration characteristics of such a system in a centrifugal force field and subjected to aerodynamic excitations, is a challenging task.

Many papers dealing with the analytical and experimental studies of the problem have appeared in the literature. The different techniques for the experimental investigation of turbomachinery blade vibrations, have been reviewed by Dokainish and Jagannath [1]*.

For the theoretical analysis of blade vibration problem, many symplifying assumptions are generally introduced. In most

---

* Numbers between brackets designates references at the end.

of the analytical work that has appeared in this field, the blade is idealized as a tapered, pretwisted cantilever beam. The effect of root flexibility, disc elasticity, shrouding and damping have not usually been included in such analysis. However, the effect of these parameters on the vibration charaterstics has been studied separately by some investigators. In such investigations several other assumptions are generally made, e.g. neglecting the pretwist, assuming the cross-section to be rectangular, treating the blade as a single degree of freedom system, etc.

The methods of analysis that have been used for blade vibration problems vary considerably - from the exact solution of differential equations of motion on the one extreme; to the empirical relations based on experience on the other. The majority of the investigators, however, have used an approximate numerical method such as the Rayleigh-Ritz energy approach, the Myklestad type lumped mass technique, the Stodola method, the matrix displacement analysis, the numerical solution of differential equations, etc. A review of the work done in the field of vibration analysis of blades has been carried out by Rawtani [2].

If the disc on which the blades are mounted is considered absolutely rigid, the blade can be treated as a separate unit for vibration analysis, as has been done in most of the investigations. However, the disc has some elasticity, and hence the blades and the disc should be considered as an

assembly. Energy from a blade can be transferred to the adjacent blades through the disc, which modifies the vibration characteristics of the blades. The existence of such rotor coupling is demonstrated by tests in which a vibration exciter is attached to a blade on a rotor, at standstill. Large vibratory amplitudes are observed on blades far from the exciter and connected to it through the rotor. The response of each blade depends not only on its own natural frequency, damping and excitation, but also on the characteristics of the other blades and the rotor.

It is known that the analytical solutions for the natural frequencies of plates and shells are possible only for a limited set of shapes, boundary conditions and thicknesses. Approximate numerical methods are, therefore, important for the analysis of such structures. The finite element method is probably the most widely used numerical method at present. A comprehensive presentation of the method and its many applications has been given by Zienkiewicz [3] and Holland and Bell [4].

For good accuracy with the finite element technique, it is necessary to have a large number of degrees of freedom, resulting in very large matrices. The central memory of presently available digital computers, therefore, becomes the restricting factor on the total number of degrees of freedom that can be used.

In the next two sections, a review is represented of the work done on the vibration analysis of bladed disks, and of the numerical methods dealing with dynamic problems that have been developed that require inordinate computer sizes.

2.2 Review of Vibration Analysis of Bladed Discs

Steam turbine blade and disk vibrations first became of importance to engineers between 1910 and 1920 when a number of turbine failures occured. The first paper to be devoted to this subject was by Campbell [5] in which the investigations of the General Electric Company into the causes of failure of a number of their turbine disks is reported.

This paper is mainly of an experimental nature. By using two electromagnetic pick-ups, situated close to and moving with a rotating turbine wheel it was possible to show the existence of a vibration in the wheel which is stationary with respect to space. Such a vibration could be induced and maintained by irregularities in the steam flow on leaving the previous nozzle row.

The resonant frequencies and mode shapes of a vibrating stationary bladed turbine wheel, the vibrations being at right angles to its plane, were also investigated by exciting the system with an electromagnetic drive, sand was used to identify the nodal pattern of each resonance. From these tests it was found that the system vibrated with nodal diameters, or nodal circles or combinations of both.

When a turbine wheel rotates it was found that the centrifugal forces increased the frequency of vibrations of the wheel. The relationship between the frequencies of the disk when rotating and when stationary could be expressed approximately by the following relationship

$$f_r^2 = f_s^2 + B\, N_s^2 \qquad (2.1)$$

where

f_r is the natural frequency, when rotating.

f_s is the natural frequency, when stationary.

B is a constant.

N_s is the rotational speed.

The value of B depends upon the shape of the wheel, the tightness and manner of support on the shaft, the tightness of the blade roots on the wheel and the internal stresses in the wheel. Because the effects of many of these factors could not be included in an analytical treatment of the problem, the practice of carrying out tests by rotating the actual bladed wheels was continued. Usually such tests were carried out when static tests showed that the difference between the resonant frequency of the disk and the excitation frequency, possible in the turbine, was so small that the increase in frequency due to centrifugal effects might cause resonant vibrations in service.

The basic method of calculating the frequencies of a bladed disk which has been proposed is due to Stodola [6]. In this method of calculating the natural frequencies of the system, use is made of the Rayleigh's principle in which an approximation to the natural frequency is obtained by equating the maximum kinetic and potential energies which the system attains. The accuracy of the estimate of frequency depends upon the extent to which the deflection assumed for calculation of the energies agrees with the actual displacement of the system. However, it can be shown that the calculated frequency is always high if an incorrect displacement form is assumed.

Stodola derived expressions for the kinetic energy of a vibrating disk and the potential energies due first to the flexure of the disk and second, to the work done against the centrifugal forces. These expressions are rather complex and for their application to a disk of varying thickness a graphical method of evaluation is suggested. This calculation should be done for at least three different forms and then from a plot of frequency against some parameter identifying the assumed modal shape, the minimum, and hence the most accurate frequency can be determined.

An attempt to accurately represent the presence of the blades on the disk is given by Malkin [7]. In this paper he proposes that the inaccuracies arising in some cases are due

to inability to choose the correct deflected shape. He then suggests that when the disk is bladed with long blades, only the outer portion of the disk participates in the motion. This idea is based on the following, rather unusual, conception.

Malkin considers the case of a rigidly fixed cantilever, Figure (1), which has sudden change in section mid-way along its length, and which is set into vibration by a sudden impulse. The fundamental mode of vibration is the only one which persists as the others decay because of the damping. He claims that in the case of such a cantilever, the lowest type of transverse vibration is characterized by the fact that only a section AC , Figure (1), of the heavier part OA is participating in the vibrations of the part AB , if the length of the latter is long enough as compared with the length of the part OA .

Malkin then links the above system to that of a bladed wheel in which the blades are long. When this is the case he suggests that only an outer ring shaped portion of the wheel will be involved in the vibrations. To allow for this effect, in one of his methods of calculation for the frequencies of the combined system, based on Rayleigh's principle, he retains the radius of this "resting core" in the expressions for the kinetic and potential energies and determines the radius of the circle to produce the fundamental frequency of the system.

If the natural frequencies of the vibration of the

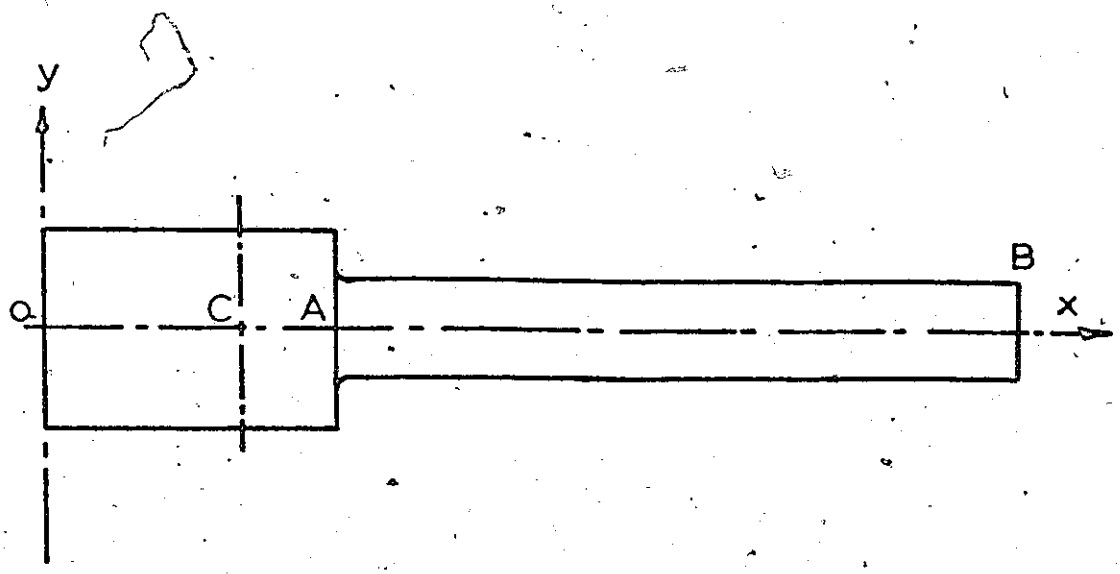

Figure 1

A Simplified Model for Bladed Disc Suggested by Malkin [7]

disc are plotted as ordinate against the number of nodal diameters K as abscissa, a number of single points are obtained. Freudenreich [8] called the curve connecting these points the "static Characteristic of the disc". Actually there will be a "characteristic" for each number of nodal circles. The blading, by reason of its mass, naturally has an influence on the natural frequencies of the vibrations, the tendency being of course to lower the frequencies. If the straight line $N=Kn$, where n is the speed of rotation, which may be called the "straight line of excitation" cuts the characteristic at a whole number of nodal diameters, reasonace will result.

The vibration of a turbine disc in its plane (in the radial and circumferential directions) has been investigated by Singh and Nandeeswaraiya [9] , Yamada [10] , Tumura and Oba [11] and Fillipov [12,2]. It was indicated that the coupling between the circumferential and radial modes of vibrations is negligible for all practical purposes. The blades were replaced by a continuous ring with the radial thickness equal to the height of the blades, and an axial width equal to the average of that of the blades. They concluded that; for the case of rigid hub mountings, it is the circumferential vibrations which are likely to be of greatest danger, while for loose hub mountings, the radial vibration modes are of greater significance. The effect of the

peripheral mass is to lower the frequencies of free vibrations in all cases. Also it was shown that for rigid hub mountings, the natural frequencies increases as the ratio of inner radius to outer radius of the disc increases.

Fillipov [12,2] has considered the problem of the tangential vibrations of the blades together with the torsional vibrations of the disc, when all the blades vibrate in phase. The effect of the rim is allowed for by introducing masses and moments at the blade roots. Satisfying the coupling conditions, a transcendetal equation for finding the frequencies is derived. The effect of the centrifugal force is accounted for by introducing a longitudinal force at the end of each blade.

Ellington and McCallion [13] have investigated the effect of elastic coupling through the rim of the disc, on the frequencies of the blades, by analyzing a simplified model. In this model, the blades are replaced by uniform beams fixed to the rim at their roots and vibrating in a plane parallel to the plane of the disc. This means that the effect of twist, taper, and obliquity is neglected. The rim is considered as a uniform elastic ring, permitting no radial displacement at the roots of the blades.

The mass of the rim is either neglected or considered as being concentrated at the roots of the blades. For the analysis, three adjacent blades(n+1, n and n-1) are assumed to be parallel to each other and the portion of the rim joining

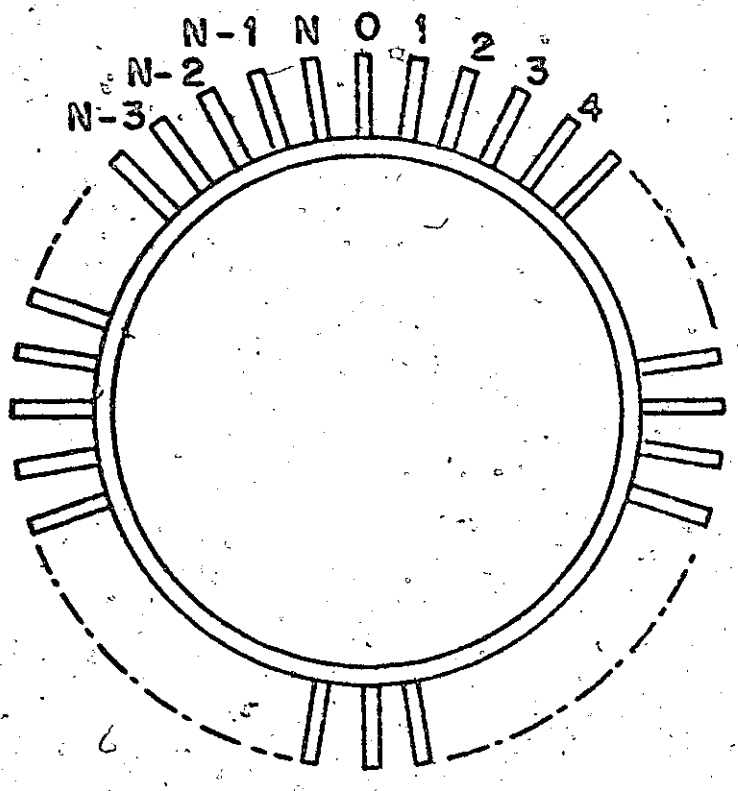

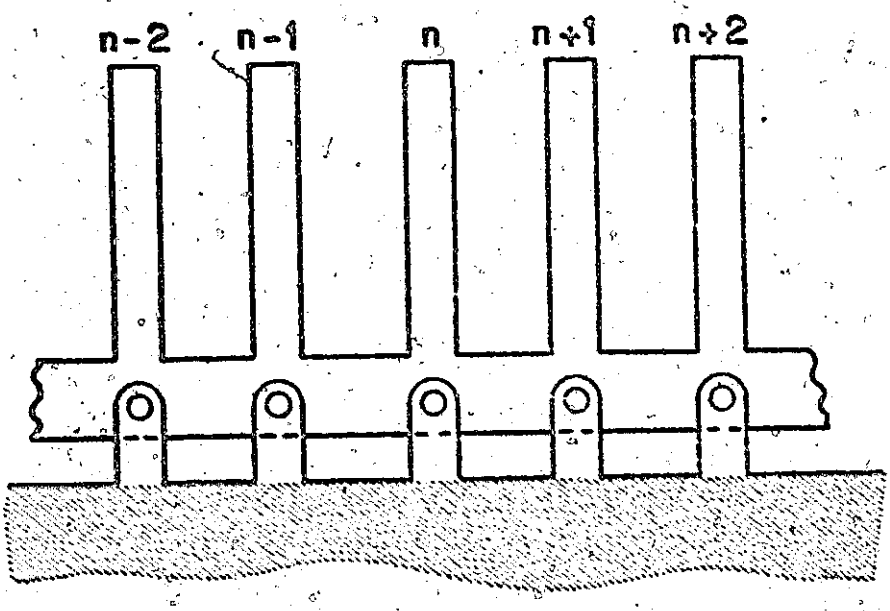

Figure 2

A Simplified Model for Bladed Disc Assembly Suggested by Ellington and McCallion [13]

them is taken as a straight beam, as shown in Figure (2). The method of analysis can be summarized as follows :

The differential equation for the cantilever blade (n) is first solved with the boundary conditions of zero shear and moment at the free end, and with zero deflection and bending moment M_n at the root. An expression for the slope θ_n at the root is thus obtained. The portion of the rim between the three adjacent blades is next treated as a continuous beam with zero deflections at the roots of the blades and acted upon by the bending couples M_{n-1} , M_n and M_{n+1} at these points. A relation between the slopes θ_{n-1} , θ_n and θ_{n+1} is thus established for each of the successive blades. Noting that the $(N+1)^{th}$ blade is in fact the same as blade numbered zero, as shown in Figure (2) , and imposing periodic solution for the slopes at the roots, the natural frequencies are obtained.

The analysis has shown that if there are N identical blades mounted on an elastic rim, the system has N fundamental frequencies, N first overtones, etc. However, if the stiffness of the rim is large compared to that of the blade, as is generally the case, these frequencies are very near to the corresponding frequency of the individual blade. Thus, instead of sharp natural frequencies, there are bands of frequencies, with the width of this band decreasing with increasing stiffness of the disc. This explains the scatter in the natural frequencies usually observed in vibration tests.

The coupling effects due to the blade ring, for the cases when either all blades have identical frequencies or alternate blades have identical frequencies, have been investigated by Sohngen [14,2].

Another simplified model for a row of blades mounted on a flexible disc is suggested by Wagner [15] and is illustrated in Figure (3). Each blade has been presented by a single degree of freedom system which has the same natural frequency and damping factor as that of a particular mode of the blade. Each subsystem is attached to a common ring support, representing the disc periphery. This ring is assumed to have flexibility and is attached to a rigid foundation representing the centre of the disc, where there is assumed to be no vibratory deflection. The equations of motion of each subsystem are derived. All the subsystems would contribute to the deflection of the flexible support at the point of attachment of any subsystem; hence the influence factors for the flexible ring are required. These factors have been derived in the paper using the analysis of curved beams on elastic foundations. It has been concluded from this analysis that multiple resonance peak vibratory stresses, can be produced by the differences in the natural frequencies among the blades and the coupling resulting from the flexibility of the disc. Coupling is also shown to average out the damping present in different blades of the same row.

Ewins [16] has found that the presence of small

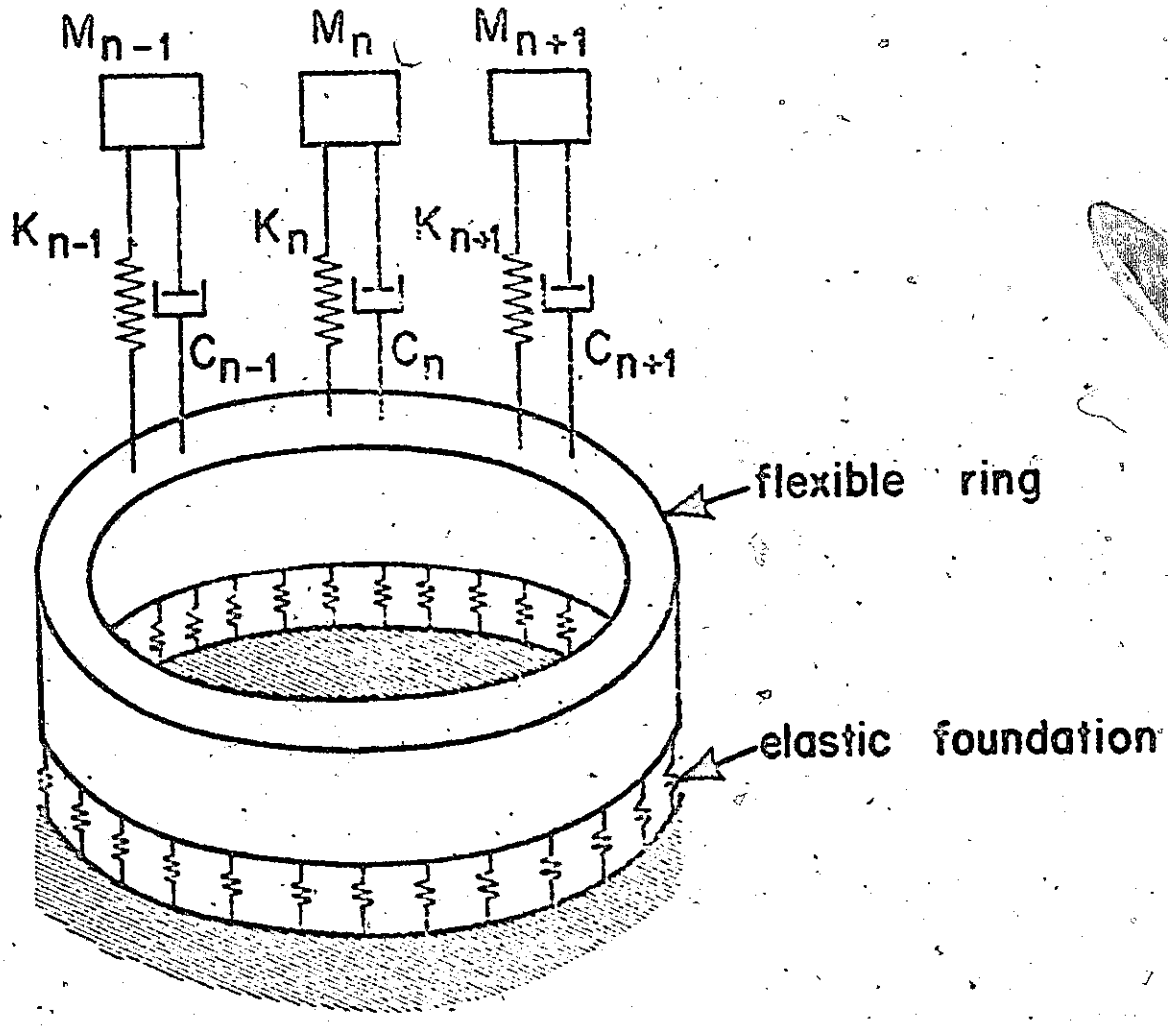

Figure 3

A Simplified Model for Blade Disc Assembly
Suggested by Wagner [15]

differences between the blades on a bladed disk - gives rise to a natural frequency "splitting" phenomenon in which a pair of modes with close natural frequencies and similar characteristics are formed in place of an apparently single mode of vibration in the perfect, or tuned, system. Furthermore, it has been found that the degree of splitting is closely related to the degree of detuning, and that within the range covered by typical blade variations (e.g. blade mass within ±2.5% of average), the maximum frequency split is of the same order of magnitude as the amplitude of the blade variation. It has been also shown that [16,17] with the random arrangements of typical blades which usually occur in practice, some blades may suffer stress levels which are 20% higher than these of the equivalent tuned systems.

Consideration of the above methods, to account for the coupling effects due to disc elasticity, indicates that: (a) The Rayleigh's method used by Stodola [6] and Malkin [7] gives only a crude estimation for the fundamental frequency, (b) The investigation of in-plane vibration of the disc limits the analysis to a specific type of motion, and (c) In the simplified models, the blades have either been considered as single degree of freedom systems [15] or as untwisted, untapered parallel beams [13] ; obviously these models are not entirely suitable for computation of actual systems, they can at most serve in the interpretation of test results and in guiding further work on this topic.

2.3 Methods Dealing with Natural Frequencies of Large Structures

The engineer frequently examines structural dynamics problems with hundreds, or even thousands, of degree of freedom. The eigenvalue solutions of full matrices however are very expensive, and even with only a few hundred degrees of freedom they may use a great deal of computer time and storage. Clearly a technique is needed to eliminate variables, so as to reduce the number of degrees of freedom in structural dynamic problems.

The technique used by Anderson, Irons and Zienkiewicz [18] retains only a small proportion of the nodal deflections, called "masters". The remaining "slave" deflections take the values giving least strain energy, regardless of what effect this has on the kinetic energy.

Given some engineering skill in choosing the master deflections, very little accuracy may be lost. The number of master nodes may be only 10% of the total, and only one deflection out of three may be retained at each node, yet the frequencies may be accurate enough for practical purposes.

However, the main disadvantage of this method is that it is possible to suppress or falsify the lower frequencies if inappropriate displacements are eliminated.

Another method which has been used for dealing with large structures is the dynamic substructuring method. The key feature of this approach, is the retention of those displacements necessary for the connection of the subject substructure to the other substructures of the complete system.

In this method the properties and the modes of the structural system are synthesized from those of the components of substructures that make up the system. Displacements related to each component are defined by a set of modal coordinates. A transformation is derived which connects component coordinates and system coordinates. By use of this transformation, mass and stiffness matrices for the system are constructed from the separate components. Using this system matrices, a matrix equation for the free vibration of an undamped elastic structure is written. The method was pioneered by Hurty [19,20], but further simplifications were introduced later by Craig and Bampton [21], Goldman [22] and Gladwell [23].

The third method, the transfer matrix method, is not completely new. It has its predecessors in the tabular methods which were successfully applied before the advert of computer. For example [24], there are Holzer's method applicable to vibrating rods and Myklestad's method for treating beam vibrations. The transfer matrix, once introduced, developed rapidly between 1950 and 1960, especially in Germany. As a matter of fact, the method was mainly used to solve problems having point masses and springs, and beams having continuous distributed mass and elasticity.

In this method [25] the state vector at a point i of an elastic system, Figure (4), is defined as a column vector whose components are the generalized displacements of the point i , and the corresponding generalized forces.

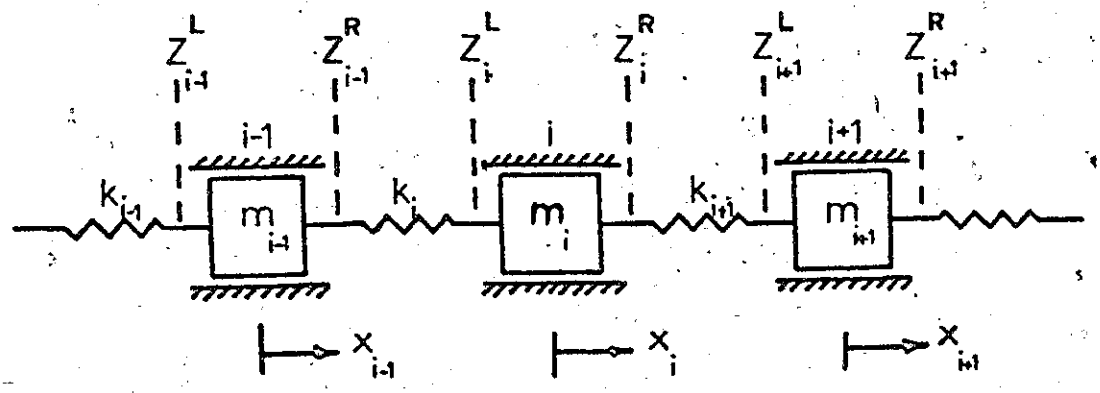

Figure 4

Spring-Mass System

The transfer matrix is defined as the matrix which relates two state vectors at different positions in the elastic system, i.e.,

$$\{Z\}_{i+1} = [T]_i \{Z\}_i \tag{2.2}$$

where $[T]_i$ is the transfer matrix, and $\{Z\}_i$ is the state vector at point i. Obviously, if there are n components in the column matrix, the transfer matrix is square and of size n. Starting from one side of the system, we can eliminate all intermediate state vectors of the system. This results in

$$\{Z\}_R = [P] \{Z\}_L \tag{2.3}$$

where $\{Z\}_R$ and $\{Z\}_L$ are the state vectors at the right and left boundaries of the system. Applying the boundary conditions we obtain the frequency determinant. In practice, the frequency determinant is plotted for different values of angular frequency, zero values of the determinant corresponding to the natural frequencies of the system.

In using a computer, which has always a finite number of digits, to find the zero value of the determinant, numerical difficulties will arise if we want to calculate higher natural frequencies. In this case, the value of the determinant depends upon differences of almost equally large

quantities, so that from the practical standpoint the zeros of the determinant cannot be found. Two procedures have been developed by Fuhrke [26] and Leckie and Pestel [27] to overcome these numerical difficulties. However, these procedures are unsuitable from the practical standpoint if applied to problems of order higher than 4.

In the static and dynamic investigations of multi-degree of freedom systems by means of transfer matrices, problems are sometimes encountered where the number of state vector component decreases, or increases, as we go from one boundary of the system to the other. Under such circumstances, it is useful to employ rectangular transfer matrices instead of the square type. Pestel [28] demonstrated how these rectangular matrices are formed.

Whitehead [29] found that, by a suitable choice of the order and signs of the elements of the state vector, the transfer matrix can, in many cases, be made symmetrical about the secondary diagonal, that is the diagonal running from the top right corner to the bottom left corner of the matrix. This property is useful in checking the derivation of transfer matrices in particular cases, and also in the preparation of computer programs.

The application of the transfer matrices was extended by Bergmann and Pestel [30] to the kinetic examination of delta wings, and by Gradowezyk [31] in connection with the exact theory of bending of prismatic shells. Also Ramaih [32]

presented a method for analysis of folded plates using transfer matrices.

The idea of the transfer matrix method has been extended by Dokainish [33] to the vibration problem of square plates. The technique is a combination of transfer matrix and finite element methods. In his work, the plate is divided into several strips, with a number of nodes on the left and right edges of each strip. Each strip is subdivided into finite elements and the stiffness and mass matrices are obtained for individual strips. The nodal equilibrium equations are arranged to obtain a relation between the edge variables of the left and the right edges. The edge variables are the forces and the displacements of all the nodes on the edge. Requirements of displacement continuity and force equilibrium at the nodes, on common edges of two adjacent strips, give the transfer matrix relation. Successive matrix multiplication finally relates the variables of the left and the right boundaries of the plate. Boundary conditions require the determinant of a portion of the overall transfer matrix to vanish at the correct natural frequency. This method has the main advantage of requiring a small computer without reducing the number of degrees of freedom of the system.

It may be mentioned that the idea of extending the transfer matrix approach to rectangular plates was also conceived by Leckie [34]. However, for obtaining the relation between the edge variables, he replaced the plate by an

equivalent network of beams, based on the Hrennikoff framework model [35]. His method of analysis, therefore, has the built-in limitations of the Hrennikoff model. In the transfer matrix- finite element approach the relation between the edge variables is based on the more versatile finite element technique and hence, the method can be used for vibration analysis of plates as well as shells of variable thickness.

Another approach has been used to solve large eigenvalue problems. This approach consists in seeking the stationary points of the Rayleigh quotient [36]

$$\lambda(x_\ell) = x_\ell^T K x_\ell / x_\ell^T M x_\ell \qquad (2.4)$$

subject to

$$x_\ell^T M x_i = 0 \quad , \quad i=1,2,\ldots,\ell-1 \qquad (2.5)$$

then

$$\min \{ \lambda(x_\ell) \} = \omega_\ell^2 \qquad (2.6)$$

where K, M, ω_ℓ and x_ℓ are the stiffness matrix, the mass matrix, the ℓ^{th} eigenvalue and eigenvector, respectively. The constraint equation (2.5) represents the imposition of the M-orthogonality condition between the eigenvector cuurently being sought and all the previously determined eigenvectors. Geometrically speaking, these constraints merely restrict the portion of vector space in which the search for

the ℓ^{th} eigenvector is carried out and in this restricted space λ has a minimum corresponding to ω_ℓ .

When minimizing the Rayleigh quotient, it is no longer necessary to physically build up the structural matrices K and M . Indeed, such an algorithm requires only the computations of the Rayleigh quotient and its gradient vector at any point. This can be performed by re-reading the elementary matrices separately from tape or disk units [36].

The first techniques for minimizing the Rayleigh quotient were confined to the "steepest descent" method, and were unsatisfactory because of the slow convergence provided by this algorithm. However, other techniques have been developed by Geradin [36] and Fried [37].

Summarizing the discussion of the various methods available for calculating natural frequencies of large structures, it can be noted that: (a) the elimination method needs some engineering skill in choosing the master deflections to avoid loss of accuracy, (b) the dynamic substructuring method becomes much too involved if the system has to be divided into many substructures, (c) the method of minimizing the Rayleigh quotient was not well developed when the work started on this thesis, and (d) the transfer matrix-finite element technique has been applied to the vibration analysis of square plates, and it seems possible to apply the same technique to more complicated structures. Hence, the transfer matrix-

finite element technique will be used to get the natural frequencies of bladed rimmed disks.

CHAPTER 3

AN ANNULAR SECTOR FINITE ELEMENT

3.1 Introduction

In two-dimensional finite element representations of problems, element shapes adopted are the triangle and the rectangle with three and four nodes, respectively. Rectangular elements are somewhat limited in their boundary shape applicability, whereas triangular elements may be used to represent almost any shape of boundary. However, for problems with curved boundaries, the use of triangular elements means that the curved boundary is being approximated by a series of straight line segments. Further, with some of the more sophosticated elements being developed today, the error introduced by this approximation may well be the limiting factor in some solutions.

Hence, there appears to be a need for elements with curved boundaries. A start in this direction has been made by Ergatoudis, Irons and Zienkiewicz [38], wherein quadrilateral plane stress elements with various curved sides are developed.

In this chapter, the stiffness and mass matrices for a plane stress element are developed in polar co-ordinates. The element has four nodal corners and is in the shape of a

segment of an annulus. The radial and tangential displacements are used as the degrees of freedom at each element node. This plane element is combined with the bending element developed by Olsen, Lindberg and Tulloch [39] to derive the total stiffness and mass matrices of an annular element having six degrees of freedom at each node. Numerical examples are carried out to check the accuracy of the in-plane element.

3.2 Theoratical Considerations

The finite element configuration to be considered is shown in Figure (5). The element is a sector of an annular plate with inside radius r_1 , outside radius r_2 , and an included angle β . The corners are numbered 1 to 4 as shown. The two displacements, in the radial and tangential directions, at each corner, are taken as the generalized coordinates for the element. The displacement vector for the finite element then becomes the 8-term column vector

$$\{\delta\} = (u_1, v_1, u_2, v_2, u_3, v_3, u_4, v_4)^T \qquad (3.1)$$

where the subscrips 1 to 4 denote the corners of the element as shown in Figure (5).

If the displacement field is to be continuous between adjacent elements it is necessary for each component of displacement to vary in a linear way along the sides of the elements. Simple displacement functions which satisfy the

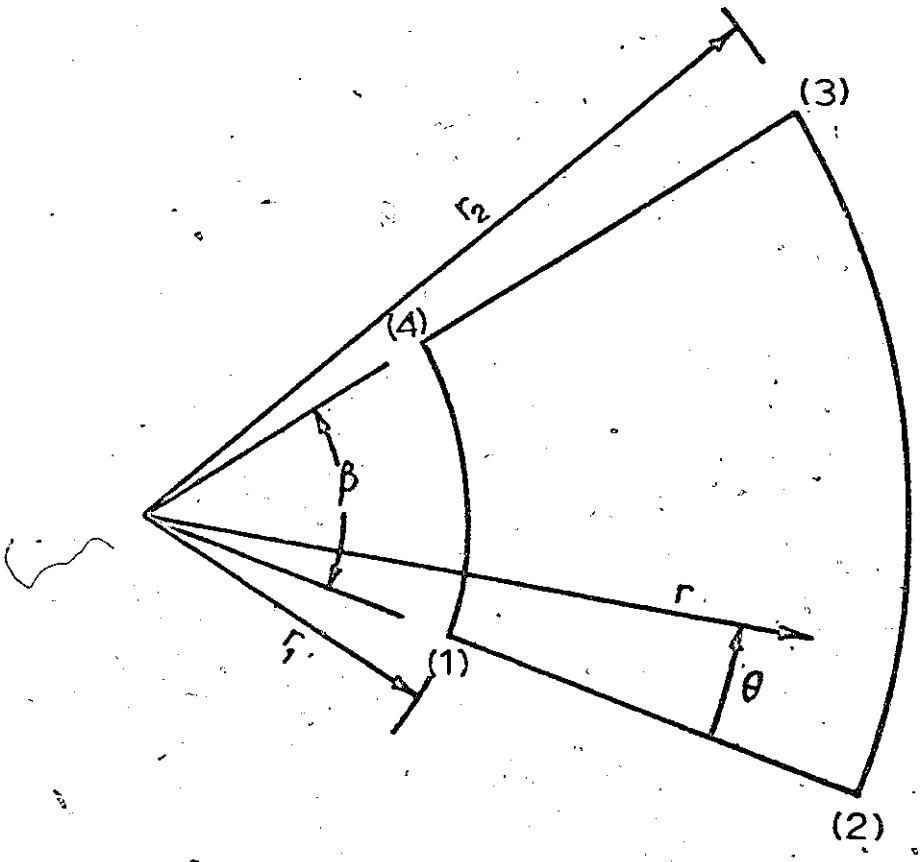

Figure 5

Annular Sector Finite Element

assumption of linearly varying boundary displacements may be taken as

$$u = \alpha_1 + \alpha_2 r + \alpha_3 \theta + \alpha_4 r\,\theta$$
$$v = \alpha_5 + \alpha_6 r + \alpha_7 \theta + \alpha_8 r\,\theta \qquad (3.2)$$

It is obvious from equation (3.2) that the distribution of the u and v displacements along any edge is linear and that it depends only on the element displacements of the two corner points defining the particular edge. Thus, the assumed form of displacement distribution ensures that the compatability of displacements on the boundaries of adjacent elements is satisfied.

It may be observed that the displacement functions are similar in form to that used for the well known eight degrees of freedom rectangular plate element [3]. In this case, the r and θ co-ordinates just replace the x and y cartesian co-ordinates, respectively, used for the rectangular element.

The eight corner displacements used in equation (3.1) may now be evaluated from equation (3.2). Carrying this leads to the matrix relation

$$\{\delta\} = [T]\,\{\alpha\} \qquad (3.3)$$

where $\{\alpha\}$ is the column vector of polynomial coefficients

$$\{\alpha\} = (\alpha_1, \alpha_2, \ldots\ldots, \alpha_8)^T \qquad (3.4)$$

and $[T]$ is the 8×8 transformation matrix given in appendix (I). Equation (3.2) can be expressed in the matrix form as

$$\begin{Bmatrix} u \\ v \end{Bmatrix} = [c]\ \{\alpha\} \qquad (3.5)$$

where

$$[c] = \begin{bmatrix} 1 & r & \theta & r\theta & 0 & 0 & 0 & 0 \\ 0 & 0 & 0 & 0 & 1 & r & \theta & r\theta \end{bmatrix} \qquad (3.6)$$

Elimination of $\{\alpha\}$ from equations (3.3) and (3.5) gives

$$\begin{Bmatrix} u \\ v \end{Bmatrix} = [c]\ [T]^{-1}\ \{\delta\} = [N]\ \{\delta\} \qquad (3.7)$$

The total strain at any point within the element can be defined by its three components [40]

$$\{\varepsilon\} = \begin{Bmatrix} \varepsilon_r \\ \varepsilon_\theta \\ \varepsilon_{r\theta} \end{Bmatrix} = \begin{Bmatrix} \partial u/\partial r \\ u/r + (1/r)\ (\partial v/\partial\theta) \\ (1/r)\ (\partial u/\partial\theta) + (\partial v/\partial r) - (v/r) \end{Bmatrix} \qquad (3.8)$$

It is noticed that in this case the strain components ε_θ and

$\varepsilon_{r\theta}$ are dependent upon the position within the element, and hence the strains are not constant throughout it.

Substituting from equation (3.2) into equation (3.8), the strains can be written in the matrix form

$$\{\varepsilon\} = [C_1] \{\alpha\} \tag{3.9}$$

where

$$[C_1] = \begin{bmatrix} 0 & 1 & 0 & \theta & 0 & 0 & 0 & 0 \\ 1/r & 1 & \theta/r & \theta & 0 & 0 & 1/r & 1 \\ 0 & 0 & 1/r & 1 & -1/r & 0 & -\theta/r & 0 \end{bmatrix} \{\alpha\} \tag{3.10}$$

Substituting for $\{\alpha\}$ from (3.3), we get

$$\{\varepsilon\} = [C_1] \quad [T^{-1}] \quad \{\delta\} \quad = [B] \quad \{\delta\} \tag{3.11}$$

Assuming the matrial to be isotropic, homogeneous, linear elastic, the constitutive relationship is

$$\{\sigma\} = \begin{Bmatrix} \sigma_r \\ \sigma_\theta \\ \sigma_{r\theta} \end{Bmatrix} = [D] \{\varepsilon\} \tag{3.12}$$

where

$$[D] = \frac{E}{1-\nu^2} \begin{bmatrix} 1 & \nu & 0 \\ \nu & 1 & 0 \\ 0 & 0 & (1-\nu)/2 \end{bmatrix} \tag{3.13}$$

and E and ν are Young's Modulus and Poisson's ratio, respectively.

The stiffness matrix for the element is obtained by applying the principle of minimum potential energy [3], and is given by

$$[K_p] = \int_{vol} [B]^T [D] [B] \, d\,vol$$

$$= [T^{-1}]^T \left[\int_{\substack{\text{area of} \\ \text{the element}}} \int [C_1] [D] [C_1] \, t \, r dr d\theta \right] [T^{-1}]$$

$$= \frac{Et}{1-\nu^2} [T^{-1}]^T [k] [T^{-1}] \qquad (3.14)$$

where the [k] matrix is given in Appendix II

3.3 Equivalent Nodal Forces for Distributed Loads

Generally, the plate is subjected to distributed external loads. The distributed loads, acting on an element must be converted to equivalent nodal forces. The principle of finding the equivalent forces is that the work done by the two systems of forces, during an arbitary virtual displacement, must be equal.

At a point within the element, let the external forces along the r and θ axis be F_r and F_θ. The external forces F_r and F_θ can be converted to a vector of equivalent nodal forces $\{F_{eq}\}$ as follows :

If $\{\delta^*\}$ denotes the virtual nodal displacements, the

virtual displacements at any point within the element, are

$$\begin{Bmatrix} u^* \\ v^* \end{Bmatrix} = [C]\ [T^{-1}]\ \{\delta^*\} \qquad (3.15)$$

Equating the work done by the actual distributed forces and the equivalent nodal forces,

$$\{\delta^*\}^T\ \{F_{eq}\} = \int_{vol} \begin{Bmatrix} u^* \\ v^* \end{Bmatrix}^T \begin{Bmatrix} F_r \\ F_\theta \end{Bmatrix} d\ vol \qquad (3.16)$$

Elimination of $\begin{Bmatrix} u^* \\ v^* \end{Bmatrix}$ from equations (3.15) and (3.16) gives

$$\{\delta^*\}^T\ \{F_{eq}\} = \{\delta^*\}^T\ [T^{-1}]^T \int_{vol} [C]^T \begin{Bmatrix} F_r \\ F_\theta \end{Bmatrix} d\ vol \qquad (3.17)$$

Since the virtual displacements $\{\delta^*\}$ are arbitary, equation (3.18) reduces to

$$\{F_{eq}\} = [T^{-1}]^T \int\int_{\substack{area \\ of\ the \\ element}} t\ [C] \begin{Bmatrix} F_r \\ F_\theta \end{Bmatrix} r\ dr d\theta \qquad (3.19)$$

This method of finding the equivalent nodal forces is known as the "consistent method".

3.4 In-plane Mass Matrix for an Element

In the case of free vibrations, the plate is acted upon by a distributed inertia load. By the application of d'Alembert principle, the dynamic problem can be treated as the static one, subjected to forces equal to the negative of the inertia loads. Since the deflection at any point within the element is $\begin{Bmatrix} u \\ v \end{Bmatrix}$, the intensity of the distributed force $\{F\}$ is given by

$$\{F\} = -\rho \begin{Bmatrix} \ddot{u} \\ \ddot{v} \end{Bmatrix} \tag{3.20}$$

where $\begin{Bmatrix} \ddot{u} \\ \ddot{v} \end{Bmatrix}$ denotes the second derivative of $\begin{Bmatrix} u \\ v \end{Bmatrix}$ with respect to time and ρ is the mass per unit volume of the plate. Substitution for $\begin{Bmatrix} u \\ v \end{Bmatrix}$ from equation (3.15) gives

$$\{F\} = -\rho\, [C]\, [T^{-1}]\, \{\ddot{\delta}\} \tag{3.21}$$

By use of equation (3.19) this distributed in-plane forces can be converted to equivalent nodal forces given by

$$\{F_{eq}\} = [T^{-1}]^T \int\int_{\substack{\text{area} \\ \text{of the} \\ \text{element}}} -\rho t\, [C]^T\, [C]\, [T^{-1}]\, \{\ddot{\delta}\}\, r\, dr d\theta \tag{3.22}$$

or

$$\{F_{eq}\} = -[M]\, \{\ddot{\delta}\} \tag{3.23}$$

where, the in-plane mass matrix is given by (Appendix III)

$$[M'_p] = \rho\ [T^{-1}]^T \left[\int_{\text{area of the element}} \int t\ [C]^T\ [C]\ r\ dr d\theta \right] [T^{-1}] \quad (3.24)$$

3.5 The Bending Annular Sector Finite Element

Two bending annular sector finite elements have been derived. Sawko and Merriman [41] developed a finite element with four degrees of freedom at each node. These are the deflection w, the slopes $\partial w/\partial r$, $(1/r)(\partial w/\partial r)$ and $(1/r)(\partial^2 w/\partial r \partial\theta)$. Sixteen undetermined constants are thus used. A cubic distribution of deflection is assumed along the radial direction. Thus the deformation function is given by

$$\begin{aligned} w(r,\theta) = {} & \alpha_1 + \alpha_2 r + \alpha_3 r^2 + \alpha_4 r^3 + \alpha_5 \cos\theta + \alpha_6 r \cos\theta \\ & + \alpha_7 r^2 \cos\theta + \alpha_8 r^3 \cos\theta + \alpha_9 \sin\theta + \alpha_{10} r \sin\theta \\ & + \alpha_{11} r^2 \sin\theta + \alpha_{12} r^3 \sin\theta + \alpha_{13} \sin 2\theta \\ & + \alpha_{14} r \sin 2\theta + \alpha_{15} r^2 \sin 2\theta + \alpha_{16} r^3 \sin 2\theta . \end{aligned} \quad (3.25)$$

Also, Olson, Lindberg and Tulloch [39] derived a flat plate-bending element in polar co-ordinates. They found that it is sufficient to use the displacement and two slopes at each

corner as the generalized co-ordinates for the element. This will allow the displacement to be cubic in r along edges 1 - 2, Figure (5) , and 3 - 4, and cubic in θ along the edges 1 - 4 and 2 - 3. Hence, the displacement will be continuous between elements with a common boundary, provided the corner displacements are made equal at the ends of that boundary. The displacement vector for the annular sector finite element then becomes the twelve - term column vector

$$\{\delta\} = \{w_1, w_{\theta_1}/r, -w_{r_1}, w_2, \ldots, w_3, \ldots, w_4, \ldots\}^T \quad (3.26)$$

where $w_\theta = \partial w/\partial\theta$, $w_r = \partial w/\partial r$ and the subscripts 1 to 4 denote the corners of the element as shown in Figure (5).

In the present analysis, this element will be used as it gave good results for vibration problems of plates, even with a rather coarse mesh.

The displacement function for this element is in the form

$$w(r,\theta) = \alpha_1 + \alpha_2 r + \alpha_3\theta + \alpha_4 r\theta + \alpha_5 r^2 + \alpha_6\theta^2 + \alpha_7 r^2\theta + \alpha_8 r\theta^2 + \alpha_9 r^3 + \alpha_{10}\theta^3 + \alpha_{11} r^3\theta + \alpha_{12} r\theta^3 \quad (3.27)$$

It may be observed that this function is similar in form to that used for the well known twelve degrees of freedom

rectangular plate bending element [3]. In this case, the r and θ co-ordinates just replace the x and y cartesian co-ordinates, respectively.

The twelve corner displacements used in equation (3.26) may now be evaluated from equation (3.27). Carrying this out leads to the matrix relationship

$$\{\delta\} = [T]\ \{\alpha\} \tag{3.28}$$

where $\{\alpha\}$ is the column vector of polynomial coefficients

$$\{\alpha\} = (\alpha_1, \alpha_2, \ldots\ldots, \alpha_{12})^T \tag{3.29}$$

and $[T]$ is the 12×12 transformation matrix given in Appendix IV.

The consistent stiffness and mass matrices of the element are given by [39]

$$[K'_b] = [T^{-1}]\ [k]\ [T^{-1}] \tag{3.30}$$

and

$$[M'_b] = [T^{-1}]\ [m]\ [T^{-1}] \tag{3.31}$$

where $[k]$ and $[m]$ are as given in Appendix V and VI, respectively.

3.6 Complete Stiffness and Mass Matrices for an Element

The next step is to combine $[K'_p]$ and $[K'_b]$ to obtain the complete stiffness matrix $[K'_e]$ for the element. In doing so, it is to be noted that the displacements prescribed for in-plane forces do not affect the bending deformation and vise-versa, also that the rotation θ'_z (about the z-axis) does not enter as a parameter into the definitions of deformation in either mode. However, when the transformation to global co-ordinates is carried out, it is necessary to have θ_z as a parameter. Hence the term θ'_z is introduced at this stage; a fictitious couple M'_z is associated with it and the appropriate number of zeros are inserted in the stiffness matrix. The stiffness matrix for the element is thus given by

$$[K'_e] = \begin{bmatrix} K_e^{11} & K_e^{12} & K_e^{13} & K_e^{14} \\ K_e^{21} & K_e^{22} & K_e^{23} & K_e^{24} \\ K_e^{31} & K_e^{32} & K_e^{33} & K_e^{34} \\ K_e^{41} & K_e^{42} & K_e^{43} & K_e^{44} \end{bmatrix} \qquad (3.32)$$

where

$$K_e^{rs} = \begin{bmatrix} K_p^{rs} & \begin{matrix} 0 & 0 & 0 \\ 0 & 0 & 0 \end{matrix} \\ \begin{matrix} 0 & 0 \\ 0 & 0 \\ 0 & 0 \end{matrix} & \begin{matrix} 0 \\ 0 \\ 0 \end{matrix} \\ \begin{matrix} 0 & 0 \end{matrix} & \begin{matrix} 0 & 0 & 0 & 0 \end{matrix} \end{bmatrix} \qquad (3.33)$$

$[K_p^{rs}]$ and $[K_p^{rs}]$ being (2×2) and (3×3) submatrices respectively, obtained by partitioning $[K'_p]$ and $[K'_b]$ in the same manner as in equation (3.32). The order of nodal displacements would be

$$\{\delta\} = \{u_1, v_1, w_1, (w_{\theta_1}/r_1), -w_{r_1}, \theta_{z_1}, u_2, \ldots\ldots$$

$$\ldots, u_3, \ldots\ldots, u_4, \ldots\ldots\}^T \qquad (3.34)$$

If an annular element has a common edge with another element, and both elements are not in the same plane, then the stiffness matrix $[K'_e]$ must be transformed to the common global co-ordinate system X, Y, Z, where the X-axis coincides with the direction given by $\theta = 0$, and the Z-axis is normal to the plane of the plate. The vector of nodal displacements $\{\delta'_e\}$ for an element in local co-ordinates is related to the corresponding vector $\{\delta_e\}$ in global co-ordinates by the relationship

$$\{\delta'_e\} = [T]\ \{\delta_e\} \qquad (3.35)$$

The same transformation is applicable for the nodal forces. Here $[T]$ is the (24×24) transformation matrix given by

$$[T] = \begin{bmatrix} \lambda & 0 & 0 & 0 \\ 0 & \lambda & 0 & 0 \\ 0 & 0 & \lambda & 0 \\ 0 & 0 & 0 & \lambda \end{bmatrix} \qquad (3.36)$$

where

$$[\lambda] = \left[\begin{array}{ccc:ccc} \cos\theta & \sin\theta & 0 & 0 & 0 & 0 \\ -\sin\theta & \cos\theta & 0 & 0 & 0 & 0 \\ 0 & 0 & 1 & 0 & 0 & 0 \\ \hdashline 0 & 0 & 0 & \cos\theta & \sin\theta & 0 \\ 0 & 0 & 0 & -\sin\theta & \cos\theta & 0 \\ 0 & 0 & 0 & 0 & 0 & 1 \end{array}\right] \quad (3.37)$$

The complete stiffness matrix for the element, in the global axes, is, therefore, given by [3]

$$[K_e] = [T]^T [K'_e] [T] \quad (3.38)$$

The same procedure is used to get the mass matrix in global co-ordinates, i.e.

$$[M_e] = [T]^T [M'_e] [T] \quad (3.39)$$

3.7 Calculation of Displacements

Having calculated the stiffness matrix, $[K_e]$ for the individual elements, the next step is to combine all these matrices, according to the sequence of node numbering employed on the structure, to obtain the complete stiffness matrix for the structure.

When all the elements joining at a particular node are in one plane, a difficulty arises. In global co-ordinates six equations that are singular are obtained. This is due to

the fact that only five equations can be independent, since rotation perpendicular to the plane is omitted. For such nodes, the rotations w_θ and $-w_r$ must be retained for assembly.

If the boundary conditions specify certain nodal displacements to be zero, the rows and the columns corresponding to such displacements must be deleted from the complete stiffness matrix to obtain the final stiffness matrix $[K]$. The vectors of the nodal forces for the elements, on assembly, give the total force vector $\{F\}$. The displacements $\{\delta\}$ can then be obtained from the equation

$$\{\delta\} = [K]^{-1} \{F\} \tag{3.40}$$

3.8 Numerical Examples

The in-plane finite element is now used to solve two numerical examples that indicate how well the element works in the various types of applications. The problems considered are the static deflections and stresses of a thin annular plate under uniform in-plane stress on the inner edge, and the tangential stresses in a circular thin ring compressed by two opposite concentrated forces.

3.8.1 Thin Annular Plate Under Uniform In-Plane Stress on the Inner Edge

The first example is the very simple thin annular

plate of Figure (6). The plate is subjected to uniform internal stress. A two dimensional finite element analysis was made of the narrow segment shown in Figure (6), utilizing the n element idealization shown in the Figure. Roller supports are assumed along the boundaries to maintain the required symmetric displacement condition, and the internal stress (or pressure) was represented by two concentrated loads acting at the interior nodal points. The inner radius of the plate is 5 inches, and the outer radius is 10 inches, the internal stress is 100 pounds per square inch.

Table I shows a comparison between the radial deformations obtained using this element and the exact values of the deformations for the analogous problem of a thick cylinder subjected to the same uniform internal stress (or pressure), as given by Wang[40]. The deformation is expressed as a nondimensional quantity given by

$$\hat{u} = \frac{uE}{\sigma_i R_o} \tag{3.41}$$

where u is the actual radial displacement at radius r, E is Young's Modulus, σ_i is the internal applied stress and R_o is the outer radius of the annular plate.

Table II shows a comparison between the stresses (radial and tangential) obtained by the present analysis and the exact values of the stresses as given by Wang. The stresses are calculated at the geometric centers of the elements, and

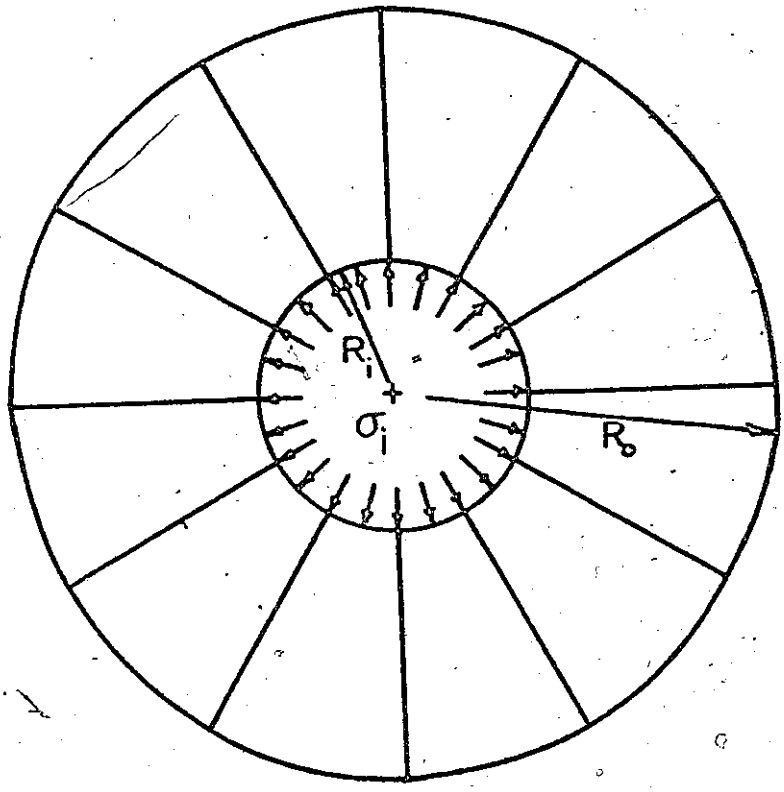

(a)

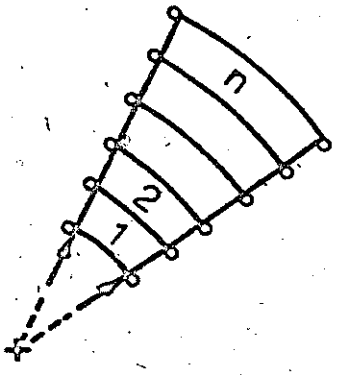

(b)

Figure 6

Thin Annular Plate under Uniform In-Plane Internal Stress σ_i on the Inner Edge

TABLE I

Nondimensional Displacements $(\hat{u})$, For a Thin Annular Plate Under Uniform In-Plane Stress On The Inner Edge

Number of Elements n	Radius At Which Deflection is Given r	Exact Value [40]	Calculated Value
3	5.00	0.9833	0.9698
	6.67	0.8066	0.7961
	8.33	0.7144	0.7068
	10.00	0.6667	0.6599
4	5.00	0.9833	0.9756
	6.25	0.8392	0.8333
	7.50	0.7528	0.7479
	8.75	0.6994	0.6952
	10.00	0.6667	0.6628
5	5.00	0.9833	0.9783
	6.00	0.8622	0.8582
	7.00	0.7824	0.7790
	8.00	0.7283	0.7254
	9.00	0.6915	0.6888
	10.00	0.6667	0.6641
10	5.00	0.9833	0.9821
	5.50	0.9162	0.9151
	6.00	0.8622	0.8612
	6.50	0.8183	0.8174
	7.00	0.7824	0.7815
	7.50	0.7528	0.7519
	8.00	0.7283	0.7276
	8.50	0.7081	0.7074
	9.00	0.6915	0.6908
	9.50	0.6778	0.6772
	10.00	0.6667	0.6660

TABLE II

Nondimensional Stresses ($\hat{\sigma}$) For a Thin Annular Plate Under Uniform In-Plane Stress On Inner Edge

Number of Elements n	Radius At Which Stress Is Given r	Radial Stress		Tangential Stress	
		Exact Value [40]	Calculated Value	Exact Value [40]	Calculated Value
3	5.833	-0.6463	-0.6465	1.3129	1.3197
	7.500	-0.2593	-0.2586	0.9259	0.9243
	9.166	-0.6336	-0.6321	0.7300	0.7265
4	5.625	-0.7202	-0.7203	1.3868	1.3918
	6.875	-0.3719	-0.3715	1.0386	1.0386
	8.125	-0.1716	-0.1712	0.8383	0.8367
	9.375	-0.0459	-0.0458	0.7126	0.7105
5	5.500	-0.7686	-0.7688	1.4353	1.4390
	6.500	-0.4556	-0.4553	1.1223	1.1228
	7.500	-0.2593	-0.2590	0.9259	0.9252
	8.500	-0.1280	-0.1279	0.7959	0.7935
	9.500	-0.0360	-0.0360	0.7027	0.7012
10	5.250	-0.8760	-0.8761	1.5427	1.5440
	5.750	-0.6749	-0.6748	1.3415	1.3422
	6.250	-0.5200	-0.5199	1.1867	1.1870
	6.750	-0.3983	-0.3982	1.0649	1.0650
	7.250	-0.3008	-0.3007	0.9675	0.9674
	7.750	-0.2216	-0.2216	0.8883	0.8881
	8.250	-0.1564	-0.1564	0.8231	0.8228
	8.750	-0.1020	-0.1020	0.7687	0.7684
	9.250	-0.0563	-0.0562	0.7229	0.7226
	9.750	-0.0173	-0.0173	0.6840	0.6836

are expressed as a nondimensional quantity given by

$$\hat{\sigma} = \sigma/\sigma_i \qquad (3.42)$$

where σ is the actual stress (radial or tangential), at radius r . Very good agreement is obtained between the theoretical and numerical results.

3.8.2 Thin Ring Compressed by Two Opposite Concentrated Forces

The second example is a thin circular ring compressed by two equal and opposite concentrated forces P acting along a diameter as shown in Figure (7). The outer radius is 10 inches and the inner radius is 5 inches. Symmetry conditions are used in order to reduce the number of degrees of freedom, so that only the right half is considered.

Table III shows the comparison between the results obtained for the ratios (σ_θ: $2P/\pi R_o$), where σ_θ is the tangential stress , for different finite element meshes, and the exact values given by Timoshemko [42]. It is to be noted that the numbers at the top of columns 3 to 6 are the number of elements in the radial direction and the tangential direction, respectively. The agreement between the theoretical and numerical results is reasonable.

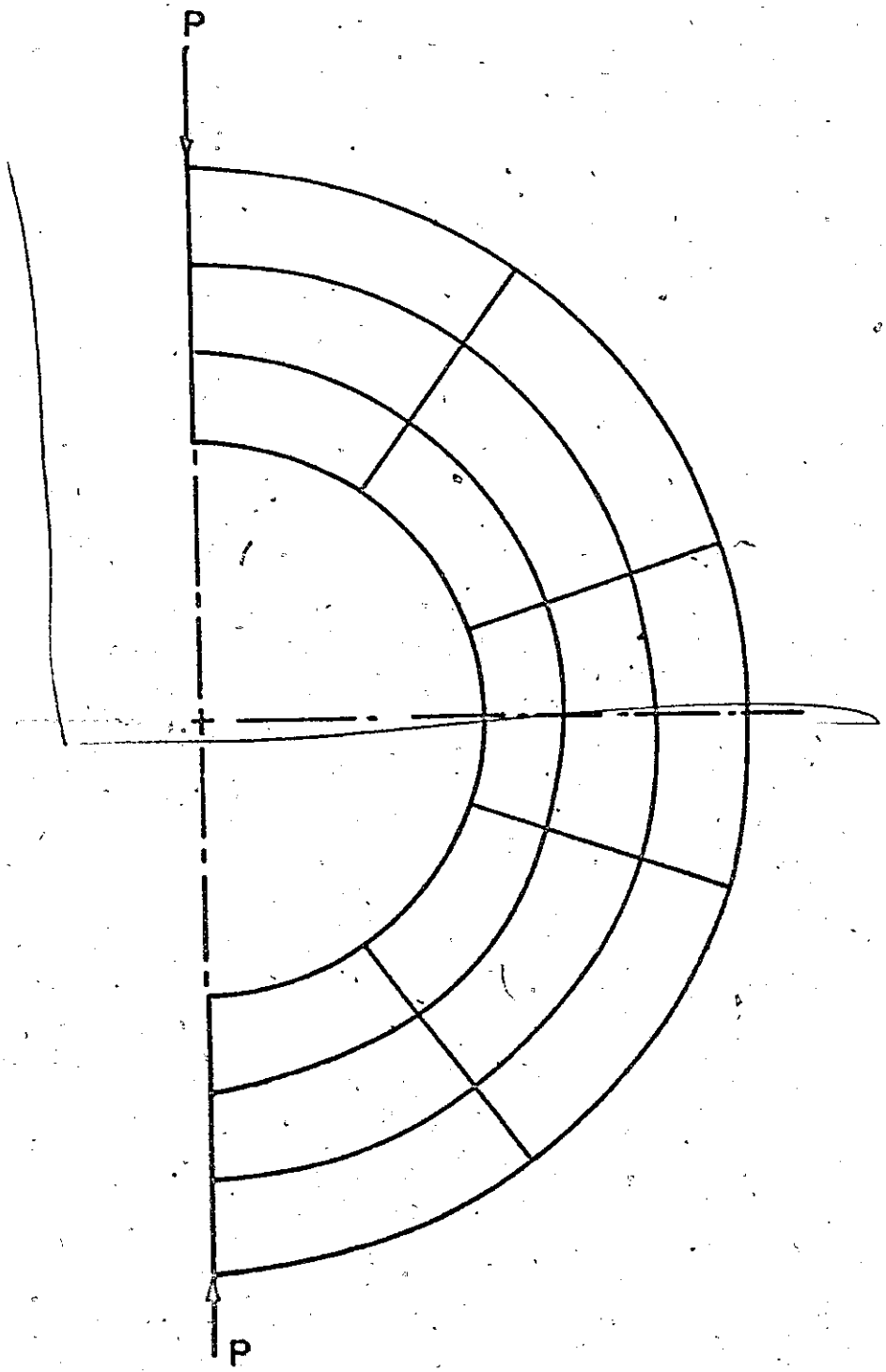

Figure 7

Circular Thin Ring Compressed by
Two Opposite Concentrated Forces

TABLE III

The Ratios ($\sigma_\theta : 2P/\pi R_0$) For a Circular Thin Ring Compressed By Two Equal Forces Acting Along a Diameter

Radius At Which The Ratio Is Given r	Exact Values Of The Ratio [42]	Calculated Values Of The Ratio			
		4x10	4x18	4x30	4x34 *
9.375	2.05	0.30	1.13	1.62	1.70
8.125	0.10	-0.42	-0.20	-0.03	0.01
6.875	-2.30	-1.51	-1.88	-2.08	-2.12
5.625	-5.85	-3.24	-4.49	-5.29	-5.42

*The numbers at the top of columns 3 to 6 represent the number of elements in the radial and tangential directions, respectively.

3.9 Concluding Remarks

The development of an in-plane annular sector finite element has been presented. The element has 8 in-plane degrees of freedom in polar coordinates corresponding to the corner displacements u and v .

The accuracy of the element was tested by two numerical examples, and it gave satisfactory results.

This element, when combined with a bending annular sector finite element, would give the complete annular sector element having six degrees of freedom at each node, three translations and three rotations.

CHAPTER 4

TWO MODIFIED CYLINDRICAL SHELL FINITE ELEMENTS

4.1 Introduction

The first application of the finite element technique to shells involved replacing the curved surface by flat triangular and rectangular elements and superimposing the "plane stress" and "plate bending" stiffness matrices. However, the major portion of the research pretaining to the development of finite elements for modelling of shells has been devoted to closed rings or conical shell segments for the modelling of shells of revolution. A closed conical shell element for use within the frame work of the displacement method was introduced by Grafton and Strome [43]. The use of closed axisymmetric shell element is restricted in that only shells of revolution can be modelled and only special types of loading can be handled. The experience gained with shells of revolution indicates that flat elements can lead to a good solution provided that a fine mesh is used. However, it appears that curved elements lead to cosiderably better results, for the same element size and shape, and therefore are more efficient. To analyze a shell of arbitary shape by the finite element method, one can use a combination of triangular and quadrilateral elements. However, rectangular

elements are particularly convenient for shells having a rectangular boundary.

Referring to the co-ordinate system defined in Figure (8), the displacement functions used by Gallegher [44,45] in deriving the 24 degrees of freedom cylindrical shell element are

$$
\begin{aligned}
u(\xi,\eta) &= \alpha_1\xi\eta + \alpha_2\xi + \alpha_3\eta + \alpha_4 \\
v(\xi,\eta) &= \alpha_5\xi\eta + \alpha_6\xi + \alpha_7\eta + \alpha_8 \\
w(\xi,\eta) &= \alpha_9\xi^3\eta^3 + \alpha_{10}\xi^3\eta^2 + \alpha_{11}\xi^3\eta + \alpha_{12}\xi^3 \\
&\quad + \alpha_{13}\xi^2\eta^3 + \alpha_{14}\xi^2\eta^2 + \alpha_{15}\xi^2\eta + \alpha_{16}\xi^2 \\
&\quad + \alpha_{17}\xi\eta^3 + \alpha_{18}\xi\eta^2 + \alpha_{19}\xi\eta + \alpha_{20}\xi + \alpha_{21}\eta^3 \\
&\quad + \alpha_{22}\eta^2 + \alpha_{23}\eta + \alpha_{24} \; .
\end{aligned}
\tag{4.1}
$$

The six degrees of freedom considered at each node (corner) of the element are u , v , w , w_ξ , w_η and $w_{\xi\eta}$.

Cantin and Clough [45] have restricted their attention to the cylindrical element and chose functions which are essentially linear in the axial and circumferential co-ordinates. The latter are modified in such a way,however, to satisfy the rigid body modes requirement. Compatability of

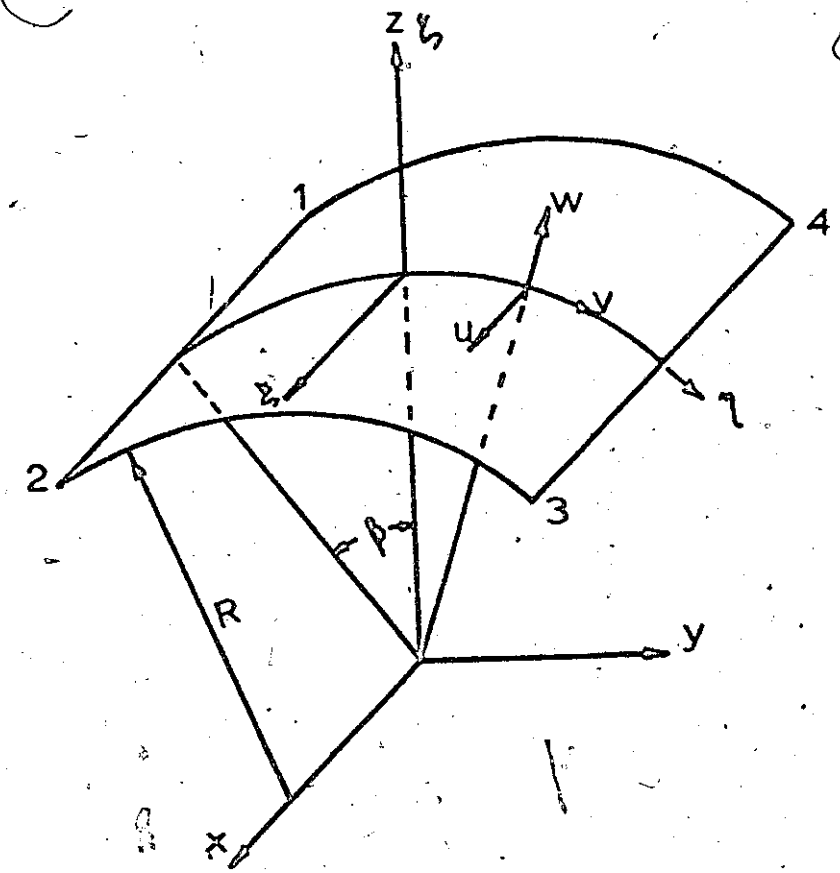

Figure 8

Definition of Geometrical Symbols for a Cylindrical Shell Element [ ]

displacements is not satisfied due to the difference in the orders of polynomials used for radial and membrane displacements, respectively. A careful numerical study is given to the significance of the rigid body modes requirement. Although convergence to the correct solution is assured, the rate of convergence for the representation which lacks adherence to this requirement is found to be poor. This conclusion is substantiated by a study of curved element representation in arch analysis.

Connor and Brebbia [46] employ the 12-term polynomial

$$w(x,y) = \alpha_1 + \alpha_2 x + \alpha_3 y + \alpha_4 x^2 + \alpha_5 xy + \alpha_6 y^2 + \alpha_7 x^3 + \alpha_8 x^2 y + \alpha_9 xy^2 + \alpha_{10} y^3 + \alpha_{11} x^3 y + \alpha_{12} xy^3 \quad (4.2)$$

to represent a four sided shallow shell element, x is measured along a cylindrical generator, and y is on the shell surface normal to the generator. Membrane behaviour is represented by linear polynomials, and shallow shell theory is used in the formulation of the strain energy.

The 48 degrees of freedom element developed by Bogner, Fox and Schmit [47], uses for both u and v the same polynomial functions as used for w in equation (4.2), and the nodal degrees of freedom include derivatives of u and v corresponding to the derivatives of w in the aforementioned degrees of freedom.

Olson and Lindberg formulated the stiffness and mass matrices for a cylindrical four-sided element, using Love's strain displacement equations [48]. The 12-term polynomial, equation (4.2), is chosen in the description of the radial displacement w, while the membrane displacements are each described by an 8-term polynomial which is linear in the axial co-ordinate and cubic in the circumferential co-ordinate. Thus, designating the axial displacement by u:

$$u(x,y) = \alpha_1 + \alpha_2 x + \alpha_3 y + \alpha_4 xy + \alpha_5 y^2 + \alpha_6 xy^2 + \alpha_7 y^3 + \alpha_8 xy^3 \qquad (4.3)$$

and the circumferential displacement v is of corresponding form. The displacements at each joint are w, u, v, w_x, w_y, u_y, and v_y - a total of 28 degrees of freedom. The rigid body mode requirements are satisfied but the displacement compatability conditions are not.

They also formulated the stiffness and mass matrices for the same element except that the membrane behaviour is represented by linear polynomials. The size of the matrices is (20x20) and the displacements at each node are u, v, w, w_x, and w_y. Actually, this is the simplest possible non-conforming representation for a cylindrical shell element.

In their analysis, the expressions for u, v and w are substituted into the strain energy and kinetic energy

integrals from cylindrical shell theory, and Castigliano's theorem is employed to yield the (28x28) and (20x20) stiffness and mass matrices for the cylindrical shell element. However, in their work, terms like $(1+t^2/R^2)$ in the energy expressions have been approximated by 1 .

In this chapter, the same displacement expressions as used by Olson and Lindberg, are used for the derivation of the 20 and 28 degrees of freedom models. The classical procedure for the derivation of the stiffness and mass matrices [3] is used and no terms have been neglected. Results are compared with those of Olson and Lindberg.

4.2 Theoretical Formulation

It is obvious that the 12-term polynomial in x and y used for plate bending may be used for the radial displacement w . Also the in-plane displacement functions may be considered the same as for a rectangular plate, so that:

$$u(x,y) = \alpha_1 + \alpha_2 x + \alpha_3 y + \alpha_4 xy$$

$$v(x,y) = \alpha_5 + \alpha_6 x + \alpha_7 y + \alpha_8 xy$$

$$w(x,y) = \alpha_9 + \alpha_{10} x + \alpha_{11} y + \alpha_{12} xy + \alpha_{13} x^2 + \tag{4.4}$$

$$+ \alpha_{14} y^2 + \alpha_{15} x^2 y + \alpha_{16} x y^2 + \alpha_{17} x^3 + \alpha_{18} y^3 +$$

$$\alpha_{19}x^3y + \alpha_{20}xy^3 \ .$$

where x is measured along a cylindrical generator, and y is on the shell surface normal to the generator, as shown in in Figure (9). The generalized corner displacements are $\partial w/\partial x$, $\partial w/\partial y$, w , u and v. Equation (4.4) can be expressed in the matrix form as

$$\begin{Bmatrix} u \\ v \\ w \end{Bmatrix} = [C] \{\alpha\} \qquad (4.5)$$

where

$$[C] = \begin{bmatrix} 1 & 0 & 0 \\ x & 0 & 0 \\ y & 0 & 0 \\ xy & 0 & 0 \\ 0 & 1 & 0 \\ 0 & x & 0 \\ 0 & y & 0 \\ 0 & xy & 0 \\ 0 & 0 & 1 \\ 0 & 0 & x \\ 0 & 0 & xy \\ 0 & 0 & x^2 \\ 0 & 0 & y^2 \\ 0 & 0 & x^2y \\ 0 & 0 & xy^2 \\ 0 & 0 & x^3 \\ 0 & 0 & y^3 \\ 0 & 0 & x^3y \\ 0 & 0 & xy^3 \end{bmatrix}^T \qquad (4.6)$$

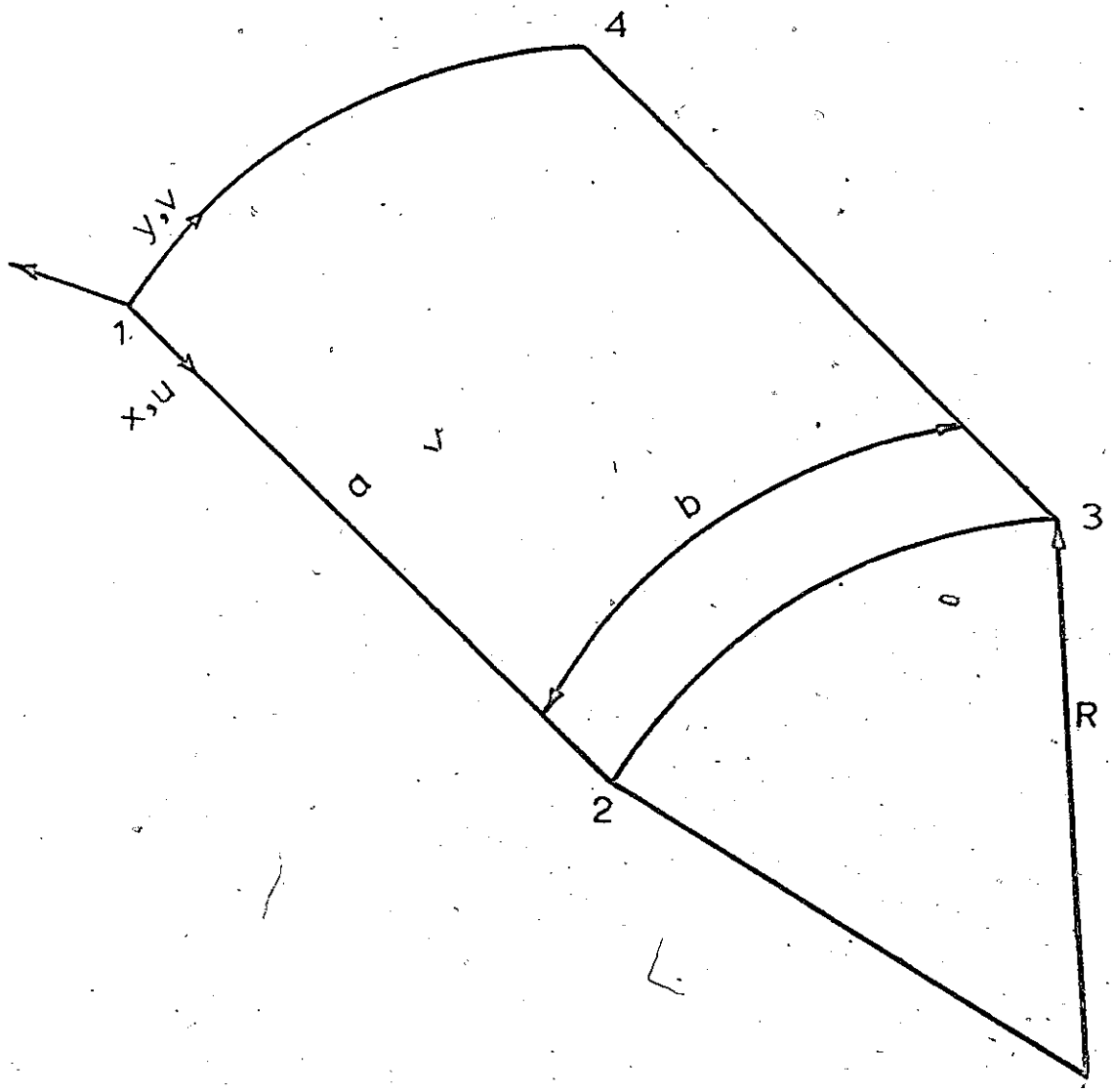

Figure 9

Cylindrical Shell Element

and $\{\alpha\}$ is the column vector of coefficients α_1 to α_{20}. The twenty displacements of the nodes and the corresponding nodal forces, expressed as vectors, are

$$\{\delta\} = \{ w_{x_1} , w_{y_1} , w_1 , u_1 , v_1 , \ldots\ldots , v_2 , \ldots\ldots , v_3 , \ldots\ldots , v_4 \}^T$$

$$\{F\} = \{ M_{x_1} , M_{y_1} , N_1 , N_{x_1} , N_{y_1} , \ldots\ldots , N_{y_2} , \ldots\ldots , N_{y_3} , \ldots\ldots , N_{y_4} \}^T \qquad (4.7)$$

Substituting for u, v and w from equation (4.5), the first of equations (4.7) can be re-written in the form

$$\{\delta\} = [T] \{\alpha\} \qquad (4.8)$$

where $[T]$ is the (20x20) transformation matrix given in Appendix VII. Elimination of $\{\alpha\}$ from equations (4.5) and (4.8) gives

$$\begin{Bmatrix} u \\ v \\ w \end{Bmatrix} = [C] \ [T]^{-1} \{\delta\} = [N] \{\delta\} \qquad (4.9)$$

The strain displacement relationships are given by[48]:

$$\varepsilon_x = \partial u/\partial x - z\,\partial^2 w/\partial x^2$$

$$\varepsilon_y = \partial v/\partial y + w/R - z\,[\,\partial^2 w/\partial y^2 - (1/R)(\partial v/\partial y)] \qquad (4.10)$$

$$\varepsilon_{xy} = \partial v/\partial x + \partial u/\partial y - 2z\,[\,\partial^2 w/\partial x \partial y - (1/R)(\partial v/\partial x)\,]$$

Substituting from equation (4.5) into equation (4.10) yields:

$$\{\varepsilon\} = \begin{Bmatrix} \varepsilon_x \\ \varepsilon_y \\ \varepsilon_{xy} \end{Bmatrix} = [C_1]\,\{\alpha\} \qquad (4.11)$$

where

$$[C_1] = \begin{bmatrix} 0 & 0 & 0 \\ 1 & 0 & 0 \\ 0 & 0 & 1 \\ y & 0 & x \\ 0 & 0 & 0 \\ 0 & 0 & 1+2z/R \\ 0 & 1+z/R & 0 \\ 0 & x+xz/R & y+2yz/R \\ 0 & 1/R & 0 \\ 0 & x/R & 0 \\ 0 & xy/R & -2z \\ -2z & x^2/R & 0 \\ 0 & y^2/R-2z & 0 \\ -2yz & x^2y/R & -4xz \\ 0 & xy^2/R-2xz & -4yz \\ -6xz & x^3/R & 0 \\ 0 & y^3/R-6yz & 0 \\ -6xyz & x^3y/R & -6x^2z \\ 0 & xy^3/R-6xyz & -6y^2z \end{bmatrix}^T \qquad (4.12)$$

Using the same procedure given in chapter 3 to get the stiffness and mass matrices, yields the stiffness matrix:

$$[K_e] = \frac{E}{1-\nu^2} [T^{-1}]^T [k] [T^{-1}] \qquad (4.13)$$

and the mass matrix:

$$[M_e] = \rho t [T^{-1}]^T [m] [T^{-1}] \qquad (4.14)$$

where [k] and [m] matrices are given in Appendices VIII and IX respectively.

4.3 The 28 Degrees of Freedom Cylindrical Shell Element

It will be shown, in the next chapter, that the use of the 20 degrees of freedom cylindrical shell element requires a large number of strips, when the transfer matrix-finite element method is applied, to get good accuracy. Naturally, this means that it requires much computing time.

For that reason, a modified 28 degrees of freedom cylindrical shell element is derived in this section. The displacement functions for this element are

$$w(x,y) = \alpha_1 + \alpha_2 x + \alpha_3 y + \alpha_4 xy + \alpha_5 x^2 + \alpha_6 y^2 +$$

$$\alpha_7 x^2 y + \alpha_8 x y^2 + \alpha_9 x^3 + \alpha_{10} y^3 +$$

$$\alpha_{11}x^3y + \alpha_{12}xy^3.$$

$$u(x,y) = \alpha_{13} + \alpha_{14}x + \alpha_{15}y + \alpha_{16}xy + \alpha_{17}y^2 \qquad (4.15)$$

$$+ \alpha_{18}xy^2 + \alpha_{19}y^3 + \alpha_{20}xy^3.$$

$$v(x,y) = \alpha_{21} + \alpha_{22}x + \alpha_{23}y + \alpha_{24}xy + \alpha_{25}y^2$$

$$+ \alpha_{26}xy^2 + \alpha_{27}y^3 + \alpha_{28}xy^3.$$

It is to be noted that since the element sides $y=0$ and $y=b$, Figure (9), are straight, it is sufficient to assume linear dependence on x for the in-plane displacements u and v. On the other hand, their dependence on y is of higher order because of the shell curvature in that direction. The displacements at each node are $\partial w/\partial x$, $\partial w/\partial y$, w, $\partial u/\partial y$, u, $\partial v/\partial y$ and v.

The derivation of the stiffness and the mass matrices for this element is exactly the same as for the 20 degrees of freedom element. The corresponding matrices [T], [k] and [m] are given in Appendices X, XI and XII, respectively.

4.4 Numerical Example

The stiffness and mass matrices, for both the 20 and 28 degrees of freedom elements, obtained from the present

analysis are used to compare the results with those of Olson and Lindberg [48]. In their work, they considered the problem of free vibrations of a curved fan blade. Such a fan blade is shown in Figure(10). This blade is a rectangular section of a cylindrical shell where y=0 and y=W are parallel cylindrical generators. The curved edge is considered built-in or clamped to an infinitely rigid foundation, while the other three sides are free. The experimental model of the blade was constructed by rolling a piece of sheet steel, 0.120 inch thick, to a radius of curvature of 24.0 inch. This curved sheet was then cut to size (W=L=12.0 inch) and welded to a steel block.

The first six vibration modes for this fan blade, using both the 20 and 28 degrees of freedom elements, are shown in Tables IV and V , respectively . It is interesting to note that the first "torsion" mode, number 1, occurs at a lower frequency than the first "bending" mode, number 2. This is the reverse of what would occur if the the blade were flat, and is a result of the stiffening due to the blade curvature.

It is obvious from both Tables that the present analysis gives better predicted results than those predicted by Olson and Lindberg for both the 20 and 28 degrees of freedom cylindrical shell elements.

It is to be noted that the numbers at the top of columns 3 to 6 in both Tables represent the number of elements in the x direction, the number in the y direction and the total number of degrees of freedom used, respectively. Note

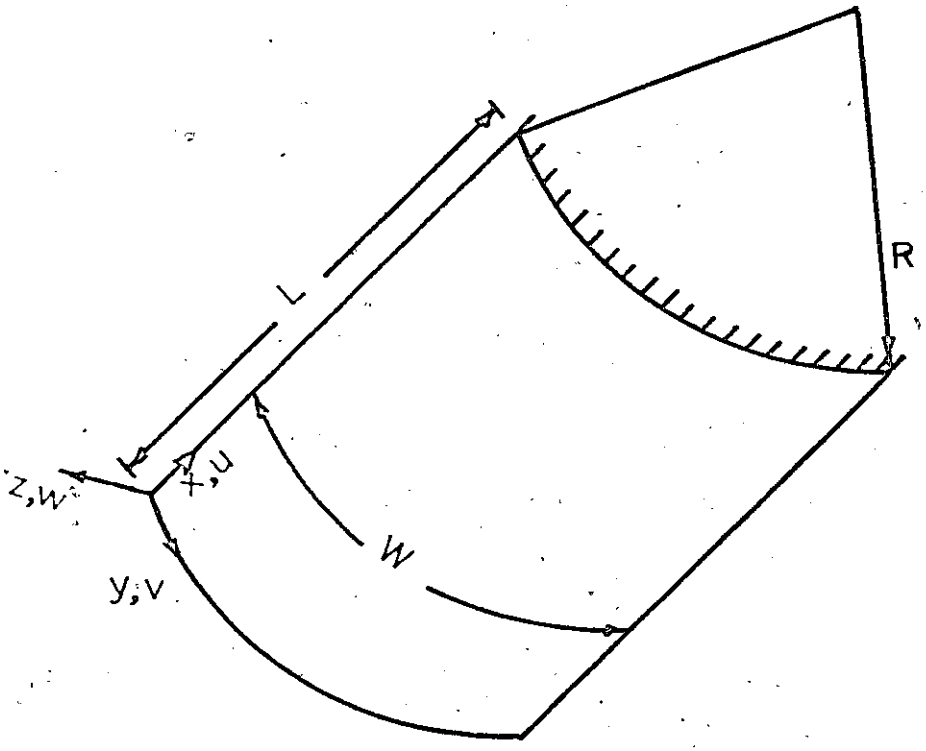

Figure 10

Curved Fan Blade

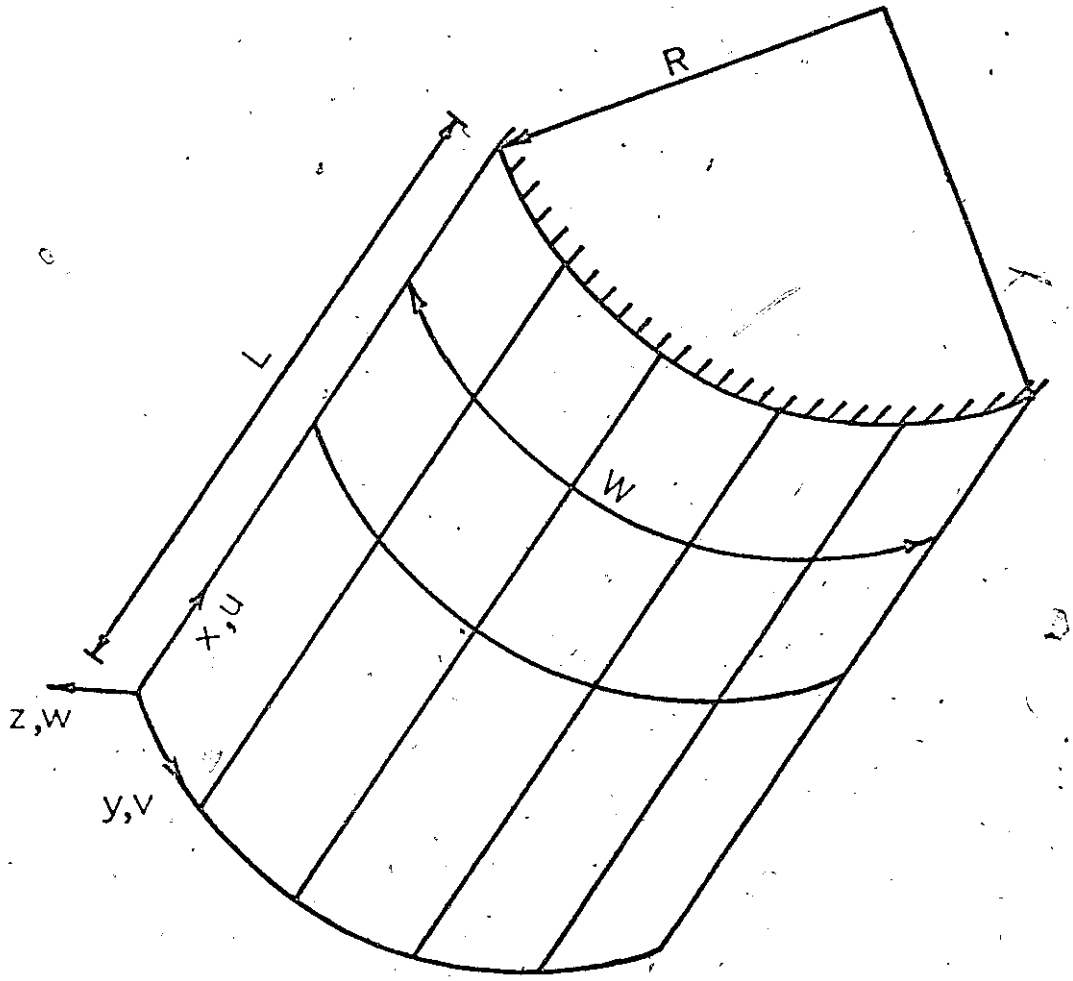

Figure 11

Curved Fan Blade divided into Finite Elements

TABLE IV

Natural Frequencies For a Curved Fan Blade

Using The 20x20 Cylindrical Shell Element

Mode Shape	Experiment [48]	3x3;60		2x5;60		2x10;60 *	
		Reference [48]	Present Analysis	Reference [48]	Present Analysis	Reference [48]	Present Analysis
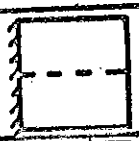	(cps) 86.6	(cps) 427	(cps) 260	(cps) 300	(cps) 205	(cps) 187	(cps) 155
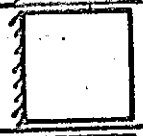	135.5	232	229	217	217	201	192
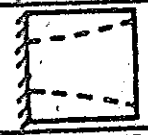	258.9	790	544	588	402	380	316
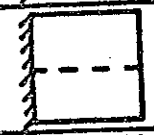	350.6	663	585	582	603	509	566
	395.2	-	-	940	664	541	611
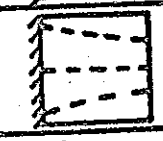	531.1	-	-	945	765	660	606

* Numbers at the top of columns 3 to 8 represent the number of elements in the x direction, the number of elements in the y direction and the total number of degrees of freedom used, respectively.

TABLE V

Natural Frequencies For A Curved Fan Blade

Using The 28x28 Cylindrical Shell Element

Mode Shape	Experiment [48]	2x2;42		3x3;84		4x4;84 *	
		Reference [48]	Present Analysis	Reference [48]	Present Analysis	Reference [48]	Present Analysis
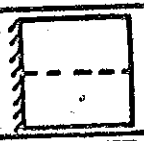	(cps) 86.6	(cps) 122.24	(cps) 109.05	(cps) 100.71	(cps) 97.66	(cps) 93.47	(cps) 92.39
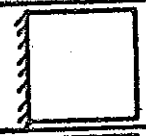	135.5	179.67	160.58	155.09	149.18	147.64	145.35
	258.9	278.71	266.92	260.94	257.53	255.14	256.07
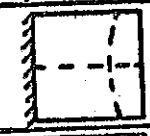	350.6	485.04	455.76	430.03	408.41	393.08	388.74
	395.2	495.80	471.16	452.90	440.09	423.50	418.85
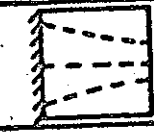	531.1	608.05	585.62	535.03	535.48	534.30	534.15

*Numbers at the top of columns 3 t 8 represent the number of elements in the x direction, the number in the y direction and the total number of degrees of freedom used, respectively.

that symmetry conditions had to be used for the 2x10 and 4x4 gridworks in order to reduce the number of degrees of freedom to a manageable size.

It may be also be noted from Table V that, in general, the frequencies converge very rapidly towards the experimental values. Furthermore, the convergence appears to be monotonic. The only possible exception may be mode number 3 , where the predicted frequency appears to undershoot the experimental value slightly. However, the difference between the two is well within the possible experimental error, so that it cannot be concluded that this is an example of nonmonotonic convergence. It should be emphasized that the present results are true only for the particular shell configuration considered herein.

It seems clear from Table IV that many more elements would have to be used before a reasonably accurate prediction of the vibratin frequencies could be obtained. On the positive side, it appears that increasing the number of elements in the circumferential direction increases the accuracy quite rapidly.

4.5 Rigid Body Modes

Another simple check of these two finite element models can be made by using them to determine the free-free vibrations of a rectangular section of a cylindrical shell. The six lowest modes for this problem are rigid body modes with zero frequency, and an approximate solution using one

finite element should include these modes.

Thus the present test for this model is to determine the eigenvalues and eigenvectors for the 28x28 matrix equation

$$(K - \lambda M)\ \vec{X} = 0 \qquad (4.16)$$

where K and M are the 28x28 matrices respectively, $\vec{X}$ is the displacement vector, and $\lambda = \rho h a^4 \omega^2 / 25200D$ is the nondimensional eigenvalue. Carrying this out for $\nu=0.3$, $a=1.0$, $b=1.0$, $R=2.0$, and $t=0.01$, yields the six lowest eigenvalues and corresponding eigenvectors presented in Table VI. The eigenvalues are tabulated in ascending order of their magnitude. The eigenvalues for the first two modes shown are exactly zero when the precision of the calculation is considered. The two associated eigevectors represent combinations of rigid body motion of the shell element in the longitudinal and circumferential directions. It may be noted that suitable linear combinations of these two eigenvectors would yield pure rigid body motion in either the longitudinal or circumferential directions alone. Hence it may be concluded that the first two rigid body modes predicted by the cylindrical shell element are pure "translations" in u and v.

The next four eigenvectors shown in Table VI are very good approximations of the following rigid body motions for the cylindrical shell element: number 3 is a translation

TABLE VI

Eigenvalues And Eigenvector Of The 28x28 Cylindrical Shell Element

(a=1 , b=1 , R=2 , t=0.01 , ν=0.3)

Eigenvalue 1	Eigenvalue 2	Eigenvalue 3	Eigenvalue 4	Eigenvalue 5	Eigenvalue 6
-6.6106E-14	4.9052E-13	2.0885E-10	2.3806E-08	1.9127E-06	2.0048E-06
Eigenvector	Eigenvector	Eigenvector	Eigenvector	Eigenvector	Eigenvector
-4.9187E-11	-4.9759E-12	4.8983E-09	1.9812E-02	-1.1907E-05	1.7939E-01
8.9663E-11	4.9729E-10	1.1472E-03	1.9400E-02	1.8221E-01	-5.3582E-03
-7.4736E-11	-8.7451E-10	4.3329E-02	-4.9515E-02	-2.1885E-01	-2.1158E-01
8.9157E-12	1.0964E-13	5.5304E-10	9.8501E-01	-4.3568E-05	-1.7509E-02
5.7944E-02	-1.5831E-02	-4.6442E-08	-9.8985E-02	1.2766E-07	4.2304E-03
2.2812E-12	5.7005E-10	-1.6283E-02	3.8799E-03	2.9416E-02	1.0763E-02
3.7370E-02	4.3728E-02	2.1666E-02	2.4741E-02	-1.0932E-03	-1.0757E-02
-4.9187E-11	-4.9759E-12	-4.8983E-09	1.9812E-02	7.9938E-05	1.7939E-01
8.9640E-11	4.9729E-10	1.1473E-03	-1.9401E-02	1.8219E-01	5.3582E-03
-7.4156E-11	-8.7293E-10	4.3329E-02	4.9524E-02	-2.1884E-01	2.1158E-01
1.0073E-12	1.1254E-13	-5.5312E-10	9.8500E-01	4.3568E-05	-1.7500E-02
5.7946E-02	-1.5835E-02	4.7121E-08	-9.8985E-02	-1.4010E-07	4.2304E-03
2.2812E-11	5.7006E-10	-1.6290E-02	-3.8799E-03	2.6392E-02	-1.0763E-02
3.7080E-02	4.3648E-02	2.1665E-02	-2.4746E-02	-1.0932E-03	1.0575E-02
-4.9184E-11	-4.9765E-12	-4.7306E-09	-1.9814E-02	-1.2614E-05	1.7939E-01
9.0021E-11	4.9773E-10	-1.0651E-03	-1.9402E-02	1.8221E-01	-5.3582E-03
7.4731E-11	8.7398E-10	4.3329E-02	-4.9514E-02	2.1885E-01	2.1158E-01
-8.9312E-12	-1.1044E-13	5.5305E-10	9.8501E-01	4.3568E-05	1.7509E-02
5.8421E-02	-1.3410E-02	3.6625E-08	9.8985E-02	1.2769E-07	4.2304E-03
-2.2800E-11	-5.7623E-10	-1.6533E-02	3.8799E-03	-2.9548E-02	-1.0763E-02
3.7367E-02	4.3701E-02	-2.1665E-02	-2.4741E-02	-1.0932E-03	-1.0575E-02
-4.9184E-11	-4.9765E-12	4.7306E-09	-1.9814E-02	7.2871E-05	1.7939E-01
9.0043E-11	4.9774E-10	-1.0653E-03	1.9400E-02	1.8219E-01	5.3582E-03
7.4146E-11	8.7264E-10	4.3329E-02	4.9524E-02	2.1884E-01	-2.1158E-01
-1.0089E-12	-1.1336E-13	-5.5314E-10	9.8500E-01	-4.3568E-05	1.7500E-02
5.8422E-02	-1.3408E-02	-3.7295E-08	9.8985E-02	-1.4006E-07	4.2304E-03
-2.2800E-11	-5.7622E-10	-1.6539E-02	-3.8799E-03	-2.6254E-02	1.0763E-02
3.7075E-02	4.3634E-02	-2.1665E-02	2.4746E-02	-1.0932E-03	1.0575E-02

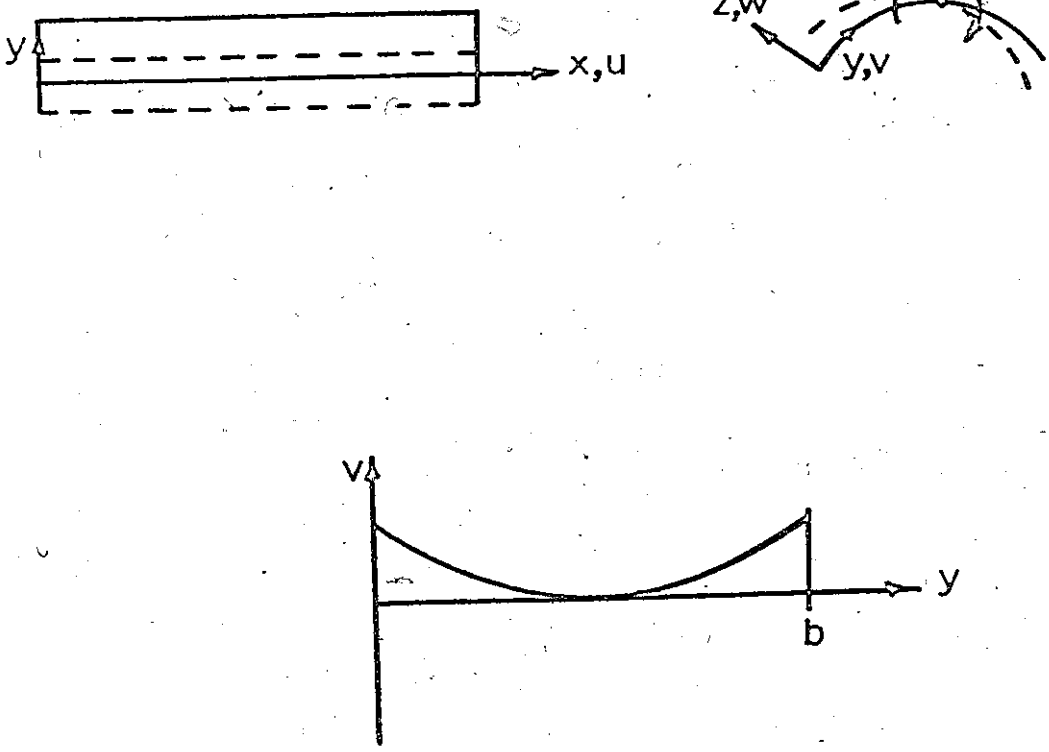

Figure 12

Rigid Body Rotation about Generator at y=b/2

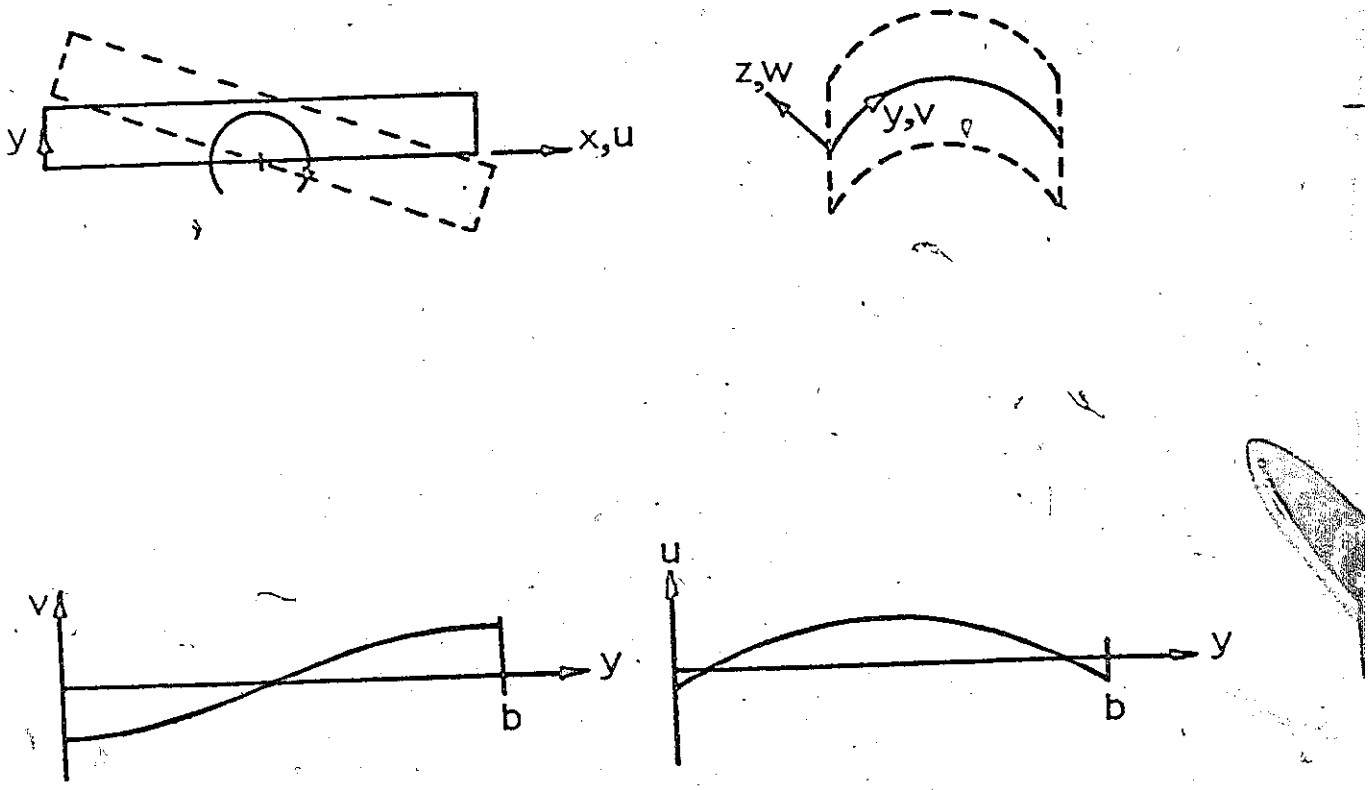

Figure 13

Rigid Body Rotation about Chord at x=a/2

parallel to a normal at x=a/2, y=b/2, number 4 is a rotation about the same normal, number 5 is a rotation about a cylindrical generator at y=b/2, (Figure(12)), and finally, number 6 is a rotation about a chord at x=a/2 (Figure(13)). It is worth noting that the ratio between eigenvalues six and seven is about 1:4000.

Hence, it may be concluded that the cylindrical shell element, having 28 degrees of freedom, provides an adequate representation of all six rigid body modes.

The same check was carried out for the 20 degrees of freedom element. The six lowest eigenvalues and corresponding eigenvectors are presented in Table VII.

The first four eigenvalues are effectively zero (the first two are exactly zero, whereas the next two are only approximately zero), and the associated eigenvectors represent rigid body modes as follows : the first three are translations in the x, y and z directions respectively, and the fourth is a pure rotation about a normal to the element at x=a/2 and y=b/2. The next two eigenvectors approximately represent rigid body rotations about an element chord at x=a/2 and a cylindrical generator at y=b/2, respectively. However, the eigenvalues associated with these latter eigenvectors are not even approximetely zero.

The fact that these eigenvalues are not zero may be attributed to the rather simple assumed distributions for the in-plane displacements. It may be observed that these last

TABLE VII

Eigenvalues And Eigenvectors Of The 20x20 Cylindrical Shell Element

(a=1 , b=1 , R=1 , t=0.01 , ν=0.3)

Eigenvalue 1	Eigenvalue 2	Eigenvalue 3	Eigenvalue 4	Eigenvalue 5	Eigenvalue 6
1.0129E-13	2.7301E-13	3.6060E-05	3.2653E-04	1.1757E+00	3.0456E+00
Eigenvector	Eigenvector	Eigenvector	Eigenvector	Eigenvector	Eigenvector
1.5441E-12	-7.0104E-12	-3.9634E-04	9.1338E-03	4.4653E-01	1.5689E-02
5.2024E-12	-1.3169E-11	-1.3222E-03	1.1313E-02	-1.2215E-01	-4.9511E-01
1.4471E-09	-2.3977E-09	-4.4759E-01	-1.8655E-03	-1.7547E-01	6.7854E-02
6.3996E-02	-4.9858E-01	-2.5392E-06	-3.5514E-01	1.6051E-14	2.8498E-03
4.9588E-01	-3.7559E-02	-2.2283E-01	3.5165E-01	-6.9971E-02	-6.2301E-14
-1.5528E-12	-2.7819E-12	3.9634E-04	9.1338E-03	4.4653E-01	-1.5689E-02
3.3346E-12	-9.0314E-13	-1.3222E-03	-1.1314E-02	1.2215E-01	-4.9511E-01
1.4471E-09	-2.3996E-09	-4.4759E-01	1.8655E-03	1.7547E-01	6.7854E-02
6.3996E-02	-4.9858E-01	2.5424E-06	-3.5514E-01	3.8174E-15	-2.8498E-03
4.9588E-01	-3.7559E-02	-2.2283E-01	-3.5165E-01	6.9971E-02	3.4752E-14
-1.7519E-12	7.0410E-12	3.9634E-04	-9.1338E-03	4.4653E-01	1.5689E-02
-4.5234E-12	1.3208E-11	1.3222E-03	-1.1313E-02	-1.2215E-01	-4.9511E-01
1.4469E-09	-2.3976E-09	-4.4759E-01	-1.8655E-03	1.7547E-01	-6.7854E-02
6.3996E-02	-4.9858E-01	2.5420E-06	3.5513E-01	-2.6192E-15	2.8498E-03
4.9588E-01	-3.7559E-02	2.2283E-01	-3.5165E-01	-6.9971E-02	-2.6983E-14
4.8369E-13	2.7034E-12	-3.9634E-04	-9.1338E-03	4.4653E-01	-1.5689E-02
-3.9889E-12	9.4947E-13	1.3222E-03	1.1313E-02	1.2215E-01	-4.9511E-01
1.4473E-09	-2.3996E-09	-4.4759E-01	1.8655E-03	-1.7547E-01	-6.7854E-02
6.3996E-02	-4.9858E-01	-2.5395E-06	3.5513E-01	-1.3788E-14	-2.8498E-03
4.9588E-01	-3.7559E-02	2.2283E-01	3.5165E-01	6.9971E-02	4.4822E-14

two rigid body rotations give rise to in-plane displacements that are of higher order than linear in the y direction. These distributions are sketched in Figures (12) and (13). Hence, it appears that, in order to obtain reasonable approximations for all the possible rigid body modes for the element, it will be necessary to include higher order terms in y for the assumed distributions of in-plane displacements u and v .

4.6 Concluding Remarks

The development of two modified, relatively simple finite cylindrical shell elements has been presented. The first element has 20 degrees of freedom corresponding to the corner displacements $\partial w/\partial x$, $\partial w/\partial y$, w, u and v, whereas the second has 28 corresponding to $\partial w/\partial x$, $\partial w/\partial y$, w, $\partial u/\partial y$, u, $\partial v/\partial y$ and v. The eigenvalues determined using the elements stiffness and mass matrices indicated that the first model contained an adequate representation of only four rigid body modes, whereas the second contained all the six.

The elements were used to predict vibration modes and frequencies for a curved, cantilevered fan blade. It was found that use of the 20 degrees of freedom element resulted in very slow convergence of the frequency predictions as the modelling was refined. On the other hand, use of the 28 degrees of freedom element resulted in quite rapid convergence.

It was found that a 4x4 grid of these latter elements predicted the first 6 vibration frequencies for the fan blade to within 10 percent. It may be concluded from this that an efficient finite element model must be capable of representing all the rigid body modes for the element.

It appears that, the present analysis gives more accurate predictions of experimental behaviour than those predictions obtained by Olson and Lindberg for both elements.

These finite elements should prove extremely useful for static and dynamic problems involving rectangular portions of cylindrical shells, especially since such configurations are very difficult to analyze by ordinary analytical techniques.

It must be noted that the 28 degrees of freedom element requires about double the storage required by the 20 degrees of freedom element.

CHAPTER 5

APPLICATIONS OF THE TRANSFER MATRIX-FINITE ELEMENT TECHNIQUE

5.1 Introduction

It is known that for satisfactory accuracy with the finite element technique, it is necessary to have a large number of nodes, resulting in very large stiffness and mass matrices. The memory of the available computer and the solution time required, therefore, become the restricting factors on the total number of nodes and degrees of freedom that can be used.

Recently, a method has been developed by Dokainish [33], to overcome the memory restriction. In this method the stiffness and the inertia matrices of individual elements are determined exactly in the same manner as in the finite element displacement type of analysis. However, the method of computation of natural frequencies is different and does not require the assembly of matrices for the entire structure. The method permits the use of large numbers of nodes and degrees of freedom, without getting involved with large matrices. A much smaller computer is, therefore, sufficient. This method is an extension of the transfer matrix method, extensively applied to beams, to system of plates and shells.

5.2 Theoretical Considerations

Figure (14) shows the plate or the shell structure divided into m strips and each strip subdivided into finite elements. Triangular elements are illustrated in the figure, although other types of elements may be used. The common lines between the adjacent strips are called the edges. Thus the edge AD is the left side of strip i and the right side of the strip $i-1$. There are a total of $2n$ nodes on strip i with n nodes on the left edge AD and n nodes on the right edge BE. The vector of nodal displacements at node p is denoted by $\{\delta_p\}$ and the corresponding vector of nodal forces is denoted by $\{F_p\}$.

A suitable function is chosen to represent the displacement distribution within the element in terms of its nodal displacements. The stiffness and mass matrices for each element are obtained using the finite element method. The stiffness and the mass matrices of all the elements on strip i are assembled to get the complete matrices for this strip. If the boundary conditions of the top edge AB and the bottom edge DE require certain displacements of nodes $n, 2n, 1$, and $n+1$ to be zero, the rows and the columns of the stiffness and the mass matrices, corresponding to such displacements are deleted. This yields the final reduced stiffness matrix $[K]_i$ and mass matrix $[M]_i$ for the strip i. This procedure is repeated for all other strips.

If ω is the natural frequency of free vibrations,

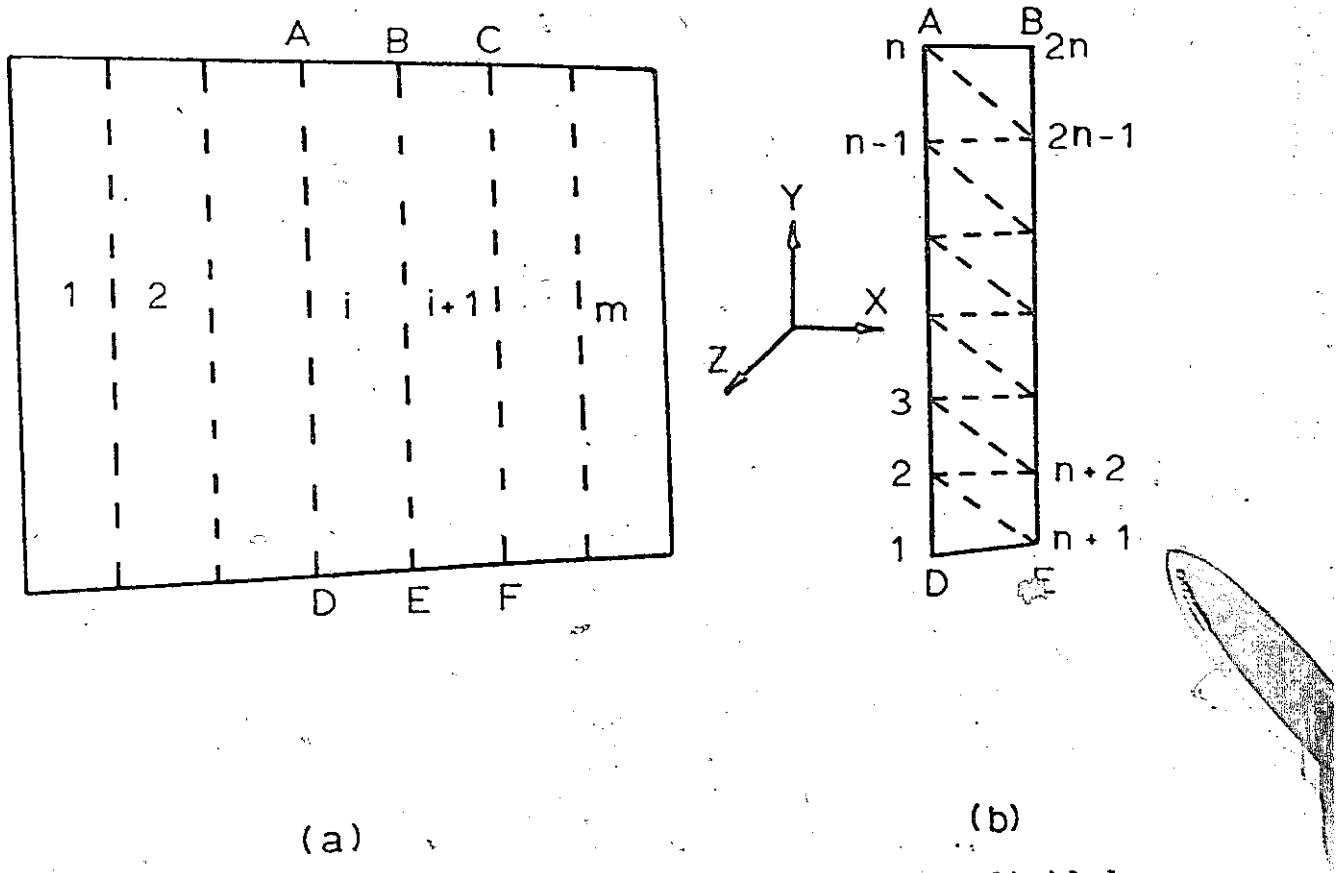

(a)

Structure divided into m Sections

(b)

Section divided into Finite Elements

Figure 14

Subdivision of Structure into sections and Finite Elements

the equilibrium equations for the nodes on strip i can be written as

$$[K]_i \begin{Bmatrix} \delta_L \\ --- \\ \delta_R \end{Bmatrix}_i - \omega^2 [M]_i \begin{Bmatrix} \delta_L \\ --- \\ \delta_R \end{Bmatrix}_i = \begin{Bmatrix} F_L \\ --- \\ F_R \end{Bmatrix}_i \qquad (5.1)$$

where $\{\delta_L\}_i$ is the displacement vector for the nodes on the left edge of strip i. This can be expressed explicitly in the form

$$\{\delta_L\}_i = \begin{Bmatrix} \text{Nonzero elements of } \delta_1 \text{ on DE} \\ \delta_2 \\ \delta_3 \\ \vdots \\ \delta_{n-1} \\ \text{Nonzero elements of } \delta_n \text{ on AB} \end{Bmatrix} \qquad (5.2)$$

where $\{F_L\}_i$ is the force vector corresponding to the displacements $\{\delta_L\}_i$. Similarly $\{\delta_R\}_i$ and $\{F_R\}_i$ are the vectors for the right edge. Obviously, $\{\delta_L\}_i$ and $\{\delta_R\}_i$ would contain an equal number of elements.

Equation (5.1) can be written as

$$[S]_i \begin{Bmatrix} \delta_L \\ --- \\ \delta_R \end{Bmatrix}_i = \begin{Bmatrix} F_L \\ --- \\ F_R \end{Bmatrix}_i \qquad (5.3)$$

where

$$[S]_i = [K]_i - \omega^2 [M]_i \qquad (5.4)$$

Matrix $[S]_i$ may be partitioned into four square matrices and equation (5.3) rewritten as

$$\left[\begin{array}{c|c} S_{11} & S12 \\ \hline S21 & S22 \end{array}\right]_i \begin{Bmatrix} \delta_L \\ --- \\ \delta_R \end{Bmatrix}_i = \begin{Bmatrix} F_L \\ --- \\ F_R \end{Bmatrix}_i \qquad (5.5)$$

With little algebraic manipulation, equation (5.5) can be rearranged to the form

$$\begin{Bmatrix} \delta_R \\ --- \\ -F_R \end{Bmatrix}_i = \left[\begin{array}{c|c} T_{11} & T_{12} \\ \hline T_{21} & T_{22} \end{array}\right]_i \begin{Bmatrix} \delta_L \\ --- \\ F_L \end{Bmatrix}_i = [T]_i \begin{Bmatrix} \delta_L \\ --- \\ F_L \end{Bmatrix}_i \qquad (5.6)$$

where

$$[T_{11}]_i = - [S_{12}^{-1}]_i [S_{11}]_i$$

$$
\begin{aligned}
[T_{12}]_i &= [S_{12}^{-1}]_i \\
[T_{21}]_i &= -[S_{21}]_i + [S_{22}]_i\ [S_{12}^{-1}]_i\ [S_{11}]_i \\
[T_{22}]_i &= [S_{22}]_i\ [S_{12}^{-1}]_i
\end{aligned}
\tag{5.7}
$$

5.3 Transfer Matrix Relation for Entire Structure

Since the nodes on the right edge of strip i are the same as the nodes on the left edge of strip $i+1$, the following identity exists

$$\{\delta_R\}_i = \{\delta_L\}_{i+1} \tag{5.8}$$

It may be mentioned that the zero components of displacements of nodes B and E, if any, are already deleted from $\{\delta_R\}_i$ and $\{\delta_L\}_{i+1}$. Equation (5.8), therefore, necessitates that the boundary conditions on AB and BC be the same; and similarly the boundary conditions on DE and EF be the same, in order that $\{\delta_R\}_i$ and $\{\delta_L\}_{i+1}$ have the same number of terms. Also, equilibrium of nodal forces on edge BE gives the relationship

$$\{F_R\}_i + \{F_L\}_{i+1} = \{F_{ext}\}_{BE} \tag{5.9}$$

where $\{F_{ext}\}_{BE}$ are the external forces acting at the nodes on edge BE. Since the problem of free vibrations is being considered, the external forces consist of the reactions at

the supported nodes only. When boundary conditions specify a certain nodal displacement to be zero, a reaction would be present in the direction of that displacement. However, the row and the column of the stiffness matrix and the mass matrix, corresponding to such a displacement and reaction, has already been deleted (since the corresponding nodal force has no influence on the deformation) . Thus, such nodal forces are not present in the force vectors $\{F_L\}_{i+1}$ and $\{F_R\}_i$. Equation (5.9) can, therefore, be written as

$$-\{F_R\}_i = \{F_L\}_{i+1} \qquad (5.10)$$

Equations (5.8) and (5.10) may be combined to give the following relationship

$$\begin{Bmatrix} \delta_R \\ -- \\ -F_R \end{Bmatrix}_i = \begin{Bmatrix} \delta_L \\ -- \\ F_L \end{Bmatrix}_{i+1} \qquad (5.11)$$

Substiution of equation (5.11) in equation (5.6) gives

$$\begin{Bmatrix} \delta_L \\ -- \\ F_L \end{Bmatrix}_{i+1} = [T]_i \begin{Bmatrix} \delta_L \\ -- \\ F_L \end{Bmatrix}_i \qquad (5.12)$$

Similarly the following relationship can be written

$$\begin{Bmatrix} \delta_L \\ --- \\ F_L \end{Bmatrix}_i = [T]_{i-1} \begin{Bmatrix} \delta_L \\ --- \\ F_L \end{Bmatrix}_{i-1} \qquad (5.13)$$

Elimination of $\begin{Bmatrix} \delta_L \\ \delta_F \end{Bmatrix}_i$ from equations (5.12) and (5.13) gives

$$\begin{Bmatrix} \delta_L \\ --- \\ F_L \end{Bmatrix}_{i+1} = [T]_i \, [T]_{i-1} \begin{Bmatrix} \delta_L \\ --- \\ F_L \end{Bmatrix}_{i-1} \qquad (5.14)$$

Proceeding in the same manner over all the m strips, the following relationship is obtained :

$$\begin{Bmatrix} \delta_L \\ --- \\ F_L \end{Bmatrix}_m = [T]_{m-1} \, [T]_{m-2} \cdots\cdots [T]_1 \begin{Bmatrix} \delta_L \\ --- \\ F_L \end{Bmatrix}_1 \qquad (5.15)$$

Multiplying both sides of equation (5.15) by $[T]_m$, and using the relationship given by equation (5.6) yields

$$\begin{Bmatrix} \delta_R \\ --- \\ -F_R \end{Bmatrix}_m = [P] \begin{Bmatrix} \delta_L \\ --- \\ F_L \end{Bmatrix}_1 \qquad (5.16)$$

where

$$[P] = [T]_m \, [T]_{m-1} \cdots\cdots [T]_1 \qquad (5.17)$$

Equation (5.16) relates the edge variables of the left boundary of the structure to the edge variables of the right boundary of the structure.

5.4 Determination of Natural Frequencies

The boundary conditions of the left edge of the structure would require some components of $\begin{Bmatrix} \delta_L \\ F_L \end{Bmatrix}_1$ to be zero. Similarly the boundary conditions on the right edge of the structure would require some components of $\begin{Bmatrix} \delta_R \\ -F_R \end{Bmatrix}_m$ to be zero.

When these conditions are incorporated, it is necessary that the determinant of a portion $[Q]$ of the matrix $[P]$ be zero at the correct natural frequency for a non-trivial solution. For example, if the left edge of the structure is clamped and the right edge of the structure is free, then

$$\{\delta_L\}_1 = \{F_R\}_m = \{0\} \tag{5.18}$$

Substitution of these boundary conditions and partitioning of matrix $[P]$ of equation (5.16) into four square matrices, gives the relationship

$$\begin{Bmatrix} \delta_R \\ \hline 0 \end{Bmatrix}_m = \left[\begin{array}{c|c} P_{11} & P_{12} \\ \hline P_{21} & P_{22} \end{array}\right] \begin{Bmatrix} 0 \\ \hline F_L \end{Bmatrix}_1 \tag{5.19}$$

This can be split into the following two equations

$$\{\delta_R\}_m = [P_{12}] \{F_L\}_1 \qquad (5.20)$$

$$\{0\} = [P_{22}] \{F_L\}_1 \qquad (5.21)$$

For a non-trivial solution of equation (5.21), it is essential that the determinant of matrix $[P_{22}]$ be zero at the correct natural frequency. The matrix $[Q]$ is, therefore, the matrix $[P_{22}]$ in this particular case.

In general, the matrix $[Q]$ is obtained from matrix $[P]$ by deleting the columns corresponding to zero elements of $\begin{Bmatrix} \delta_L \\ F_L \end{Bmatrix}_1$ and deleting the rows corresponding to the non-zero elements of $\begin{Bmatrix} \delta_R \\ -F_R \end{Bmatrix}_m$.

The method of determining the natural frequencies consists of the following steps [33] :

1. The stiffness and the mass matrices of all the strips are calculated using the finite element method. The boundary conditions of the top and bottom edges are incorporated.

2. A numerical value is assumed for the natural frequency ω.

3. Matrices $[S]_i$ and hence the matrices $[T]_i$ are obtained, using equations (5.4) to (5.7).

4. Matrix $[P]$ is determined using equation (5.17).

5. By substituting the boundary conditions of the left and the right boundaries of the structure in equation

(5.16) and deleting the appropriate columns and rows, matrix [Q] is obtained.

6. The determinant of matrix [Q] is calculated.

7. Steps 2 to 6 are repeated for different values of ω.

8. The determinants of [Q] are plotted as ordinate with the corresponding values of ω as abscissa. The points of intersection with ω axis (zero value of the determinant) are the natural frequencies of the structure.

5.5 Determination of Mode Shapes

To illustrate the procedure for determining the mode shape corresponding to a particular natural frequency, let us consider, once again, the particular case in which the left edge of the structure is clamped and the right edge is free. For this case, equation (5.16) is equivalent to equations (5.20) and (5.21). Matrix $[P_{22}]$ is obtained for the particular natural frequency for which the mode shape is required. Since equation (5.21) cannot give absolute values for $\{F_L\}_1$, but only the relative ratios of its components, we assume that the first component of $\{F_L\}_1$ is unity. Incoporation of this condition in equation (5.21) gives the relationship

$$\{R\} = [Q_1] \{F_L\}_1 \qquad (5.22)$$

Here $\{R\}$ is a column vector with the first element unity and all the other elements equal to zero. The matrix $[Q_1]$ is obtained from matrix $[P_{22}]$, by replacing the elements of the first row by zeros; with the exception of the first element, which is replaced by unity.

Solution of equation (5.22) yields the value of $\{F_L\}_1$. Substitution of zeros for the displacements $\{\delta_L\}_1$ of the clamped left edge, gives the vector of edge variables $\begin{Bmatrix}\delta_L \\ F_L\end{Bmatrix}_1$. Successive applications of transfer matrix equation (5.12) gives the edge variables of all the edges and hence the mode shape.

5.6 Numerical Examples

5.6.1 Rectangular Plates

Natural frequencies, using the present method, are calculated for two rectangular plates with two different boundary conditions, Figure (15). The first plate is a cantilever plate and the second has all its edges simply supported. The strips of the plates are subdivided into triangular elements as shown in Figure (15). The local cartesian co-ordinate axes x', y', z' for each triangular element are so chosen that the z-axis is normal to the plate surface and the y-axis is along the hypotenuse of the triangle, as shown in Figure (16). Within each element, the deflection w along the z-axis is assumed in the form

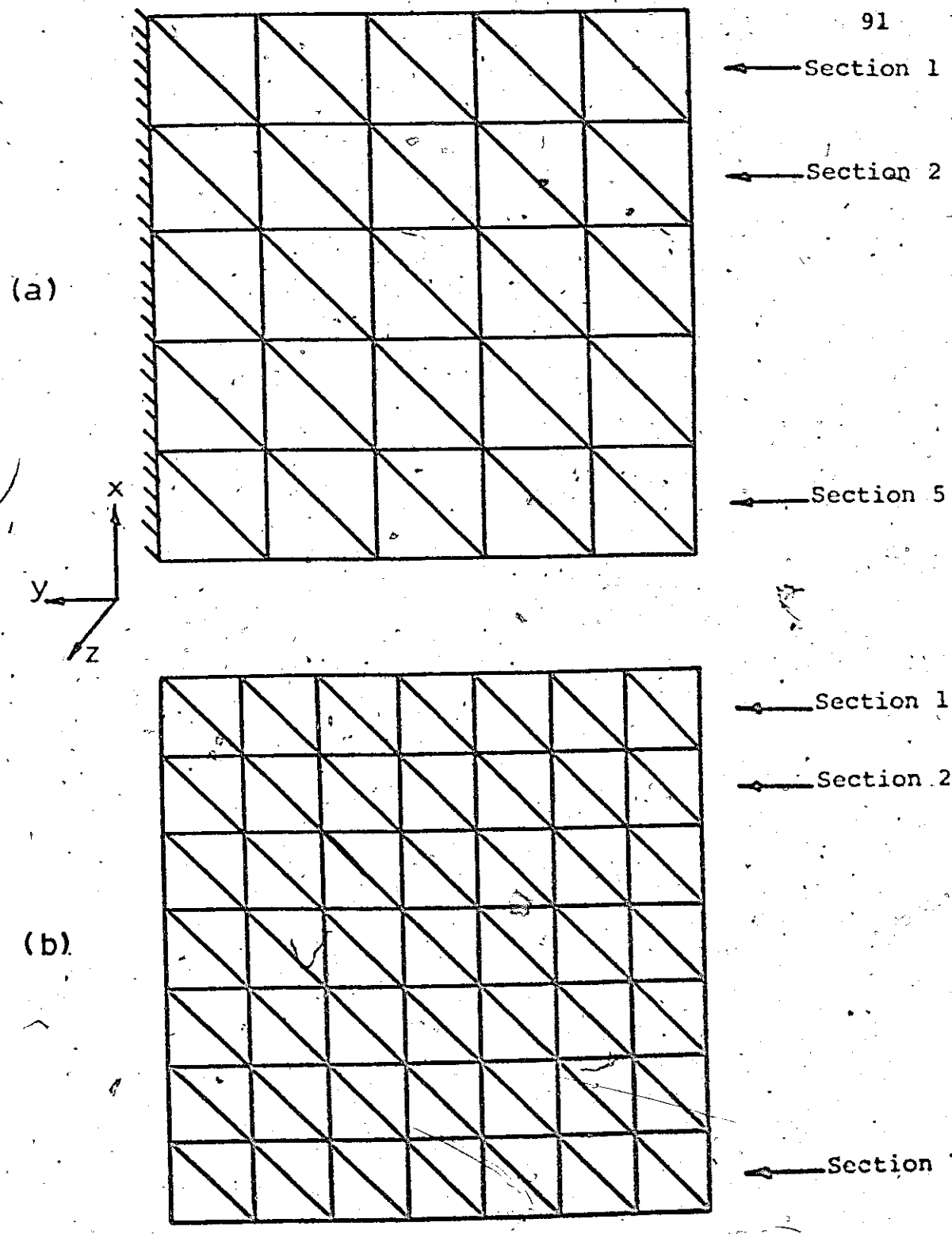

Figure 15

Subdivision of Square Plate into Sections and Finite Elements
(a) Cantilever Plate
(b) Simply Supported Plate

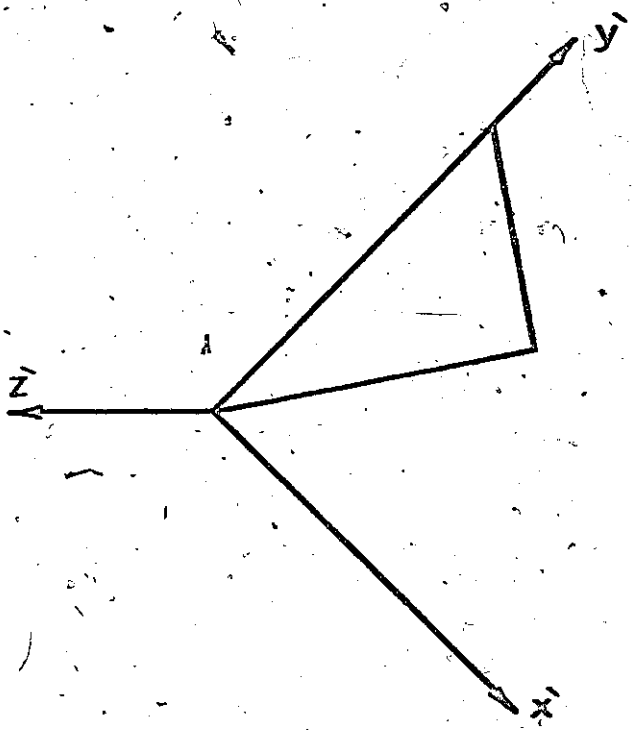

Figure 16

Local Coordinate Axes for a Triangular Element

$$w'(x',y') = \alpha_1 + \alpha_2 x' + \alpha_3 y' + \alpha_4 x'^2 + \alpha_5 x'y' + \alpha_6 y'^2 + \alpha_7 x'^3 + \alpha_8 x'^2 y' + \alpha_9 y'^3 \quad (5.23)$$

This expression for w' along with the system of local co-ordinate axes selected is partially conforming. In addition to displacement continuity along all the edges between the adjacent elements, it also satisfies transverse slope continuity along the hypotenuse of the triangle. The regular finite element analysis with this expression is known [49,50] to give a good rate of convergence for static as well as dynamic problems. However, any other assumption for deflection may be used if so desired.

The stiffness and the mass matrices of individual elements are obtained using the regular displacement type finite element approach. These matrices are transformed to common global axes x,y,z. The assembly of element matrices is carried out for all the elements on one strip, to give the total stiffness and mass matrices for each strip.

In examples (a),(b) and (5.6.3), the frequency is expressed as a nondimensional quantity given by

$$\Omega = \omega L^2 \sqrt{\rho t/D} \quad (5.24)$$

where L is the length, t is the thickness, and ρ is the mass per unit volume of the plate. D is the flexral rigidity

of the plate given by

$$D = Et^3/\ 12(1 - \nu^2) \qquad (5.25)$$

E and ν are Young's modulus and Poisson's ratio, respectively.

(a) Square Cantilever Plate

The plate is divided lengthwise into 5 strips and each strip is subdivided into 10 elements. Since the top edge of each strip is clamped, the displacements of nodes 6 and 12 are zero. The rows and the columns corresponding to these displacements are deleted from the assembled stiffness and mass matrices for each strip.

Since the left and the right edges of the plate are free, equation (5.16) can be written in partitioned form as

$$\left[\begin{array}{c|c} P_{11} & P_{12} \\ \hline P_{21} & P_{22} \end{array}\right] \left\{\begin{array}{c} \delta_L \\ \hline 0 \end{array}\right\}_1 = \left\{\begin{array}{c} \delta_R \\ \hline 0 \end{array}\right\}_5 \qquad (5.26)$$

yielding

$$[P_{11}]\ \{\delta_L\}_1 = \{\delta_R\}_5 \qquad (5.27)$$

$$[P_{21}]\ \{\delta_L\}_1 = \{0\} \qquad (5.28)$$

For a nontrivial solution, the determinant of matrix $[P_{21}]$ must vanish at the correct frequency. The matrix [Q] is,

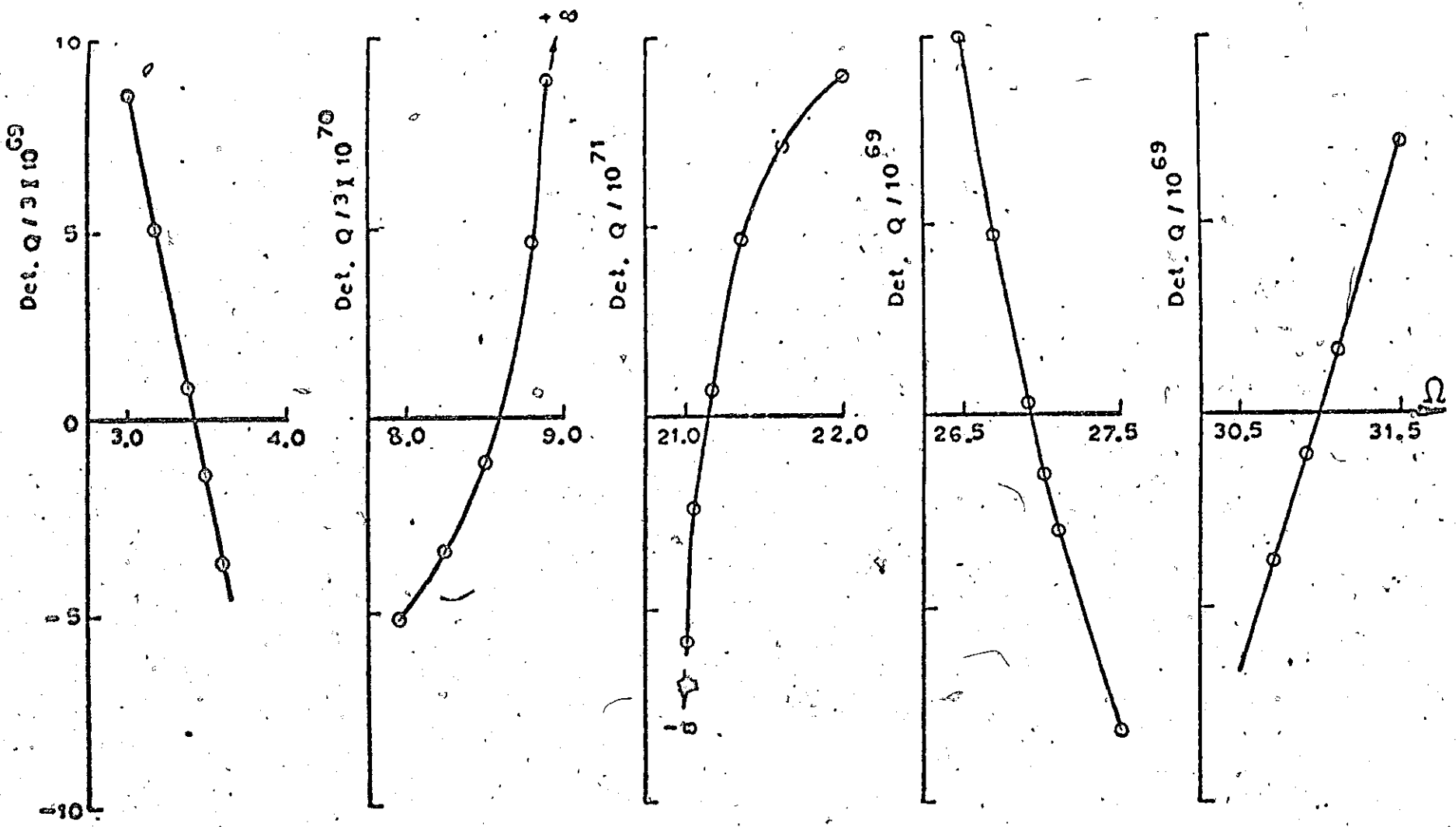

Figure 17

Variation of Determinant of Matrix Q with Frequency for a Square Cantilever Plate

TABLE VIII

Nondimensional Natural Frequencies (Ω) For a Square Cantilever Plate

Vibration Mode	Calculated Value	Ritz Method Value [51]	% Difference
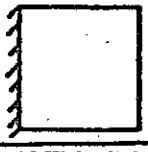	3.44	3.49	1.43
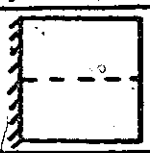	8.55	8.55	0.00
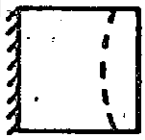	21.18	21.44	1.21
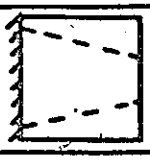	26.93	27.46	1.93
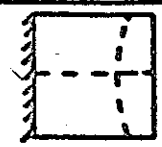	30.98	31.17	0.61

therefore, the matrix $[P_{21}]$ in this case.

The variation of this determinant with frequency is plotted in Figure (17). The curve of the determinant vs. frequency is observed to have a discontinuity at a value of Ω in the vicinity of 16 . The value of the determinant at this point changes from $+\infty$ to $-\infty$. The reason for this is that at this value of frequency the matrix $[S_{12}]$ of equation (5.5) has a determinant equal to zero. The inverse of this matrix and hence the transfer matrices [T] and [P] do not exist at this frequency.

The values of the natural frequencies, for the first five modes of vibration as obtained from the present analysis, are given in Table VIII. The Ritz method values given by Young [51] are also included for comparison. The present values are observed to be lower than the Ritz method values, the maximum difference being 1.93%.

Each strip has a total of 30 degrees of freedom. The natural frequencies are obtained from the determinant of a 15 × 15 matrix [Q]. Conventional finite element technique for the same subdivision would require the determination of eigenvalues of a 90 × 90 matrix.

(b) Square Simply Supported Plate

The plate is divided lengthwise into 7 strips and each strip is subdivided into 14 elements. The top and the bottom edges of the plate are taken to be parallel to the

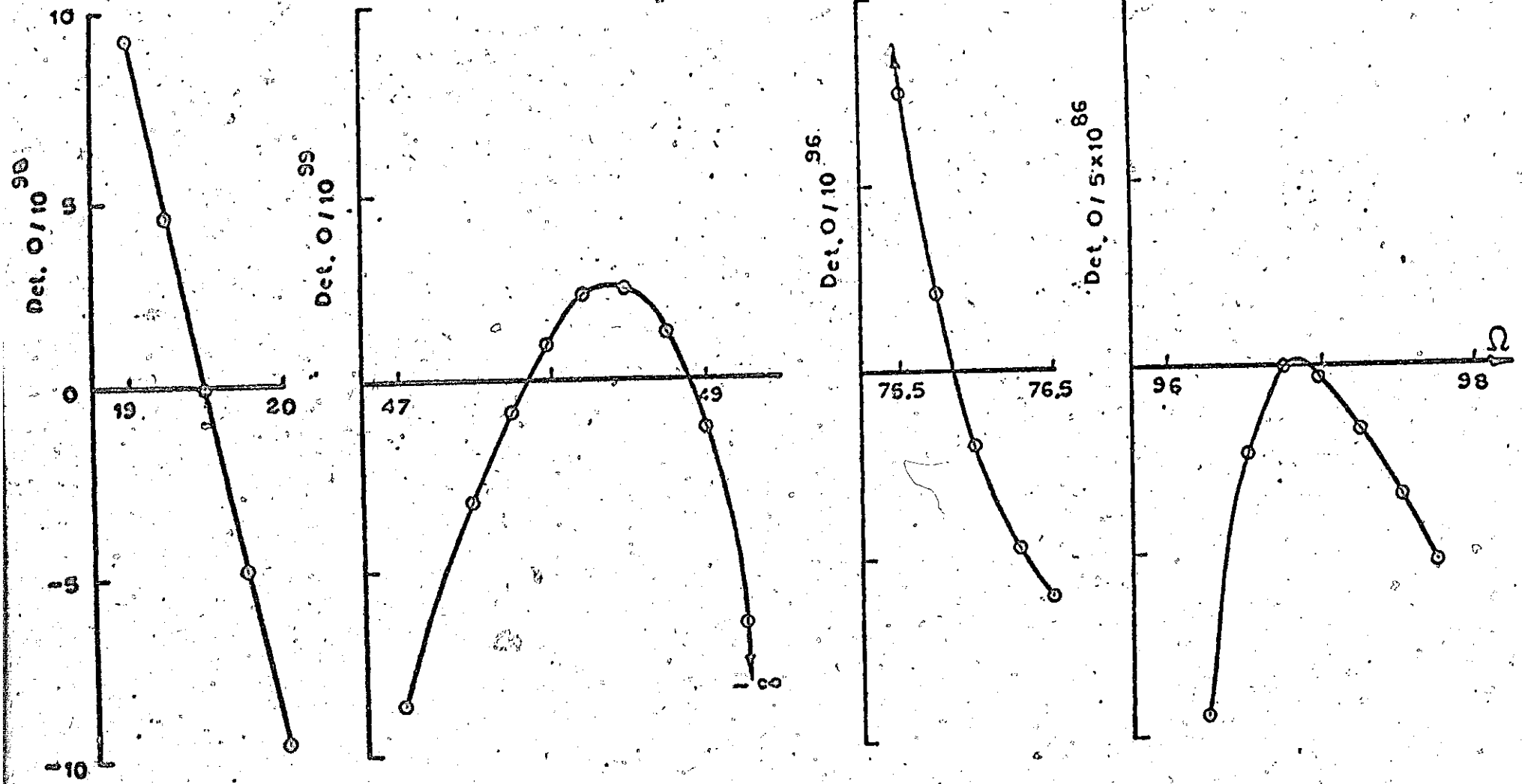

Figure 18

Variation of Determinant of Matrix Q with Frequency for a Square Simply Supported Plate

TABLE IX

Nondimensional Natural Frequencies (Ω) For a Square Simply Supported Plate

Vibration Mode	Calculated Value	Exact Value [52]	% Difference
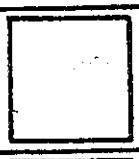	19.49	19.74	1.29
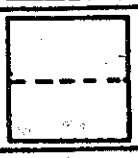	47.85	49.35	3.06
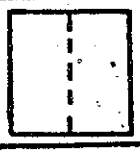	48.90	49.35	0.93
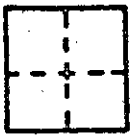	75.88	78.96	3.92
	96.78	98.70	1.96
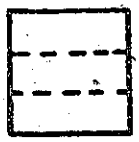	96.90	98.70	1.84

global x axis. Since the top and the bottom edges are simply supported, the value of w and $\theta_y = -\partial w/\partial x$ are zero for nodes 1,8,9 and 16 of each strip. The rows and the columns of the stiffness and mass matrices, corresponding to these displacements, are deleted for each strip. The overall transfer matrix [P] is then determined, giving the relationship

$$[P] \begin{Bmatrix} \delta_L \\ --- \\ F_L \end{Bmatrix}_1 = \begin{Bmatrix} \delta_R \\ --- \\ -F_R \end{Bmatrix}_7 \qquad (5.29)$$

The left edge of the plate is simply supported. For the nodes on this edge, therefore, the boundary conditions are $w = 0$, $\theta_x = \partial w/\partial y = 0$ and $M_y = 0$. The columns of matrix [P], corresponding to these zero elements of $\begin{Bmatrix} \delta_L \\ F_L \end{Bmatrix}_1$, are deleted. The right edge of the plate is also simply supported. For the nodes on this edge we have $w = \theta_x = M_y = 0$ as well. The rows of the matrix [P] cprresponding to the non-zero elements of $\begin{Bmatrix} \delta_R \\ -F_R \end{Bmatrix}_7$ are deleted to give the matrix [Q]. At the correct frequency the determinant of matrix [Q] must be zero for the existence of non-zero elements of $\begin{Bmatrix} \delta_L \\ F_L \end{Bmatrix}_1$.

The variation of this determinant with frequency is plotted in Figure (18). The curve is observed to have a discontinuity at Ω approximately equal to 60. This also

corresponds to the frequency where the matrix $[S_{12}]$ becomes singular and hence the transfer matrices do not exist.

The values of the natural frequencies, for the first six modes of vibration as obtained from the present analysis are given in Table IX.The exact theory [52] is available for this plate. These exact frequencies are also given in the Table for comparison. The maximum error in the natural frequencies is observed to be 3.92%.

5.6.2 Annular Cantilever Plates

Natural frequencies, using the present method, are calculated for annular plates clamped at the inner edge and free at the outer edge. The annular plate may be divided into strips in two different ways, in the radial or tangential direction, as shown in Figure (19). It is advantageous in both cases to cosider only one quarter of the plate, with the appropriate boundary conditions, to reduce the number or size of strips, and hence the computing time. Each strip is subdivided into finte elements as shown in Figure (19). The finite element used in this analysis is the annular sector finite element developed in reference [39].

In this example, one quarter of the plate is considered, and is divided into 3 strips, and each strip is subdivided into 3 finite elements, as shown in Figure (19-b).

Since the inner edge is clamped and the outer edge is free, equation (5.16) can be rewritten as

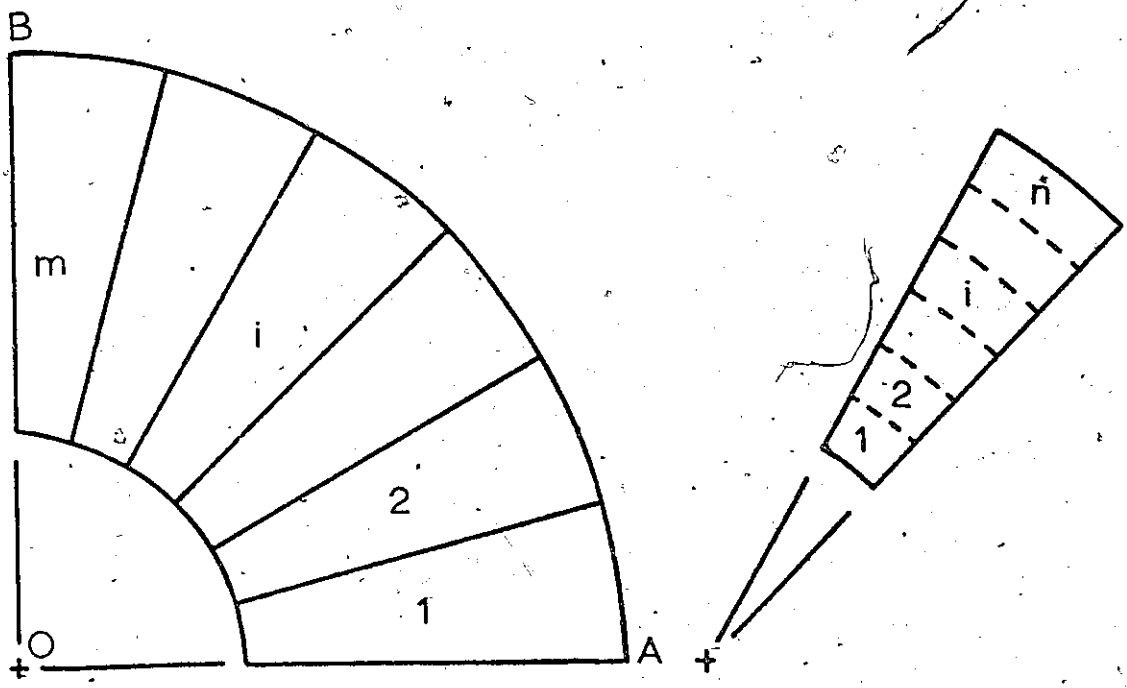

(a)

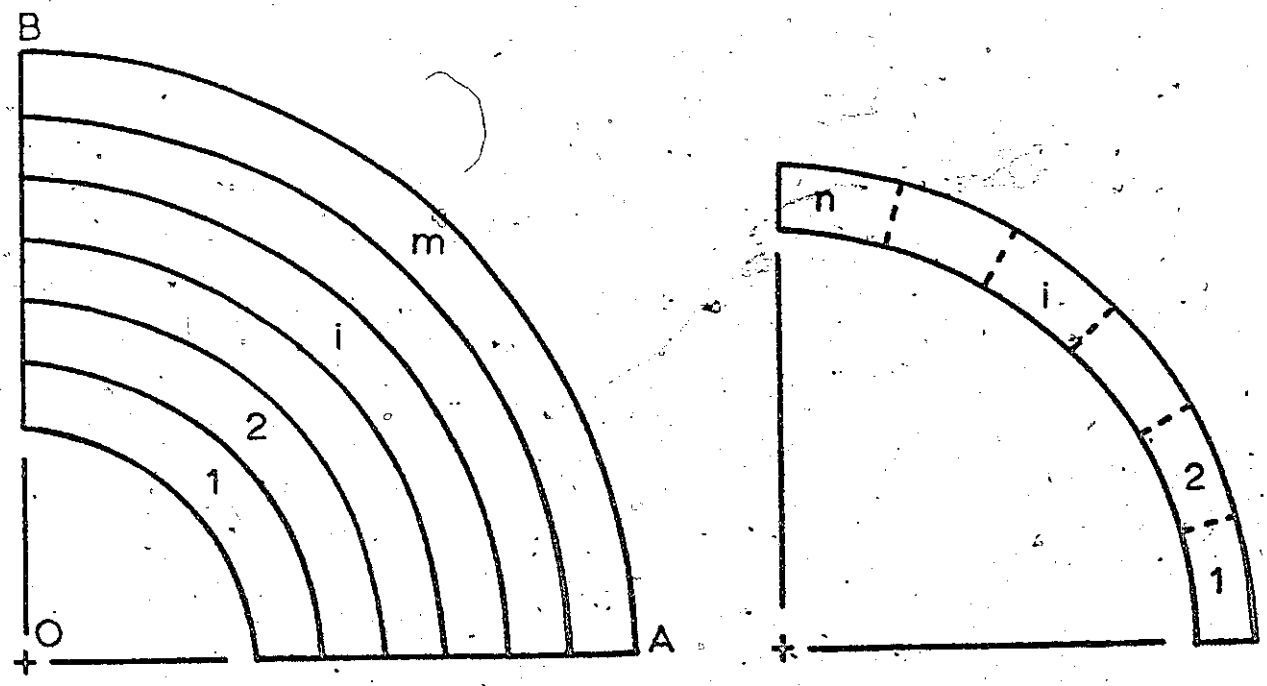

(b)

Figure 19

Subdivision of Annular Plate into Sections and Finite Elements

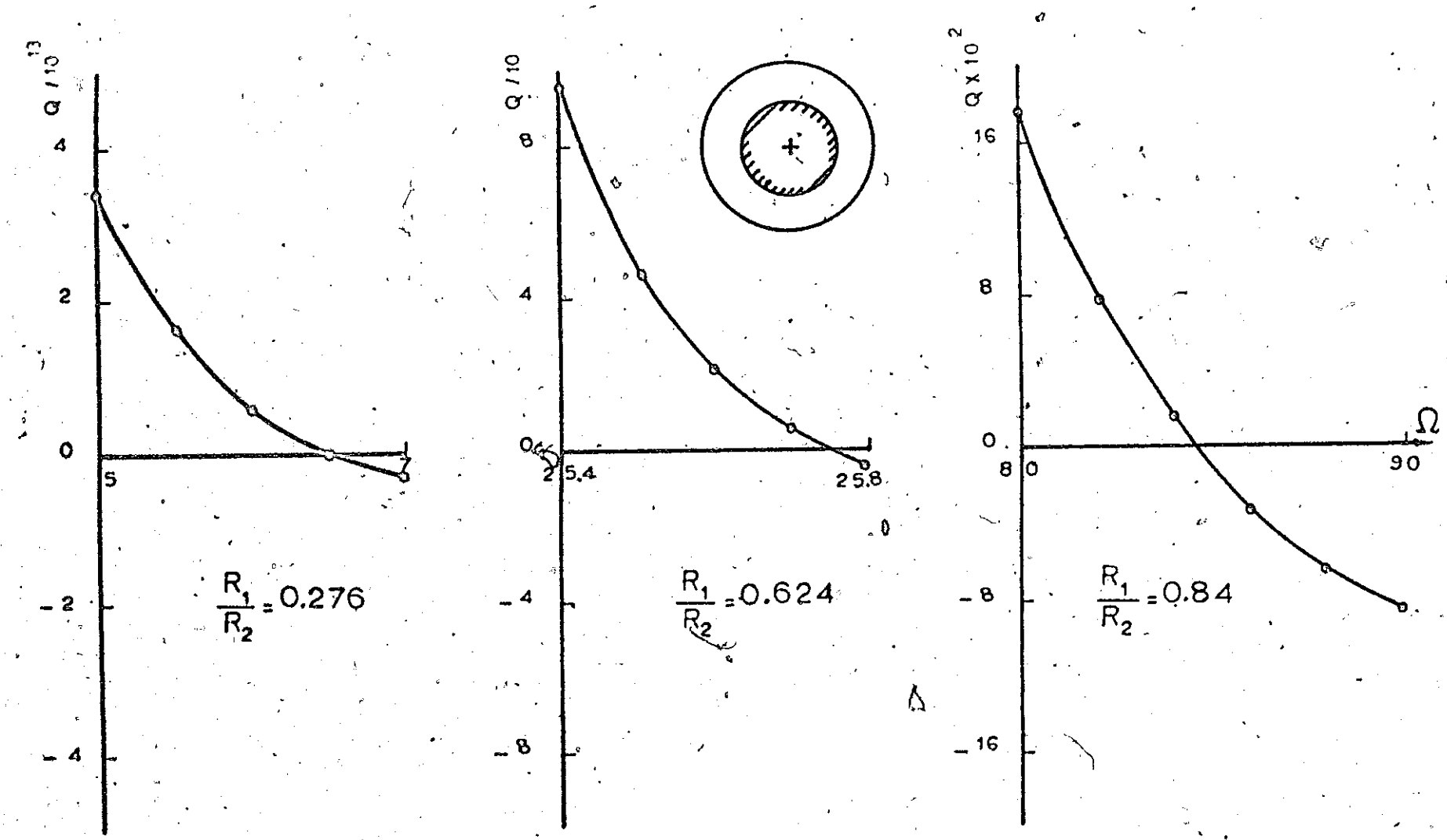

Figure 20

Variation of Determinant of Matrix Q with Frequency for Annular Cantilever Plates (First Mode Shape)

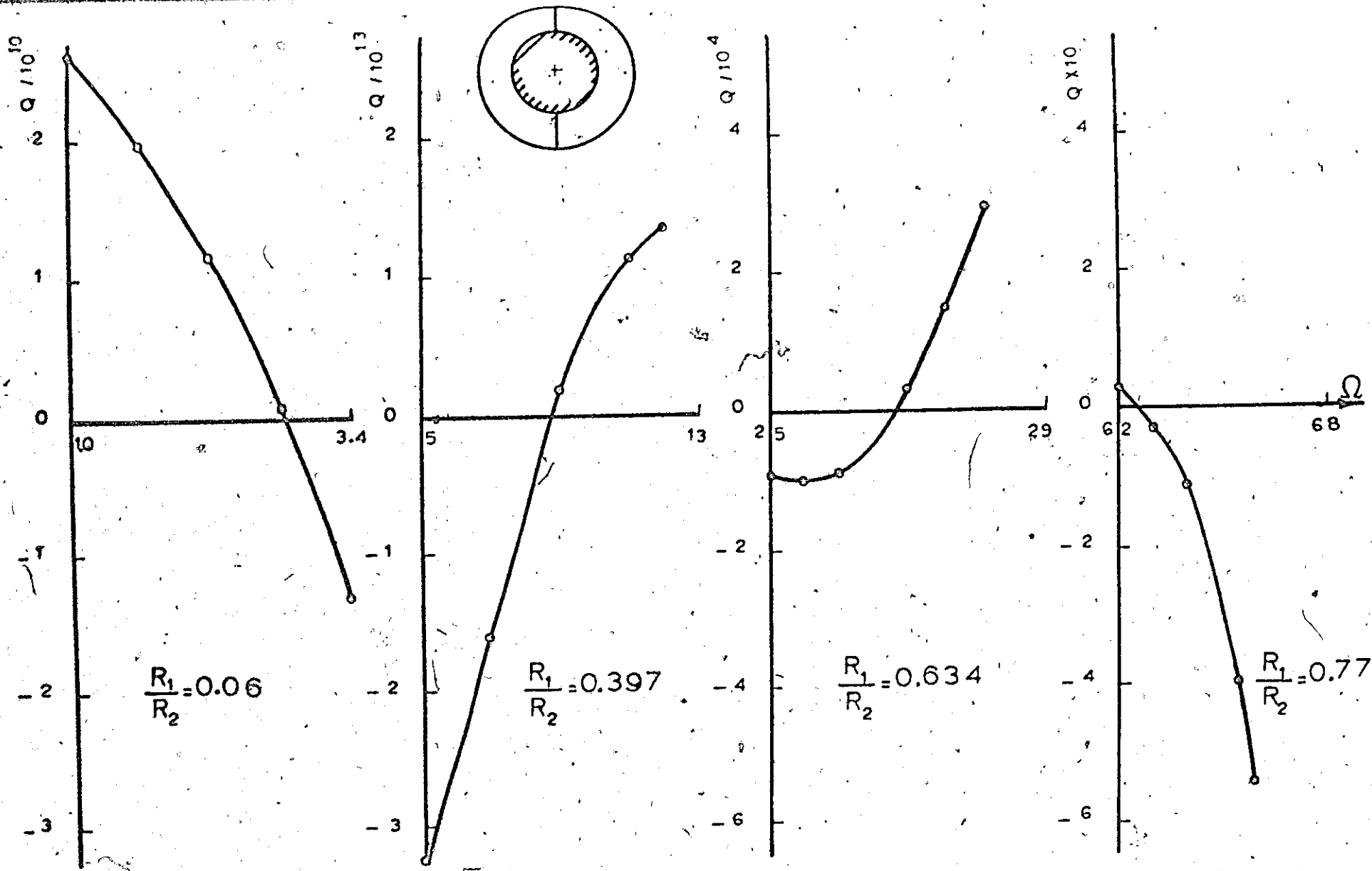

Figure 21

Variation of Determinant of Matrix Q with Frequency for Annular Cantilever Plates (Second Mode Shape)

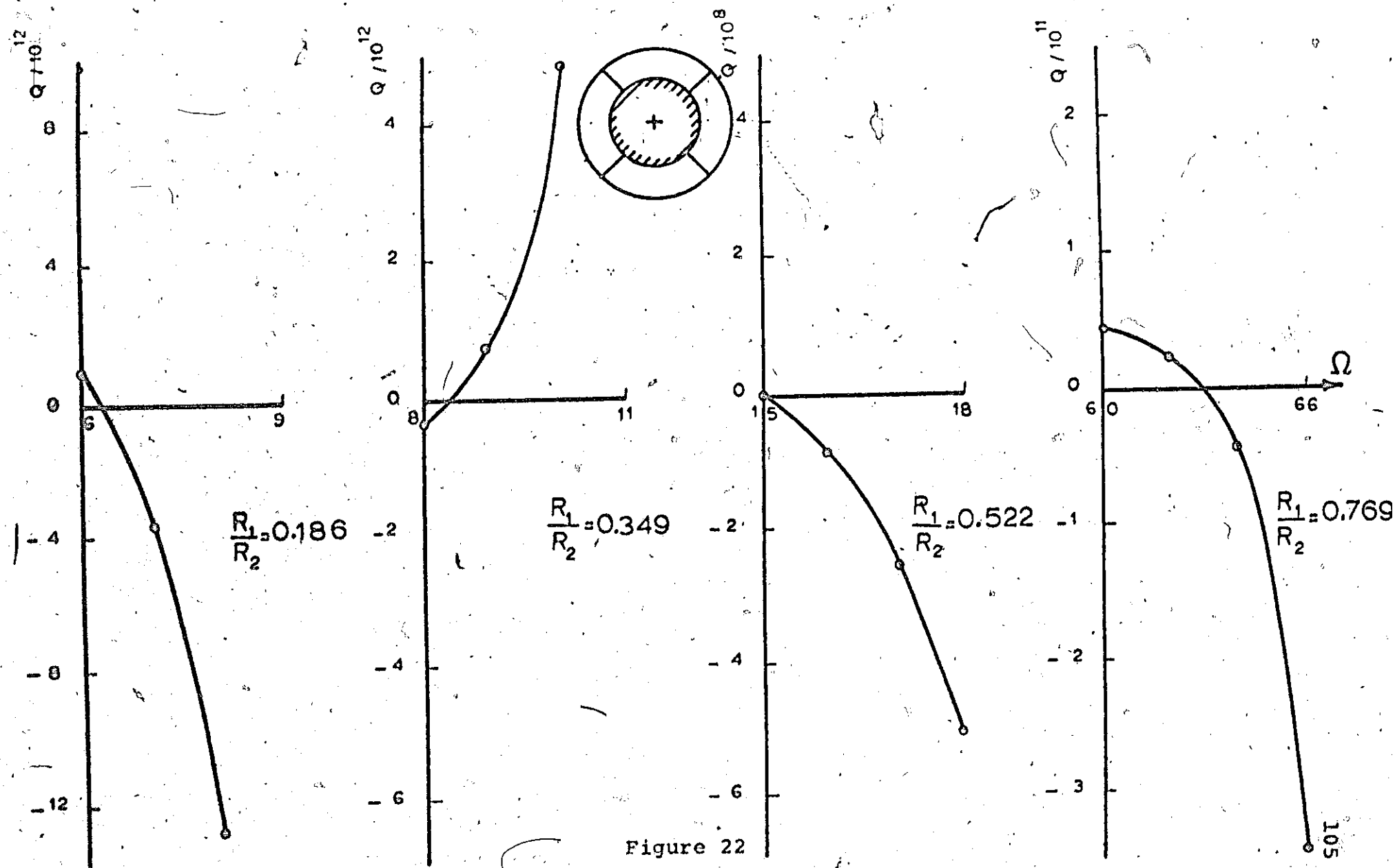

Figure 22

Variation of Determinant of Matrix Q with Frequency for Annular Cantilever Plates (Third Mode Shape)

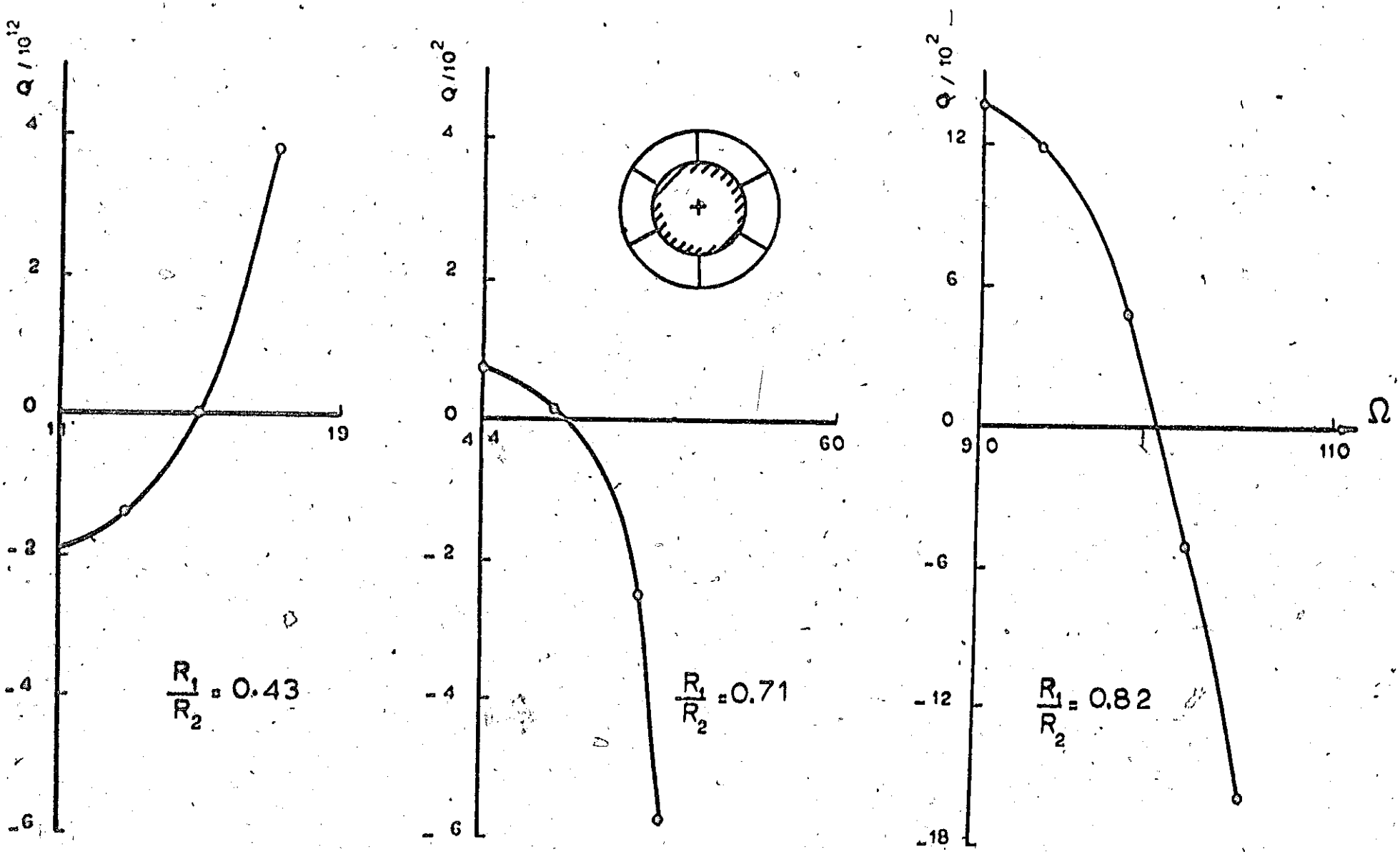

Figure 23

Variation of Determinant of Matrix Q with Frequency for Annular Cantilever Plates (Fourth Mode Shape)

TABLE X

Nondimensional Natural Frequencies (Ω) For

Annular Cantilever Plates

Vibration Mode	R_i/R_o	Calculated Value	Exact Value [52]	% Difference
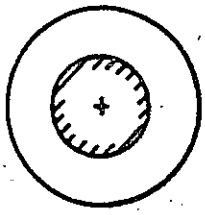	0.276	6.45	6.25	3.2
	0.642	25.76	25.00	3.1
	0.840	84.60	81.00	4.5
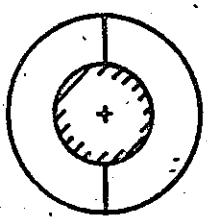	0.060	2.83	2.82	0.4
	0.397	8.80	9.00	2.2
	0.634	26.80	25.00	7.2
	0.771	62.60	64.00	2.2
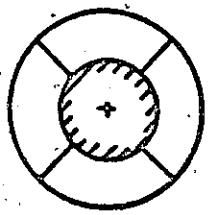	0.168	6.30	6.25	0.8
	0.349	8.45	9.00	6.1
	0.522	15.00	16.00	6.3
	0.769	62.80	64.00	1.9
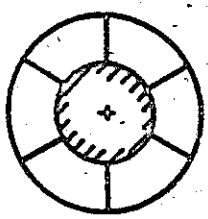	0.430	15.05	16.00	5.9
	0.710	48.80	49.00	0.4
	0.82	100.40	100.00	0.4

$$\left[\begin{array}{c|c} P_{11} & P_{12} \\ \hline P_{21} & P_{22} \end{array}\right] \left\{\begin{array}{c} 0 \\ \hline F_{in} \end{array}\right\}_1 = \left\{\begin{array}{c} \delta_{out} \\ \hline 0 \end{array}\right\} \qquad (5.30)$$

Thus $$[P_{22}]\ \{F_{in}\}_1 = \{0\} \qquad (5.31)$$

and the matrix $[Q]$ in this case is $[P_{22}]$.

The variation of the determinant of matrix $[Q]$ with the frequency is plotted in Figures (20), (21), (22) and (23), for different mode shapes and for different ratios of the inner to the outer radii. The frequency is expressed as a non-dimensional quantity Ω defined as

$$\Omega = \omega R_o^2 \sqrt{\rho t/D} \qquad (5.32)$$

where R_o is the outside radius of the plate.

The values of the natural frequencies as obtained from the present analysis are given in Table X . The exact values of the natural frequencies as given in Reference [52] are also given for comparison. The maximum deviation from the exact answer is 7.2%.

Naturally, more accurate results could be obtained, using the present method, by increasing the number of strips. This of course will not increase the size of the matrices.

5.6.3 Rectangular Cantilever Plate with Irregular Boundaries

Figure (24) shows a special shape cantilever plate, divided into two parts A and B . Part A is divided into m_1 strips and part B is divided into m_2 strips. Each

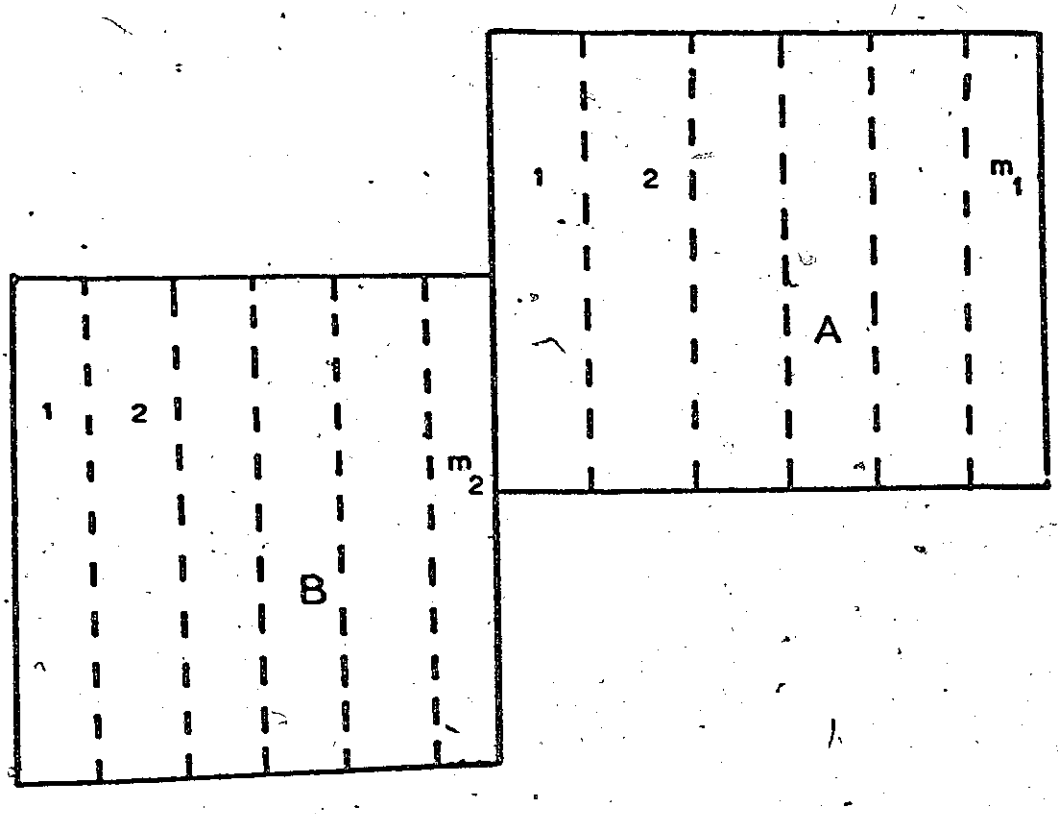

Figure 24

Division of a Plate with Irregular Boundaries into Two Parts, and Subdivision of each Part into Sections

strip in A and B is subdivided into n_1 and n_2 finite elements respectively.

For part A of the plate, we get

$$\begin{Bmatrix} \delta_R \\ --- \\ -F_R \end{Bmatrix}_A = [T]_{m_1} [T]_{m_1-1} \cdots\cdots [T]_1 \begin{Bmatrix} \delta_L \\ --- \\ F_L \end{Bmatrix}_A = [R] \begin{Bmatrix} \delta_L \\ --- \\ F_L \end{Bmatrix}_A \quad (5.33)$$

Equation (5.33) relates the edge variables of the left boundary of part A to the edge variable of the right boundary of part A .

A similar expression may be obtained for part B in the form

$$\begin{Bmatrix} \delta_R \\ --- \\ -F_R \end{Bmatrix}_B = [T]_{m_2} [T]_{m_2-1} \cdots\cdots [T]_1 \begin{Bmatrix} \delta_L \\ --- \\ F_L \end{Bmatrix}_B = [V] \begin{Bmatrix} \delta_L \\ --- \\ F_L \end{Bmatrix}_B \quad (5.34)$$

To get the transfer matrix for the entire plate, it is more convenient to rearrange the columns matrix [R] , so that the nodes of the left boundary of part A are separated into two groups, free and common, thus

$$\begin{Bmatrix} \delta_R \\ --- \\ -F_R \end{Bmatrix}_A = \left[\begin{array}{c:c} R_1 & R_2 \end{array}\right] \begin{Bmatrix} \delta_{Lf} \\ F_{Lf} \\ --- \\ \delta_{Lc} \\ F_{Lc} \end{Bmatrix}_A \quad (5.35)$$

where $\begin{Bmatrix} \delta_{Lf} \\ F_{Lf} \end{Bmatrix}_A$ is the column vector of nodal displacements and forces of the free nodes on the left edge of A and $\begin{Bmatrix} \delta_{Lc} \\ F_{Lc} \end{Bmatrix}_A$ is the column vector of nodal displacements and forces of the common nodes on the left edge of A .

Similarly arranging the rows of matrix [V], so that the nodes on the right boundary of part B are separated into free and common nodes, we get

$$\begin{Bmatrix} \delta_{Rc} \\ -F_{Rc} \\ \hline \delta_{Rf} \\ -F_{Rf} \end{Bmatrix}_B = \begin{bmatrix} V_1 \\ \hline V_2 \end{bmatrix} \begin{Bmatrix} \delta_L \\ \hline F_L \end{Bmatrix}_B \qquad (5.36)$$

But since

$$\begin{Bmatrix} \delta_{Lc} \\ \hline F_{Lc} \end{Bmatrix}_A = \begin{Bmatrix} \delta_{Rc} \\ \hline -F_{Rc} \end{Bmatrix}_B \qquad (5.37)$$

With a little algebraic manipulation, the following relationship can be obtained

$$\begin{Bmatrix} \delta_R \\ -F_R \\ \hline \delta_{Rf} \\ -F_{Rf} \end{Bmatrix}_B = \left[\begin{array}{c|cc} [R_1] & [R_2] & [V_1] \\ \hline [0] & [V_2] & \end{array}\right] \begin{Bmatrix} \delta_{Lf} \\ F_{Lf} \\ \hline \delta_L \\ F_L \end{Bmatrix}_A \qquad (5.38)$$

Equation (5.38) relates the edge variables of : (a) the right boundary of part A , (b) the non-common (free) nodes of the left boundary of part A , (c) the left boundary of part B , and (d) the non-common (free) nodes of the right boundary of part B .

The boundary conditions determine the matrix [Q], whose determinant is zero at the correct natural frequencies.

Natural frequencies using the present method, are calculated for a cantilever plate which is divided into two parts A and B as shown in Figure (25). The right edge of the plate is fixed. Each part is divided into three strips, and each strip into four triangular elements. The stiffness and mass matrices for a strip is obtained.

Since the right boundary of part A is fixed and the left boundary of part B is free, thus $\{\delta_R\}_A = 0$ and $\{F_L\}_B = 0$. Also since some of the nodes at the left boundary of part A , and some of the nodes at the right boundary of part B , are free, thus $\{F_{Lf}\}_A = 0$ and $\{F_{Rf}\}_B = 0$.

In this case, equation (5.38) can be written as

$$\begin{Bmatrix} 0 \\ -F_R \\ \delta_{Rf} \\ 0 \end{Bmatrix}_B = \left[\begin{array}{c|cc} [R_1] & [R_2] & [V_1] \\ \hline [0] & & [V_2] \end{array}\right] \cdot \begin{Bmatrix} \delta_{Lf} \\ 0 \\ \delta_L \\ 0 \end{Bmatrix}_A \qquad (5.39)$$

The matrix [Q] whose determinant vanishes at the correct values of the natural frequencies, is obtained by

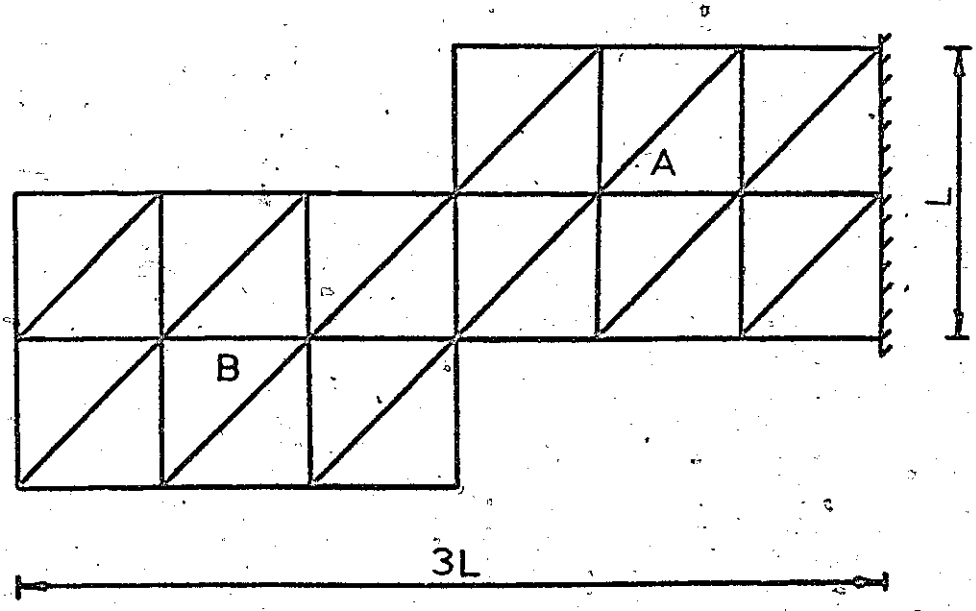

Figure 25

Subdivision of the Plate into Two Parts A and B, Each Part has 3 Strips, and Each Strip is Divided into 4 Finite Elements

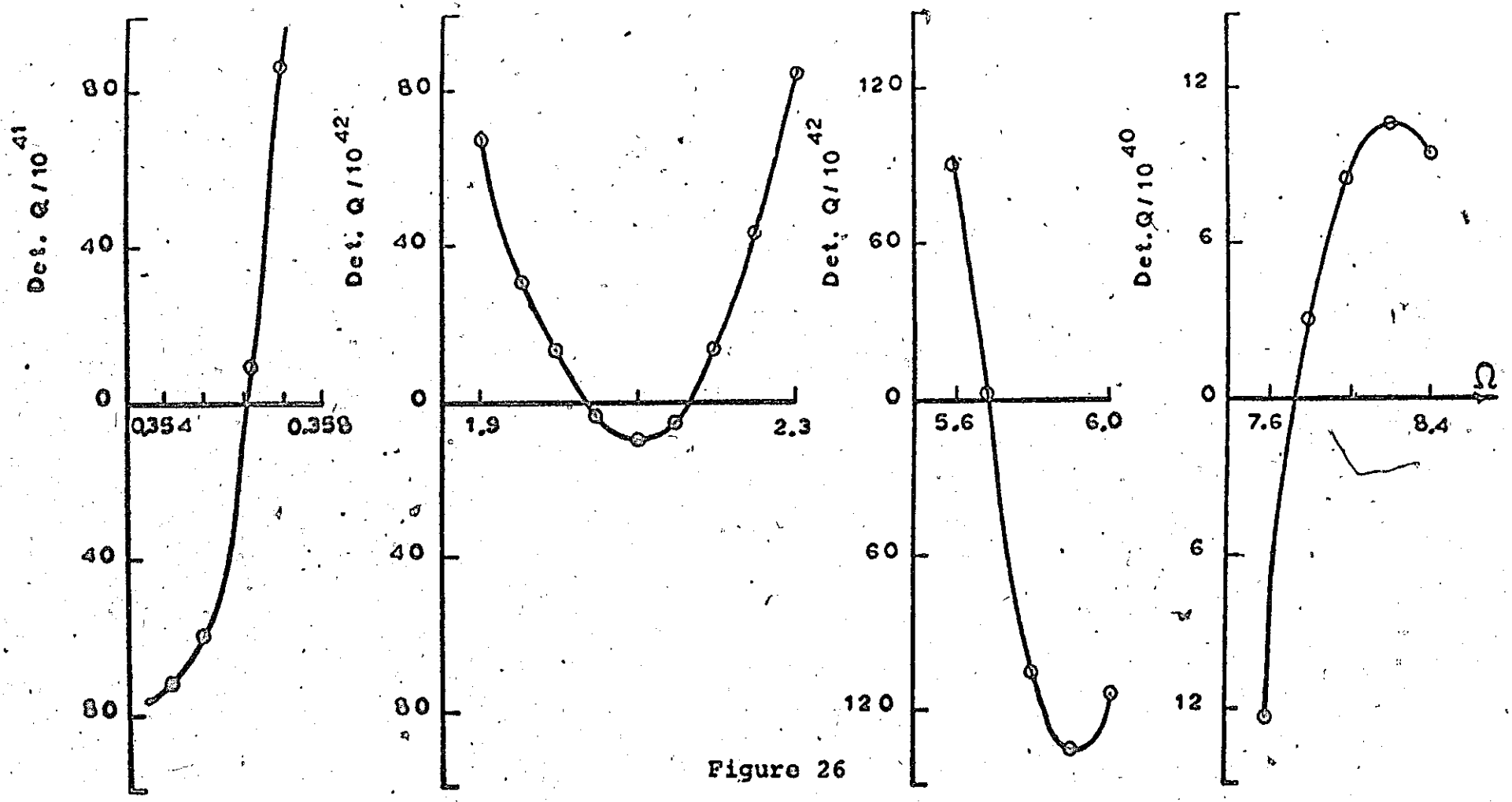

Figure 26

Variation of Determinant of Matrix Q with Frequency for a Rectangular Cantilever Plate with Irregular Boundaries

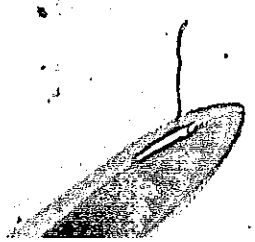

TABLE XI

Nondimensional Natural Frequencies (Ω) For a Rectangular Cantilever Plate With Irregular Boundaries

Vibration Mode	Transfer Matrix -Finite Element Method Value	Finite Element Method Value	% Difference
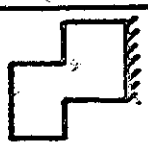	0.36	0.36	0.00
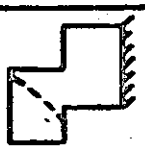	2.04	1.99	2.45
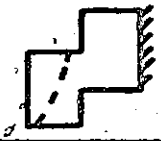	2.17	2.17	0.00
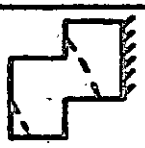	5.70	5.60	1.76
	7.72	7.99	3.50

deleting the columns corresponding to the zero elements of the right hand side column vector and deleting the rows corresponding to the non-zero elements of the left hand side column vector.

The variation of the determinant of matrix [Q] with the frequency is plotted in Figure (26).

The values of the natural frequencies, for the first five modes of vibration, as obtained from the present analysis are given in Table XI . The values for these frequencies as obtained by the usual finite element analysis are also included in the Table for comparison. The maximum deviation from the finite element method value is 3.5%.

5.6.4 Cantilever Fan Blade

The same curved fan blade, whose natural frequencies were obtained in the last chapter using the finite element method alone, will be studied in this section using the transfer matrix - finite element technique.

The shell is divided into m strips and each strip is subdivided into finite elements as shown in Figure (27). The modified 20 degrees of freedom cylindrical shell element, and the modified 28 degree of freedom element, are both used in the analysis. The assembly of element matrices is carried out for all elements on each strip, to give the total stiffness and mass matrices for each strip.

Since the left edge of the shell is free and the right

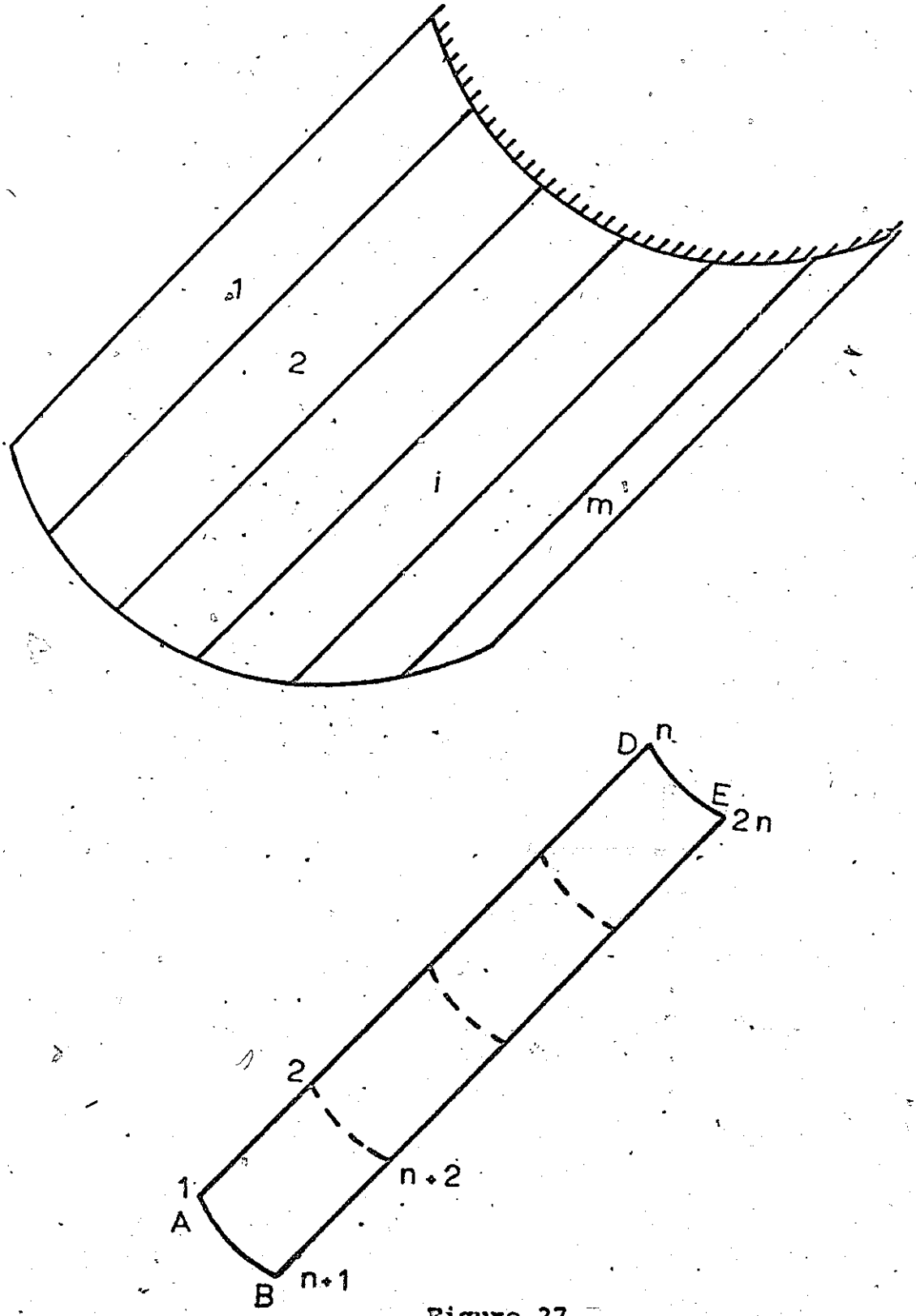

Figure 27

Division of Curved Fan Blade into Sections, and Subdivision of a Section into Finite Elements

edge is also free, equation (5.16) can be written as

$$\left[\begin{array}{c|c} P_{11} & P_{12} \\ \hline P_{21} & P_{22} \end{array}\right] \left\{\begin{array}{c} \delta_{\ell} \\ \hline 0 \end{array}\right\}_1 = \left\{\begin{array}{c} \delta_R \\ \hline 0 \end{array}\right\}_m \tag{5.40}$$

This can be split into two equations

$$[P_{11}]\ \{\delta_{\ell}\}_1 = \{\delta_R\}_m \tag{5.41}$$

and

$$[P_{21}]\ \{\delta_{\ell}\}_1 = \{0\} \tag{5.42}$$

The matrix [Q] whose determinant vanishes at the correct value of natural frequencies is, therefore, the matrix $[P_{21}]$ in this case.

The variation of the determinant of matrix [Q] with the frequency is plotted in Figures (28) to (30). The 20×20 cylindrical shell element is used in this case, and the frequency is expressed in cycles per second.

Table XII shows a comparison between the results obtained by the present analysis and the experimental results obtained by Olsen and Lindberg [48]. It should be noted that the numbers at the top of columns 2 to 5 in the Table represent the number of strips and the number of elements in each strip, respectively. It is obvious from the Table that the present analysis gives much better predictions than those obtained using the finite element method alone. The maximum deviation of the natural frequencies, for the first five modes,

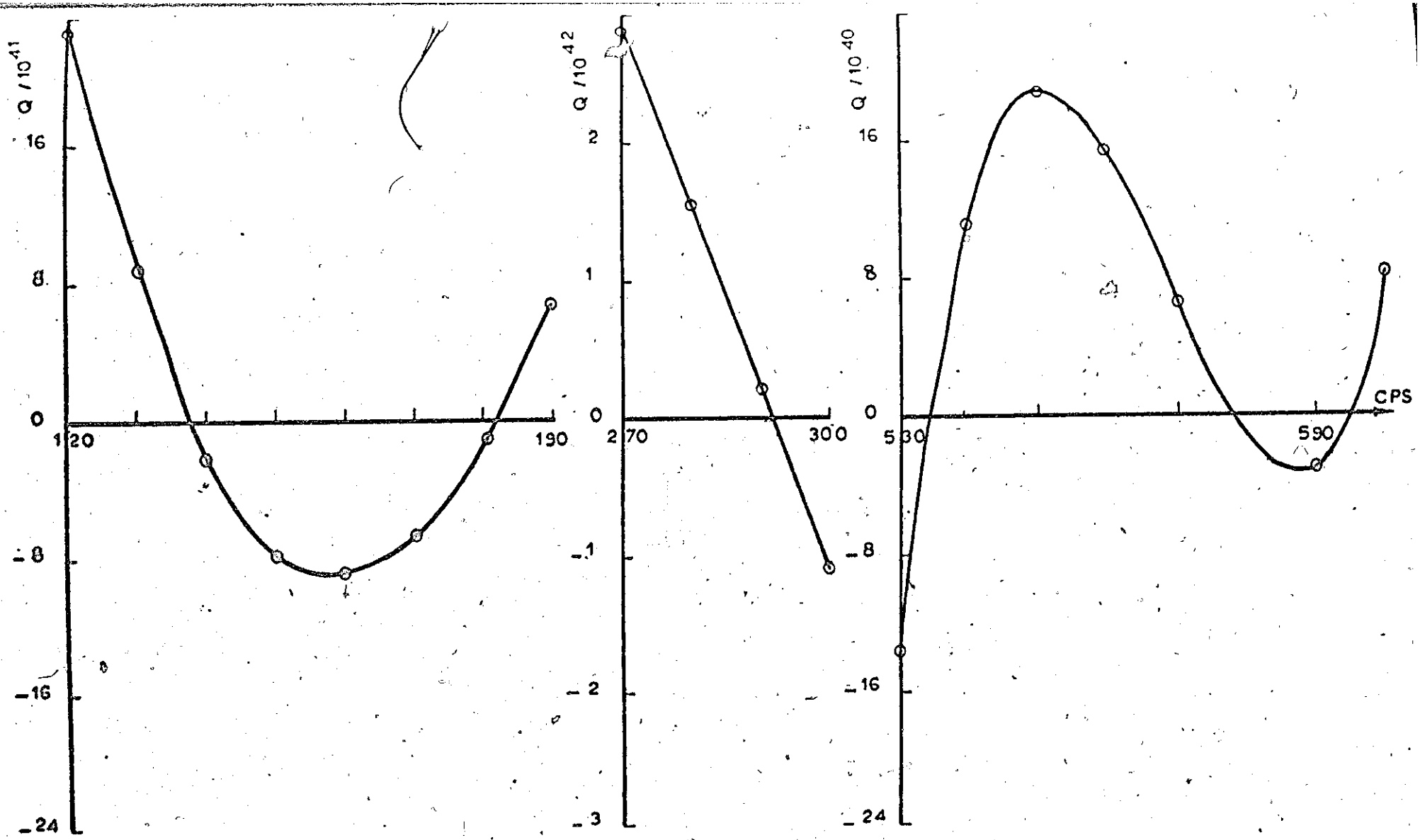

Figure 28

Variation of Determinant of Matrix Q with Frequency for a Cantilever Fan Blade (20x2 mesh; the 20x20 Element is used)

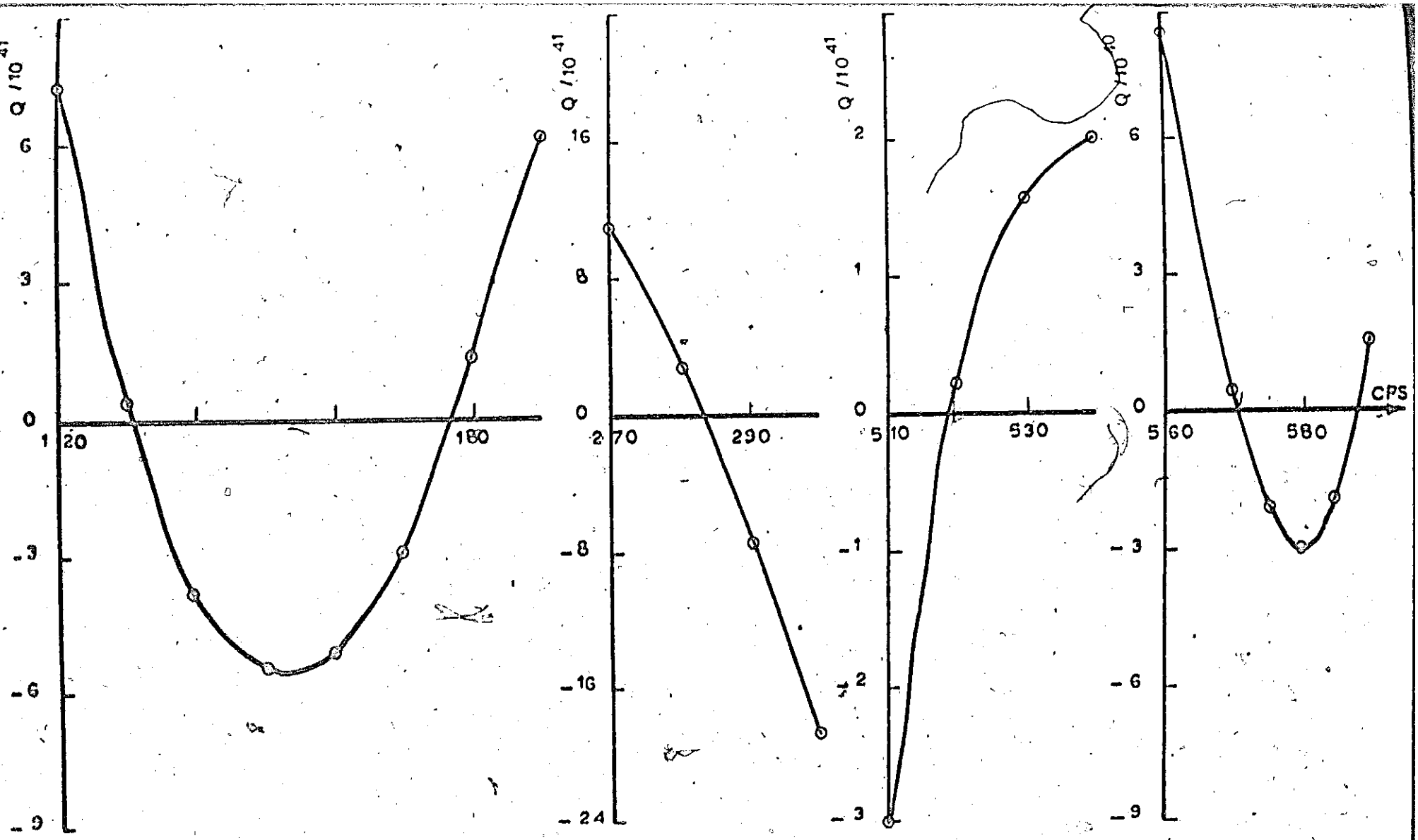

Figure 29

Variation of Determinant of Matrix Q with Frequency for a Cantilever Fan Blade (100x2 mesh; the 20x20 Element is used)

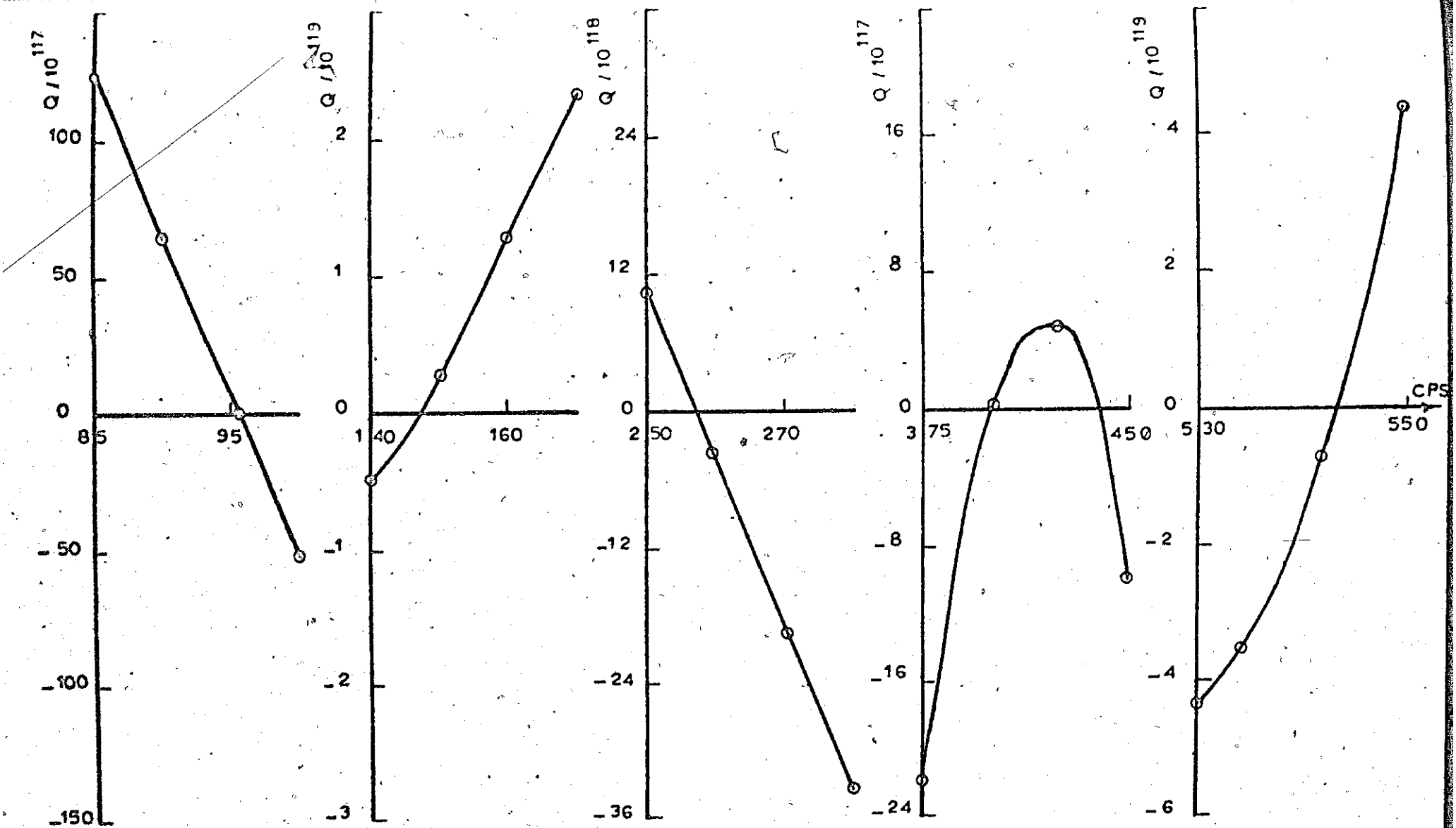

Figure 30

Variation of Determinant of Matrix Q with Frequency for a Cantilever Fan Blade (60x4 mesh; the 20x20 Element is used)

TABLE XII

Natural Frequencies For Curved Fan Blade

Using The Transfer Matrix-Finite Element Method

(The 20x20 Shell Element Is Used)

Mode Shape	Experiment Ref. [48]	20x2	100x2	60x4 *
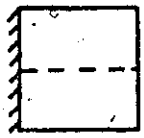	(cps) 86.6	(cps) 137	(cps) 131	(cps) 95
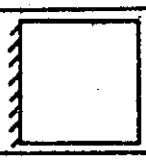	135;5	182	177	147
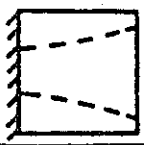	258.9	292	283	257
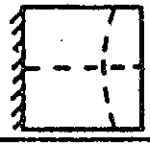	350.6	535	520	399
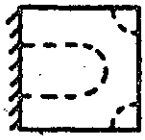	395.2	578	571	439

* The numbers at the top of columns 3 to 5 represent the number of strips, and the number of elements in each strip, respectively.

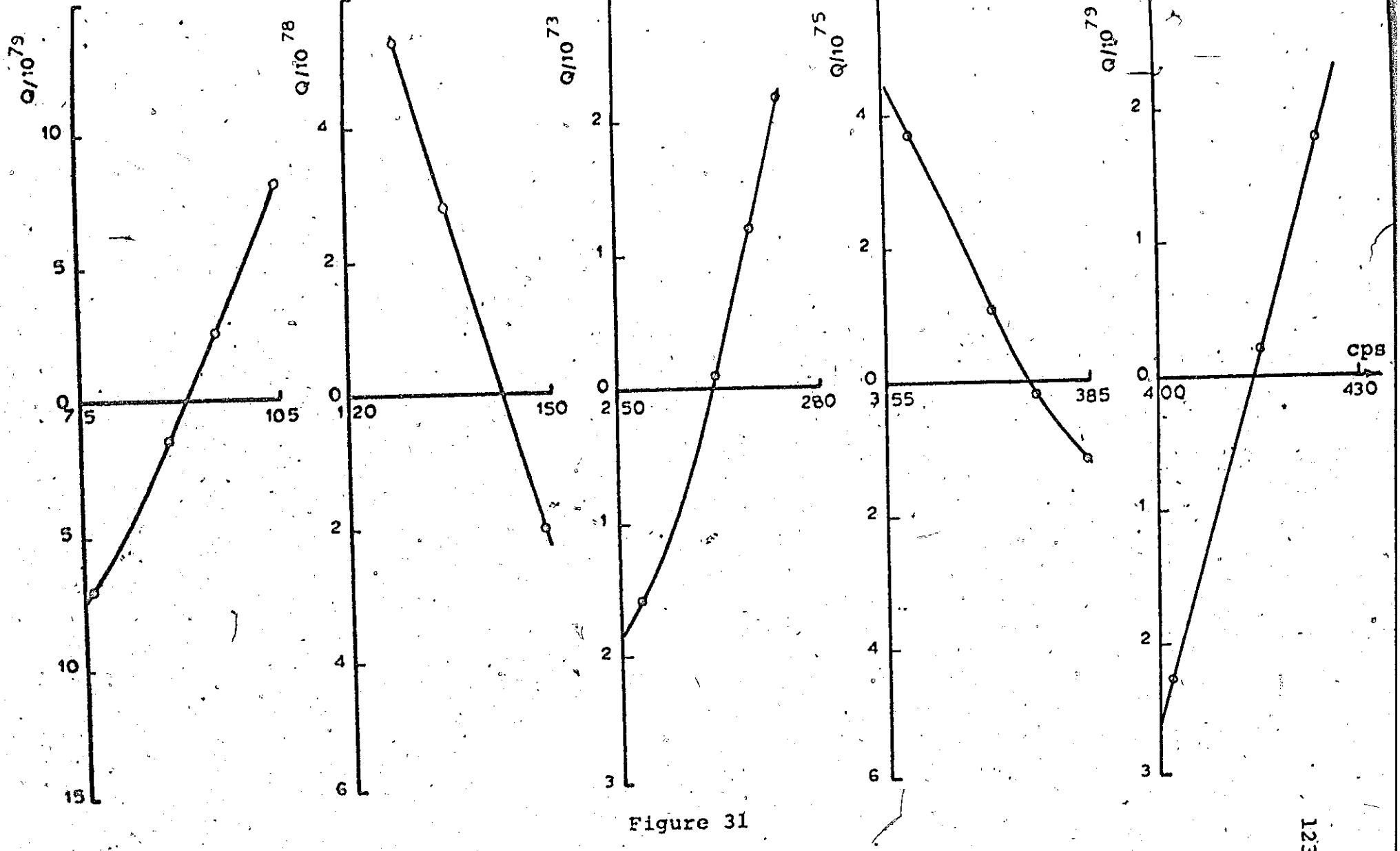

Figure 31

Variation of Determinant of Matrix Q with Frequency for a Cantilever Fan Blade (6x4 mesh; the 28x28 Element is used)

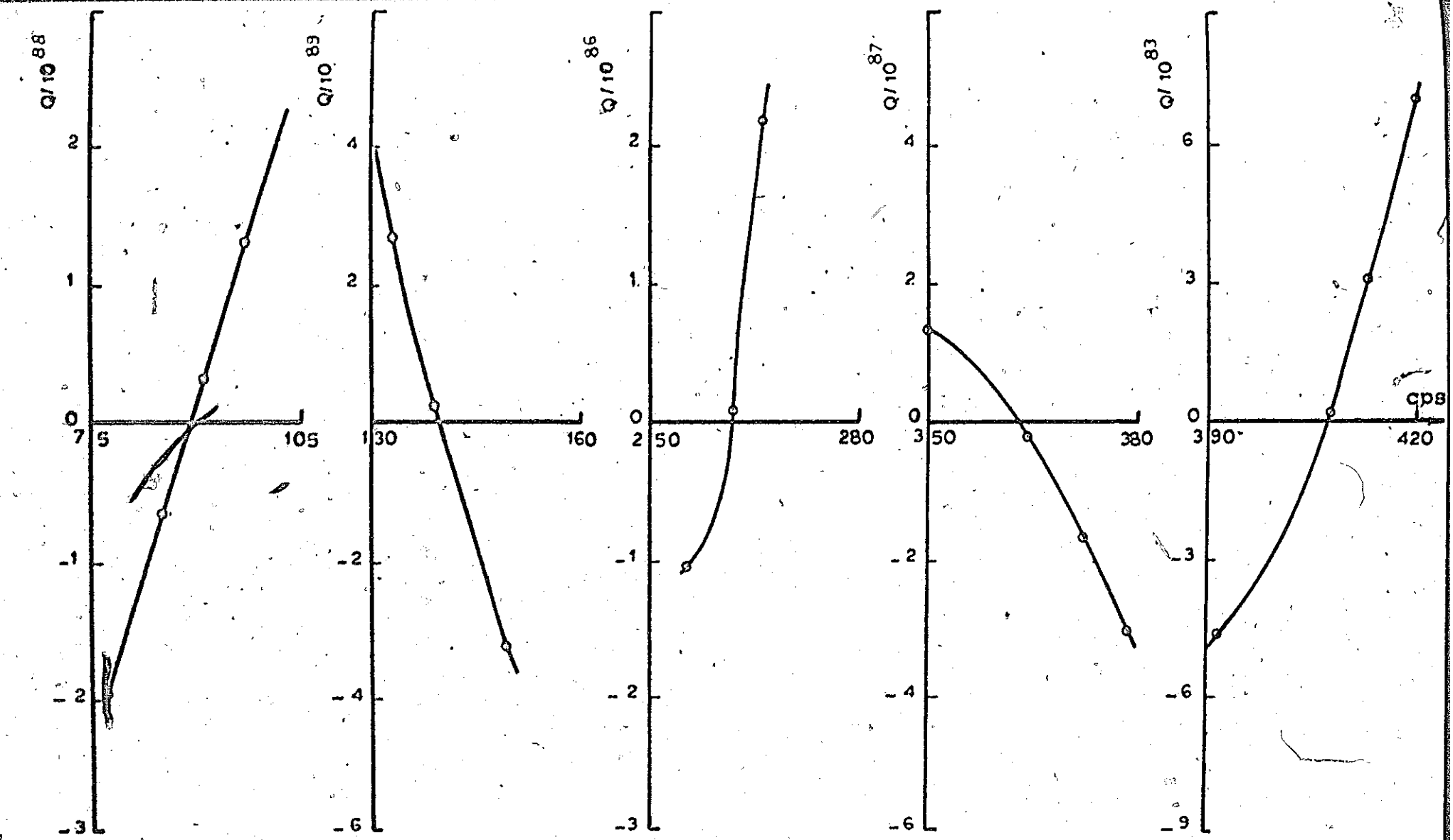

Figure 32

Variation of Determinant of Matrix Q with Frequency for a Cantilever Fan Blade (8x4 mesh; the 28x28 Element is used)

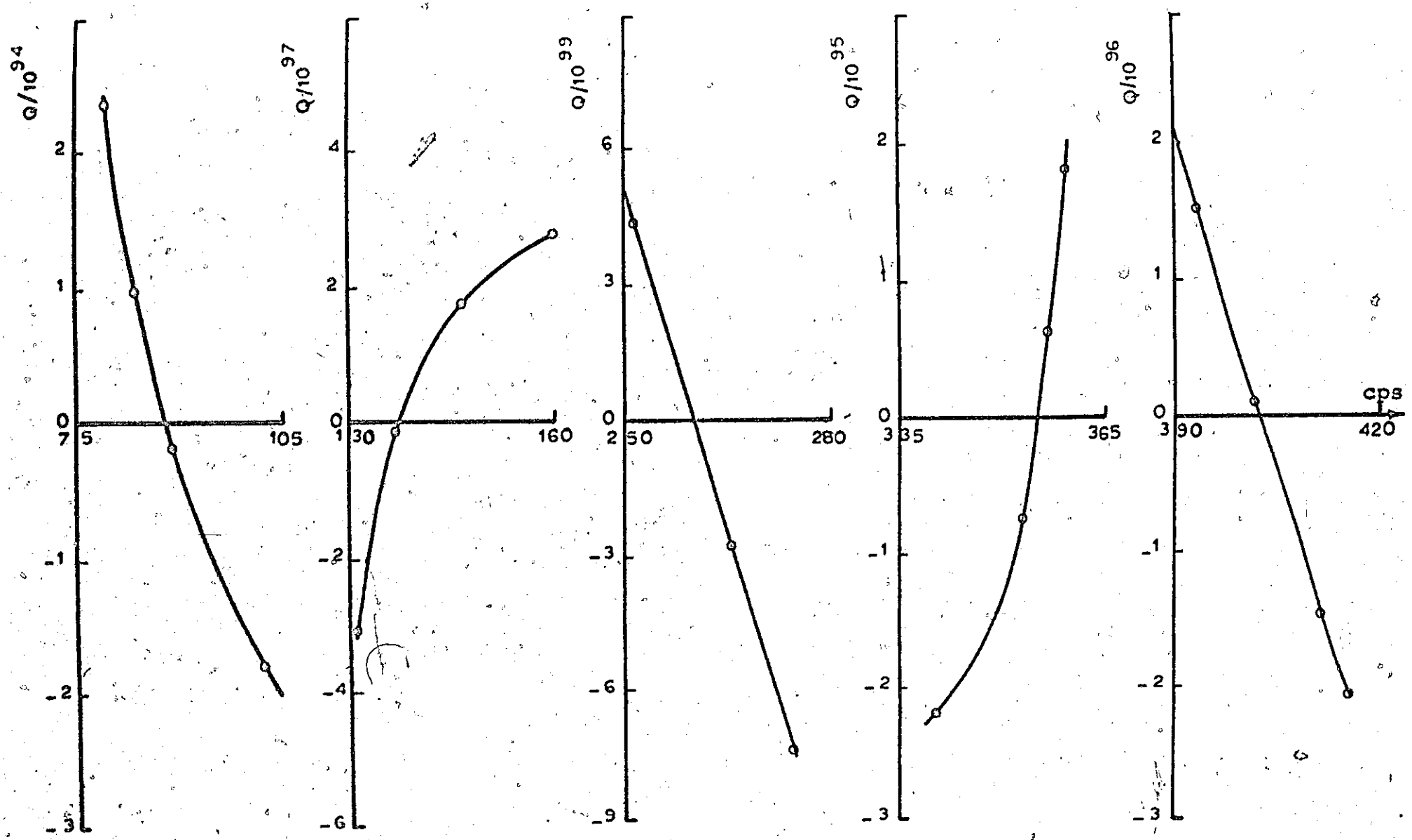

Figure 33

Variation of Determinant of Matrix Q with Frequency For a Cantilever Fan Blade (10x4 mesh; the 28x28 Element is used)

TABLE XIII

Natural Frequencies For Curved Fan Blade

Using the Transfer Matrix-Finite Element Method

(The 28x28 Shell Element Is Used)

Mode Shape	Experiment Ref. [48]	6x4	8x4	10x4 *
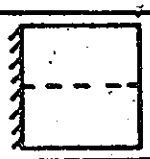	(cps) 86.6	(cps) 90.7	(cps) 88.9	(cps) 87.8
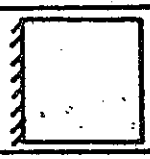	135.5	142.7	139.5	137.4
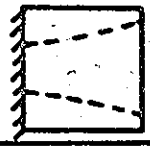	258.9	263.6	262.4	260.1
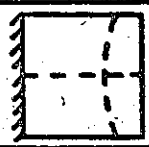	350.6	375.9	362.8	355.1
	395.2	414.1	407.0	402.8

*The numbers at the top of columns 3 to 5 represent the number of strips , and the number of elements in each strip, respectively.

is 14 %. If the same problem is solved by the usual finite element method for the cases given in Table XII, the size of the matrices will be 210 , 1010 and 1220 respectively, which would require a huge computer size.

Table XIII shows the same comparison, but using the 28×28 modified cylindrical shell element. The variation of the determinant of matrix [Q] with the frequency is plotted in Figures (31) to (33). The maximum deviation of the natural frequencies from the experimental results, using the 4×10 division, is less than 2 %. It is quite clear from this Table that the present method is a powerful method for the vibration analysis of shells and it gives very accurate predictions, using a comparatively small computer.

5.6.5 Clamped - Ring - Stiffened Circular Cylindrical Shell

Another example which can be solved using the transfer matrix - finite element technique is the vibration analysis of the clamped-ring-stiffened circular cylindrical shell shown in Figure (34). This problem has received very little attention. Sharma and Jones [53] formulated the problem using the Rayleigh-Ritz technique to obtain an approximate solution.

In the present analysis, the shell is divided into 16 strips, and each strip is subdivided into one annular sector finite element and five cylindrical shell elements as shown in Figure (34). The 28×28 modified cylindrical shell element is used in this case. The assembly of element matrices is carried

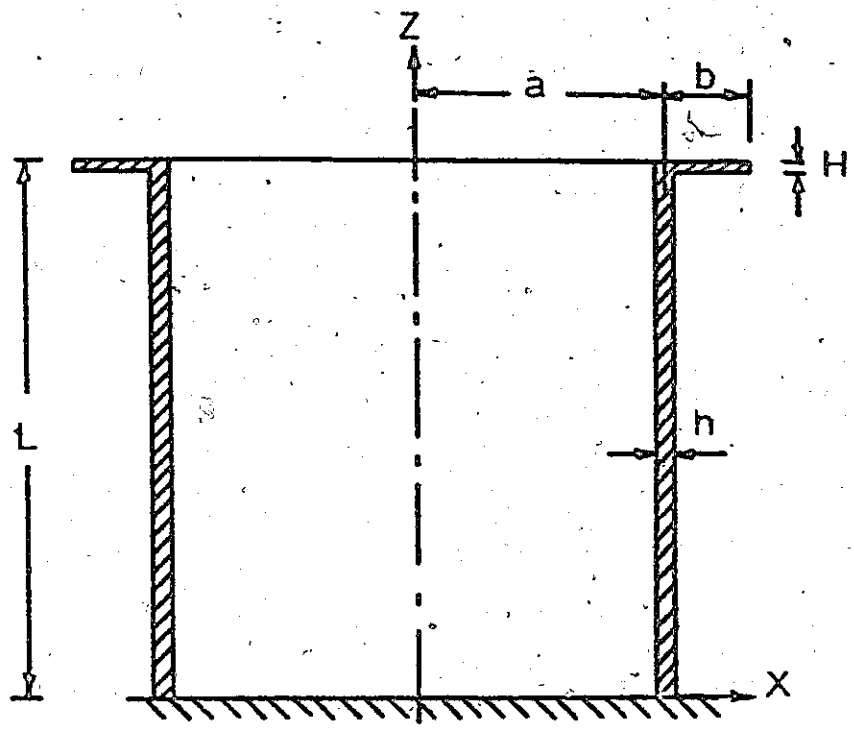

(a)

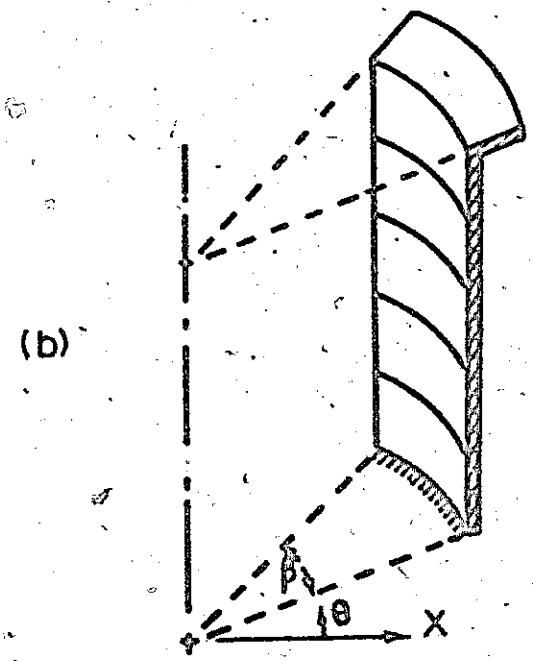

Figure 34

Clamped-Ring-Stiffened Circular Cylindrical Shell and Subdivision of a Section into Finite Elements

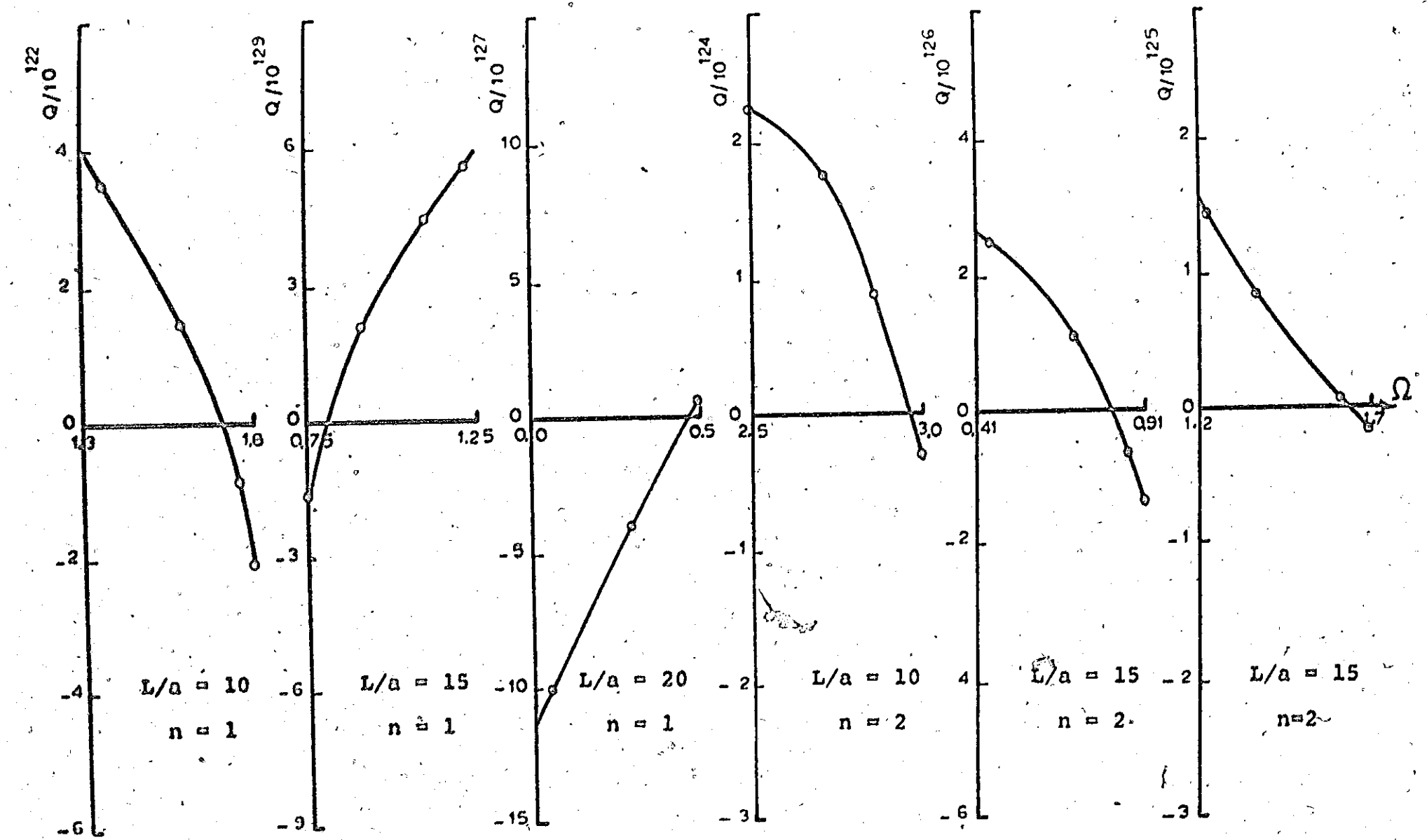

Figure 35

Variation of Determinant of Matrix Q with Frequency for a Clamped-Ring-Stiffened Circular Cylindrical Shell (a/h=50)

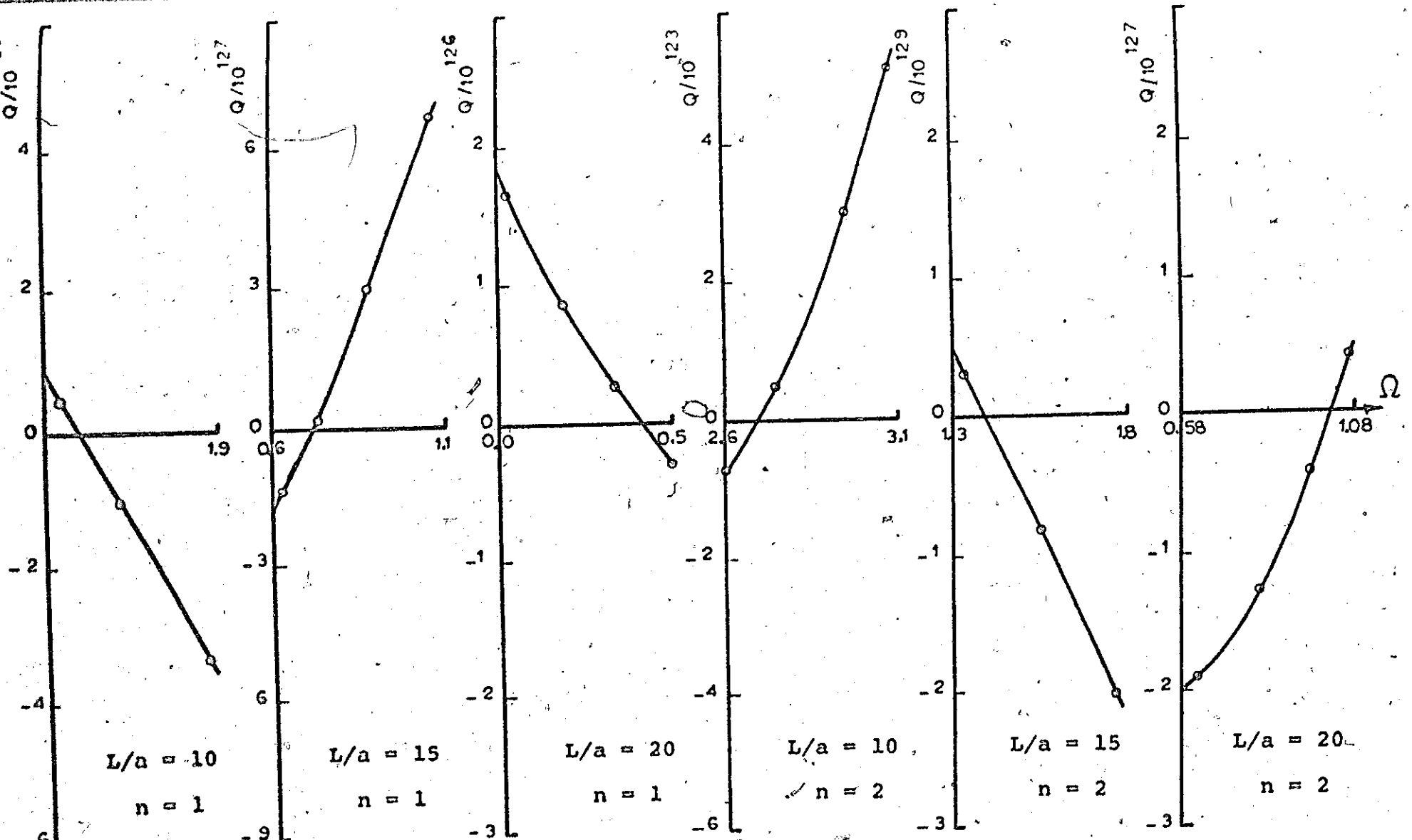

Figure 36

Variation of Determinant of Matrix Q with Frequency for a Clamped-Ring-Stiffened Circular Cylindrical Shell (a/h=100)

TABLE IXV

Nondimensional Natural Frequencies (Ω) For Clamped Ring-Stiffened Shells

L/a	Mode Shape Number n	a/h			
		50		100	
		Present Analysis	Reference [53]	Present Analysis	Reference [53]
10	1	1.71	1.7824	1.49	1.5486
15	1	0.81	0.8513	0.73	0.7681
20	1	0.47	0.4952	0.41	0.4573
10	2	2.96	3.0667	2.69	2.7915
15	2	1.89	1.9664	1.38	1.4384
20	2	1.63	1.6986	0.99	1.0341

out to give the total stiffness and mass matrices for each strip. Since in this case the system is closed, we can write

$$\begin{Bmatrix} \delta \\ -- \\ F \end{Bmatrix}_{\theta_1=0} = [P] \begin{Bmatrix} \delta \\ -- \\ F \end{Bmatrix}_{\theta_1=0} \tag{5.43}$$

or

$$[P - I] \begin{Bmatrix} \delta \\ -- \\ F \end{Bmatrix}_{\theta_1=0} = \{0\} \tag{5.44}$$

where [I] is an identity matrix.

Hence the matrix [Q] whose determinant vanishes at the correct values of natural frequencies is the matrix [P-I].

The dimensions of the shell, Figure (34), are as follows: a/h=50 and 100, L/a=10,15 and 20, H/a=0.1, and b/a= 0.3. The variation of the determinant of matrix [Q] with frequency is plotted in Figures (35) and (36) for values of n=1 and 2, where n is the circumferential mode number (n=1 is the cantilever mode, and n=2 is the first ovalling mode).The frequency is expressed as a nondimensional quantity defined by

$$\Omega = \omega a \sqrt{\rho(1 - \nu^2)/E} \times 100 \tag{5.45}$$

Table IXV shows a comparison between the results obtained by the present analysis and the approximate solution obtained by Sharma and Jones. The present values are observed to be lower than the approximate values, the maximum difference is about 5%. Conventional finite element technique for the same subdivision would require the determination of eigenvalues

TABLE XV

Comparison Between The Time Used By The Present Method And The Finite Element Method

Frequency (Ω)	Range of Trials	No. of Trials	Time Used (sec)
3.44	3.2 - 3.6	3	39.671
8.55	8 - 9	5	58.353
21.18 26.93 30.98	18 - 34	29	328.336
Total time used by the present method			426.360
Time used by the finite element method			52.328

for a 656 x 656 matrix, while the size of matrix [Q] is only 82.

5.7 Time comparison

The first five natural frequencies of the square cantilever plate , Figure (15) , are obtained using the finite element method alone, i.e. without dividing it into strips. The plate is divided into 50 elements. The size of the stiffness and mass matrices in this case is 90. The power method is used to get the required eigenvalues.

Table XV shows a comparison between the computing time used (on a CDC 6400 computer) by both methods. It is observed that the present method took about 8 times the computing time required by the finite element method, while the storage utilized is one ninth of that required by the finite element method. It should also be noted that if the range of the natural frequencies is not known, a lumped mass approximation may be done before using the transfer matrix-finite element technique. However, the present method has still the great advantage of requiring a smaller computer size as compared with the size required by the finite element method.

5.8 Concluding Remarks

The present method, based on the combination of transfer matrix and finite element techniques, is observed to

give satsfactory results fo the natural frequencies of plates and shells. In the conventional finite element approach the size of the matrix to be considered is equal to the total number of degrees of freedom for the entire structure. In the present method the size of the matrix is equal to the number of degrees of freedom for one strip. A much smaller computer is thus sufficient.

In the case of the finite element method , the natural frequencies are determined from the eigenvalue problem obtained from the equilibrium equations of the nodal forces. In the present method, these frequencies are determined by calculating the determinant of the boundary conditions matrix [Q] at various assumed values for the frequency. The size of the matrix [Q] is equal to half the number of degrees of freedom of one strip.

The computing time used by this method is usually greater than the time required by the finite element method.

CHAPTER 6

VIBRATION ANALYSIS OF BLADED RIMMED DISCS

6.1 Introduction

As was mentioned earlier, most of the studies of the vibrations of turbine blades assumed that the disc on which the blades are mounted is absolutely rigid. Hence, the blades are treated as cantilevered beams or plates (sometimes considered twisted or tapered).

In the present work, the transfer matrix - finite element technique is used to predict the lowest few natural frequencies of a bladed rimmed disc. The bladed rimmed disc is divided into sections, each section is a sector of the whole structure with included angle β. The disc is assumed to be rigidly fixed at its inner radius. Every section consists of two consecutive blades, and the part of the disc and rim within the included angle β as shown in Figure (37). Each section is then subdivided into finite elements.

The disc is subdivided into annular sector finite elements, and the rim into cylindrical shell elements. The annular sector finite element derived in Chapter 3 will be used for the disc and the 28x28 modified cylindrical shell element obtained in Chapter 4,will be used for the rim.

The blades are divided into flat plate triangular

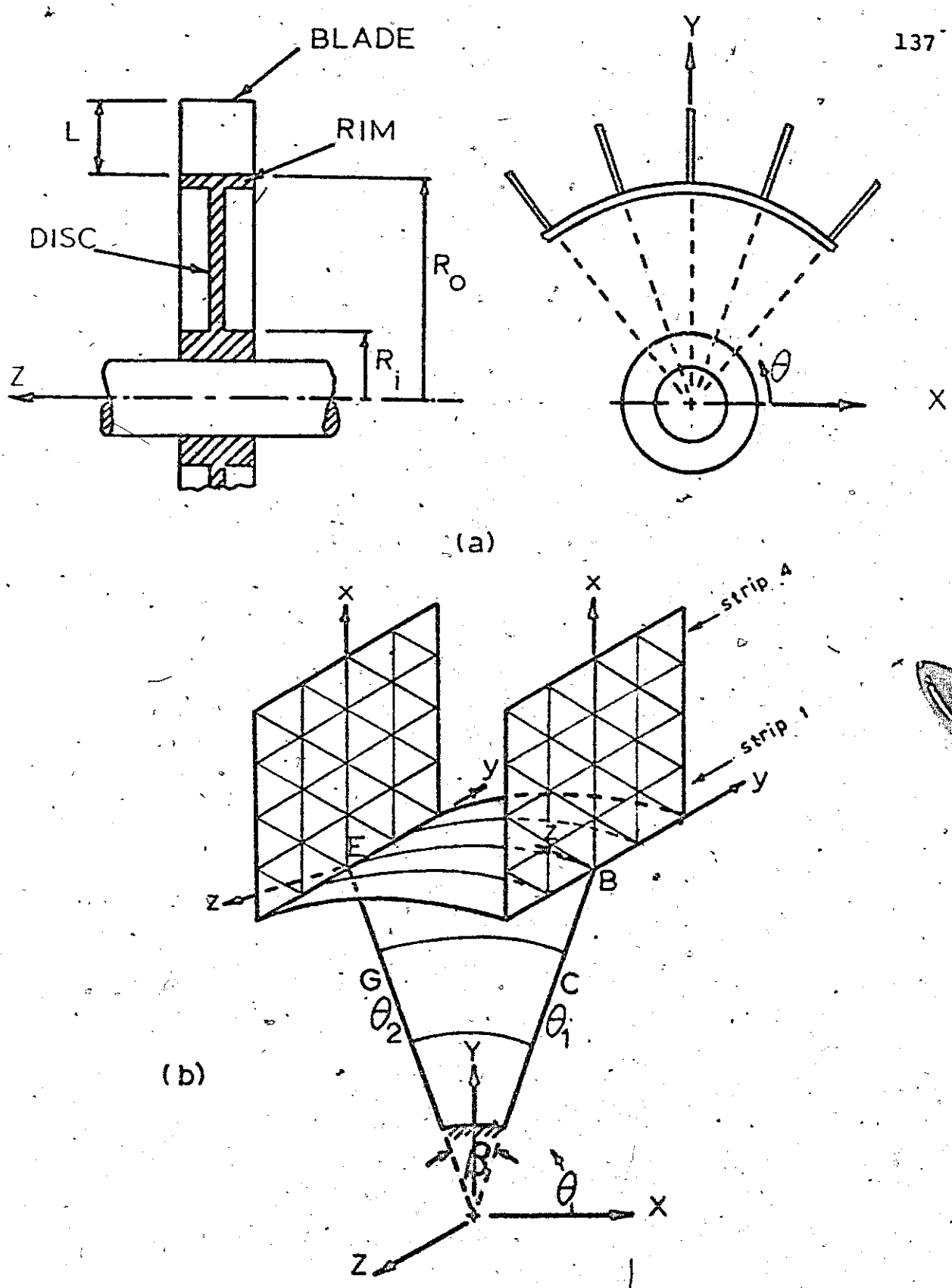

Figure 37

Bladed Rimmed Disc divided into Sections, and Subdivision of a Section into Finite Elements

elements. The flat plate bending triangular element utilized in Chapter 5 will be used here.

6.2 Complete Stiffness and Mass Matrices for the Triangular Plate Element

A shell element is, generally, subjected to bending as well as in-plane forces. For a flat element these forces cause independent deformations and, therefore, the in-plane stiffness and mass matrices can be derived independent of the bending matrices.

At each node of the triangular element two in-plane degrees of freedom are assigned. These are the displacements u' and v' along the x' and y' axes (Figure (16)).

The complete stiffness and mass matrices, which include the effects of both the in-plane and bending forces, are derived, in local coordinates, in reference [2]. The order of nodal displacements would be

$$\{\delta'_e\} = \{ u'_1 , v'_1 , w'_1 , \theta'_{x1} , \theta'_{y1} , \theta'_{z1} , .. , \theta'_{z2} , .. , \theta'_{z3} \}^T \qquad (6.1)$$

where u', v' and w' are the displacements along x', y' and z' respectively. θ'_x, θ'_y and θ'_z are the rotations about x', y' and z' axes respectively.

Since the stiffness matrix $[K'_e]$ refers to the

local coordinate system of an element, it must be transformed to common global coordinate system xyz. The procedure for transformation is given in reference [2].

6.3. Theoretical Analysis of the Bladed Rimmed Disc

In the present analysis we assume that all the blades are identical, and have the form of rectangular plates. Each blade is divided into a number of strips, and each strip is subdivided into triangular elements as shown in Figure (37). The local cartesian coordinate axes x', y', z' for each triangular element are so chosen that the z'-axis is normal to the blade surface and the y'-axis is along the hypotenuse of the triangle (Figure (16)).

The common global axes of the blade are such that the x-axis is along the length of the blade, the y-axis is in the plane of the blade and the z-axis is normal to the blade surface as shown in Figure (37).

The stiffness and the mass matrices of individual elements are obtained using the regular displacement type finite element approach. These matrices are transformed to the blade common global axes x, y, z. The assembly of element matrices is carried out for all the elements on one strip, to give the total stiffness and mass matrices for each strip.

Following the procedure of the last chapter, the transfer matrix relating the state vectors at the free end and the root of the blade is of the form:

$$\left[\begin{array}{c|c} P_{11} & P_{12} \\ \hline P_{21} & P_{22} \end{array}\right] \left\{\begin{array}{c} \delta_{root} \\ \hline F_{root} \end{array}\right\} = \left\{\begin{array}{c} \delta_{free} \\ \hline -F_{free} \end{array}\right\} \qquad (6.2)$$

Applying the boundary conditions, and splitting the last equation into two equations, yields

$$[P_{11}]\ \{\delta_{root}\} + [P_{12}]\ \{F_{root}\} = \{\delta_{free}\} \qquad (6.3)$$

and

$$[P_{21}]\ \{\delta_{root}\} + [P_{22}]\ \{F_{root}\} = \{0\} \qquad (6.4)$$

From the second equation

$$\{F_{root}\} = -\ [P_{22}^{-1}]\ [P_{21}]\ \{\delta_{root}\}$$
$$= [W']\ \{\delta_{root}\} \qquad (6.5)$$

This equation gives the relationship between the forces and deflections at the root of the blade due to the vibrations of the blade in the local coordinates of the blades xyz. Each section, of the whole structure includes two blades, with one blade at an angle θ_1 and the other at an angle θ_2, as shown in Figure (37). Equation (6.5) applies to both blades. Actually, this equation must be transformed to global coordinates XYZ. The transformation is carried out as follows:

$$\{F_B\} = [T_1]^T\ [W']\ [T_1]\ \{\delta_B\} = [W_1]\ \{\delta_B\} \qquad (6.6)$$

and

$$\{F_B\} = [T_2]^T [W'] [T_2] \{\delta_E\} = [W_2] \{\delta_E\} \qquad (6.7)$$

The subscript B corresponds to the root of the blade at θ_1, and the subscript E corresponds to the root of the blade at θ_2 as shown in Figure (37). The matrices $[T_1]$ and $[T_2]$ have the same form given by equation (3.36), where $[\lambda]$ is as follows

$$[\lambda] = \left[\begin{array}{ccc|ccc} \cos\theta & \sin\theta & 0 & 0 & 0 & 0 \\ 0 & 0 & -1 & 0 & 0 & 0 \\ -\sin\theta & \cos\theta & 0 & 0 & 0 & 0 \\ \hline 0 & 0 & 0 & \cos\theta & \sin\theta & 0 \\ 0 & 0 & 0 & 0 & 0 & -1 \\ 0 & 0 & 0 & -\sin\theta & \cos\theta & 0 \end{array}\right] \qquad (6.8)$$

Now, consider the rest of the section of the whole structure, which includes part from the disc and the rim which has an included angle β. The stiffness and mass matrices of all the annular elements and the cylindrical shell elements are obtained with respect to the global axes XYZ. Following the procedure of the last chapter yields

$$[S]_i \left\{\begin{array}{c} \delta_L \\ --- \\ \delta_R \end{array}\right\}_i = \left\{\begin{array}{c} F_L \\ --- \\ F_R \end{array}\right\}_i \qquad (6.9)$$

and this can be partitioned as follows

$$\left[\begin{array}{c|c|c|c} S_{11} & S_{12} & S_{13} & S_{14} \\ \hline S_{21} & S_{22} & S_{23} & S_{24} \\ \hline S_{31} & S_{32} & S_{33} & S_{34} \\ \hline S_{41} & S_{42} & S_{43} & S_{44} \end{array}\right]_i \left\{\begin{array}{c} \delta_E \\ \hline \delta_G \\ \hline \delta_B \\ \hline \delta_C \end{array}\right\}_i = \left\{\begin{array}{c} F_E \\ \hline F_G \\ \hline F_B \\ \hline F_C \end{array}\right\}_i \qquad (6.10)$$

where δ_E and δ_G are the deflections on the left edge of the section and δ_B and δ_C are the deflections on the right edge of the section, and, F_E, F_G, F_B and F_C are the corresponding forces, respectively.

Now, since there are additional forces at the roots of the blades (i.e. edges B and E), their effect must be added to the last equation. Therefore, from equations (6.6), (6.7) and (6.10);

$$\left[\begin{array}{c|c|c|c} S_{11}+W_1 & S_{12} & S_{13} & S_{14} \\ \hline S_{21} & S_{22} & S_{23} & S_{24} \\ \hline S_{31} & S_{32} & S_{33}+W_2 & S_{34} \\ \hline S_{41} & S_{42} & S_{43} & S_{44} \end{array}\right]_i \left\{\begin{array}{c} \delta_E \\ \hline \delta_G \\ \hline \delta_B \\ \hline \delta_C \end{array}\right\}_i = \left\{\begin{array}{c} F_E \\ \hline F_G \\ \hline F_B \\ \hline F_C \end{array}\right\}_i \qquad (6.11)$$

Following the same steps of the previous chapter, the transfer matrix relation for the section is in the form:

$$\left\{\begin{array}{c} \delta_R \\ \hline -F_R \end{array}\right\}_{\theta=\theta_1} = [T]_i \left\{\begin{array}{c} \delta_L \\ \hline F_L \end{array}\right\}_{\theta=\theta_2} \qquad (6.12)$$

Starting from the section where $\theta_1 = 0$, the transfer matrix for each section is obtained. Since this is a closed system, by successive matrix multiplication of the transfer matrices;

$$\begin{Bmatrix} \delta \\ -- \\ F \end{Bmatrix}_{\theta=0} = [P] \begin{Bmatrix} \delta \\ -- \\ F \end{Bmatrix}_{\theta=0} \qquad (6.13)$$

Thus the matrix whose determinant vanishes at the correct natural frequency is given by

$$|P - I| = 0 \qquad (6.14)$$

6.4 Numerical Examples

The present method is used to obtain the lowest few natural frequencies of a bladed rimmed disc. The disc has the shape of an annular plate of constant thickness and clamped at the inner edge. All the dimensions of the structure are measured with respect to the blade length, i.e. assuming the blade length is unity.

The inner radius of the disc is 1 , the outer radius of the disc is 3 and its thickness is 0.25 , and the total width of the rim is 1 and its thickness is 0.25 , unless mentioned otherwise.

In all the cases, the number of blades is assumed to be 16 , hence the whole structure is divided into 16 sections.

The reason for this is that the rim must be divided into at least 16 divisions in the tangential direction to obtain good accuracy: within 2%. In the axial direction, the rim is divided into 4 equal divisions. The disc is divided into 16 divisions in the tangential direction and 3 divisions in the radial direction.

Each blade is divided into four divisions in each direction. It is known that these numbers of divisions, whether on the disc, the rim or the blades give results to 3% accuracy.

Also, unless mentioned otherwise, the value of Poisson's ratio is taken as 0.3 in all the computations.

The natural frequency is expressed as a nondimensional quantity, defined as

$$\Omega = \omega L^2 \sqrt{\rho t/D} \qquad (6.15)$$

where L is the length, t is the thickness of the blade, D is the flexural rigidity and t=L/16.

6.4.1 Square Plates on a Rimmed Disc

In the first example, the blades are considered as flat rectangular plates of aspect ratio 1 and thickness 1/16. Using the present method, the problem of a bladed rimmed disc is investigated.

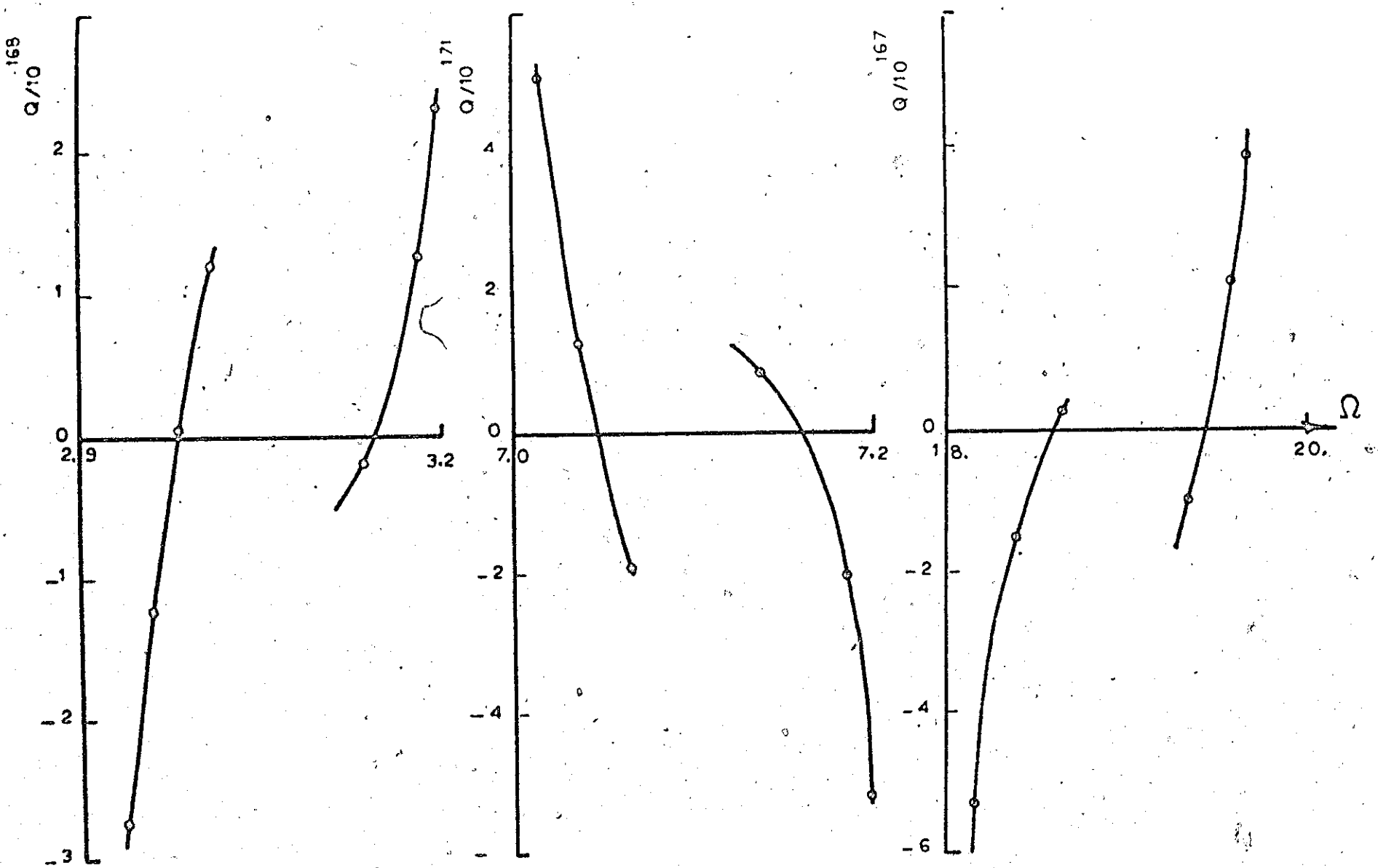

Figure 38

Variation of Determinant of Matrix Q with Frequency for a Bladed Rimmed Disc (Blades considered as Square Plates, $R_i/R_o=0.33$)

TABLE XVI

Nondimensional Frequencies (Ω) of Square Plates on a Rimmed Disk

Blades' Mode Shape	Cantilever Plates	Plates Mounted on a Rimmed Disk
	Finite Element Method	Transfer Matrix-Finite Element Method
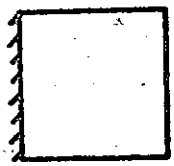	3.44	2.98-3.14
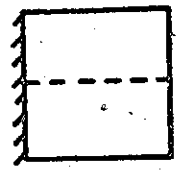	8.51	7.05-7.16
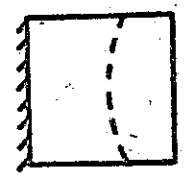	21.18	18.6-19.36

Figure (38) shows the variation of the determinant with the frequency. Results for the first 3 natural frequencies are given in Table XVI.

For cantilever plates of constant thickness, the first few natural frequencies are obtained using the finite element method, and the results are included in Table XVI for comparison. It should be emphasized that both cases; the cantilever plates and the plates on a rimmed disc; are for identical mesh sizes of the plates (4x4).

It is observed from Figure (38) and Table XVI that, for the bladed rimmed disc, there is not a single frequency corresponding to a specified mode shape for the blades, but a band of frequencies all lower than the one obtained for the cantilever plate. The differences between the results for cantilever plate and a bladed rimmed disc varies between 9% and 17%. It is to be mentioned that each band contains a number of frequencies equal to the number of blades on the disc, which is 16 in our case, and some of the frequencies, within a band, may be repeated.

6.4.2 Pretwisted Plates on a Rimmed Disc

The method is applied to the case of pretwisted plates on a rimmed disc, as this shape closely resembles a turbo - machinery blade. The blades are assumed to have a total pretwist of 40°. A linear variation of pretwist along the length of the blade is assumed. The blades have aspect ratio

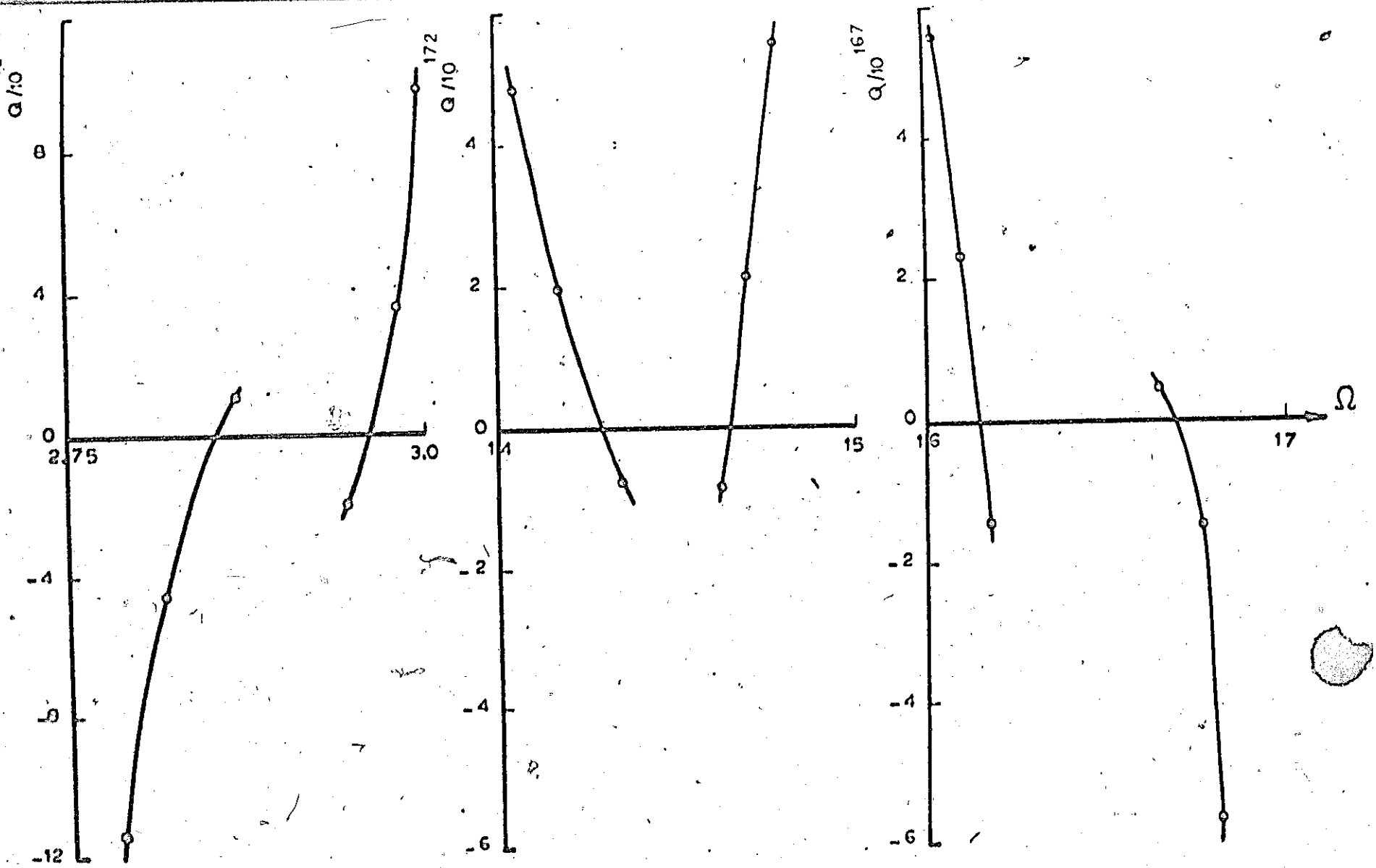

Figure 39

Variation of Determinant of Matrix Q with Frequency for a Bladed Rimmed Disc (Blades considered as Pretwisted Square Plates, $R_i/R_o=0.33$)

TABLE XVII

Nondimensional Frequencies (Ω) of Pretwisted Square Plates on a Rimmed Disk

(Pretwist Angle = 40°)

Blades' Mode Shape	Cantilever Plates	Plates Mounted on a Rimmed Disk
	Finite Element Method	Transfer Matrix-Finite Element Method
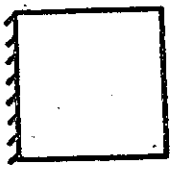	3.30	2.85-2.96
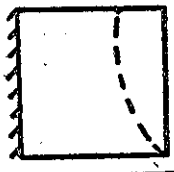	16.67	14.3-14.66
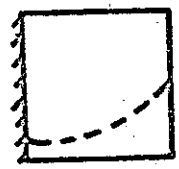	18.03	16.16-16.70

of 1 and their thickness is 1/16.

The variation of the value of the determinant with frequency is shown in Figure (39). The results of the computations are given in Table XVII. Also given in the Table are the values of the natural frequencies of pretwisted cantilever plates as obtained by the finite element method [2].

Again, in this case the natural frequencies are lower than those obtained for the case of pretwisted cantilever plates.

Comparing the results for this case, with the results obtained in case (6.4.1), would give an indication on the effect of pretwist on the natural frequencies.

6.4.3 Effect of Increasing the Inner Radius of the Disc

This case is similar to case (6.4.1), except that the inner radius of the disc is assumed to be equal to 2.0. The blades again have aspect ratio of 1 and thickness of 1/16.

The variation of the determinant with the frequency is shown in Figure (40). The results of the computations are given in Table XVIII.

It is observed that the natural frequencies are higher than those obtained in case (6.4.1), and also the frequency band width is decreased.

6.5 Concluding Remarks

The transfer matrix - finite element technique was

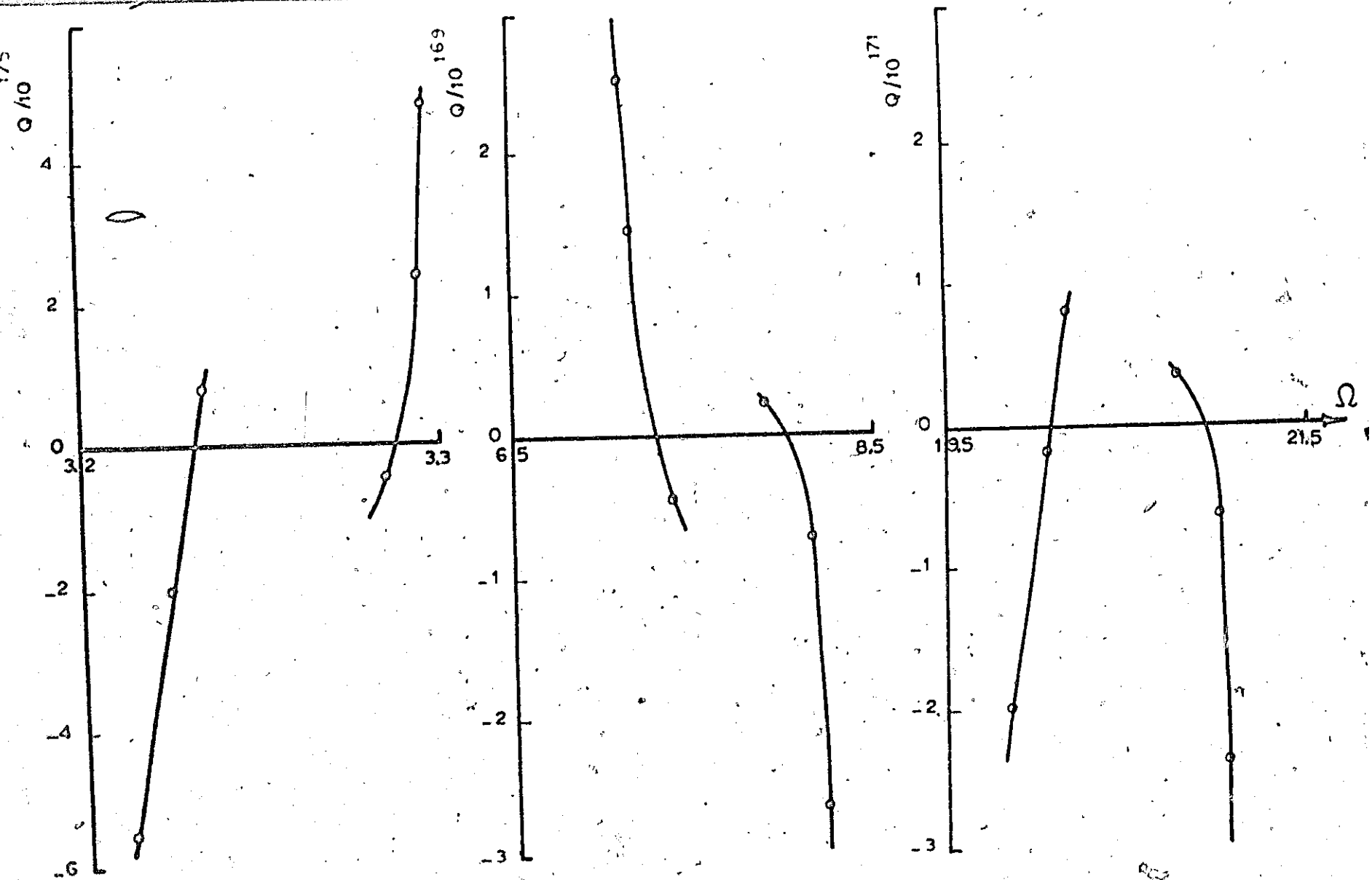

Figure 40

Variation of Determinant of Matrix Q with Frequency for a Bladed Rimmed Disc (Blades considered as Square Plates, R_i/R_o=0.47)

TABLE XVIII

Nondimensional Frequencies (Ω) of Square Plates on a Rimmed Disk

Effect of Changing R_i/R_o of the Disk

Blades' Mode Shape	Transfer Matrix-Finite Element Method	
	$R_i/R_o = 0.33$	$R_i/R_o = 0.67$
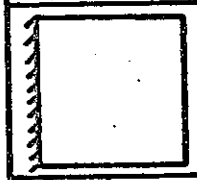	2.98-3.14	3.23-3.29
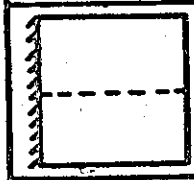	7.05-7.16	7.30-8.02
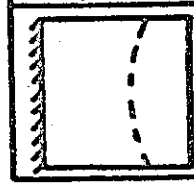	18.60-19.36	20.10-20.94

applied to a bladed rimmed disc. The disc and the rim were assumed to be more rigid, or thicker, than the blades, which is usually the case, so that vibrations will be mainly confined to the blades (the lowest nondimensional frequency of the disc alone is about 240). The first three natural frequencies were obtained for two different cases, first the blades were assumed as square plates of constant thickness, then they were assumed as pretwisted plates. It was found that there is not a single frequency for a specific mode shape for the blades, but a band of frequencies. The range of this band is lower than for the corresponding cantilever blades case, the average difference being about 12%. It is to be mentioned that each band contains a number of frequencies equal to the number of blades on the disc.

Also, it was found that as the ratio of the inner to outer radius of the disc increases, and consequently the disc becomes more rigid, the width of the bands decreases and the frequencies approach more closely to the cantilever blades case.

It is to be noted that similar conclusions were obtained by Ellington and McCallion [13]. The computing time used by the present method (on CDC 6400 Computer) to get a single value of the determinant is about 7 minutes.

CHAPTER 7

CONCLUSIONS

The development of an in-plane annular sector finite element has been presented. The element has 8 degrees of freedom in polar coordinates. The accuracy of the element was tested by two numerical examples, and it gave satisfactory results.

Also the development of two modified, relatively simple finite cylindrical shell elements has been presented. The first element has 20 degrees of freedom and the second has 28 degrees of freedom.

It has been found from eigenvalue analysis of the elements that the first model contained an adequate representation of only four rigid body modes, whereas the second contained all six. Naturally the second element gives better results, but it requires about double the computer size required by the first element. These two elements should prove extremely useful for static and dynamic problems involving rectangular portions of cylindrical shells, particularly since such configurations are very difficult to analyze by ordinary analytical techniques.

It was found that many elements, using the 20 degrees of freedom element, would have to be used before a reasonably accurate prediction of the vibration frequencies of a curved

fan blade could be obtained. On the other hand, use of the 28 degrees of freedom element resulted in quite rapid convergence.

The accuracy of the transfer matrix - finite element method is tested by solving several vibration problems of plates and shells, for which analytical or experimental results are available. The method is observed to give good predictions for the test problems, and much more accuracy can be obtained with this method, than is obtained with the finite element method.

In the finite element approach the size of the matrix to be considered is equal to the total number of degrees of freedom for the entire structure. In the present method, the size of the matrix is equal to the number of degrees of freedom for one strip. A much smaller digital computer is thus sufficient. The frequencies are determined by calculating the determinant of a matrix $[Q]$ at various values for the frequency. The size of the matrix $[Q]$ is equal to half the number of degrees of freedom on one strip.

Since the present method is a trial method, it usually takes more computing time than that required by the finite element method. However, a lumped mass approximation may be done before using the transfer matrix - finite element technique to get the ranges of the natural frequencies.

Finally, the present method was used to calculate the first few natural frequencies of nonrotating low aspect ratio

turbo-machinery blades mounted on a rimmed disc. The disc was treated as assembly of annular sector finite elements, the rim was treated as an assembly of cylindrical shell elements and the blades were considered as an assembly of small flat triangular elements.

It was found that the natural frequencies obtained are lower than those obtained for cantilever blades. The average difference is about 12%. Also it is observed that there is not a single frequency, for a specific mode shape of the blades, but a band of frequencies.

The method was applied to two cases, first the blades were considered as square flat plates, and then the blades were considered as pretwisted plates. Reasonable results were obtained in both cases. It is also found that as the ratio of the inner to outer radius of the disc increases and consequently the disc becomes more rigid, the width of the frequency bands decreases and the frequencies approach the cantilever blades case.

It is obvious that the present work could be extended to study the effect of: (a) rotation, (b) shrouding of the blades, (c) root flexibility of the blades and (d) existence of small variations between the blades; on the natural frequencies and mode shapes of the whole structure.

REFERENCES

1. Dokainish, M.A. and Jagannath, D.V., "Experimental investigation of Gas Turbine Blade Vibration - A Review", ASME Paper No. 69-Vibr-59, 1969.
2. Rawtani, S., "Vibration Analysis of Rotating Low Aspect Ratio Blades", Ph.D. Thesis, McMaster University, 1970.
3. Zienkiewicz, O.C., "The Finite Element Method in Engineering Science", McGraw-Hill Co., 1971.
4. Holland, I., and Bell, K., "Finite Element Methods in Stress Analysis", TAPIR (Technical Univ. of Norway Press) Trondheim, 1969.
5. Campbell, W., "The Protection of Steam Turbine Disk Wheels from Axial Vibration", ASME Trans., Vol. 46, 1924.
6. Stodola, A., "Steam and Gas Turbines", Translated by L.C. Loewenstein, -Hill Book Company, Inc., New York, N.Y., 2 Volumes, 1927.
7. Malkin, I.,""On a Generalization of Kirchoff's Theory of Transversal Plate Vibrations in the Vibration Problem of Steam Turbine Disks", Journal of Franklin Institute, 1942, 355-370.
8. Freudenreich, J.V.) "Vibrations of Steam Turbine Disc", Engineering, Jan. 2, 1925, 2-4.

9. Singh,B.R. and Nandeeswaraiya,N.S.," Vibration Analysis of Turbine Disc in its Plane", Journal of the Institution of Engineers, India, Vol. 40, NO. 1, Pt. 2, Sept. 1959.

10. Yamada , K.,"Vibrations of Turbine Disc in its Plane", Proc. of the second Japan National Congress for Applied Mech., 1952.

11. Tumura, T. and Oba, Z.,"Circumferential Vibrations of a Turbine Disc",Proc. of the first Japan National Congress for Applied Mech., 1951.

12. Fillipov, A.P.,"Tangential Vibrations of Turbine Blades Taking into Account Vibrations of Disc in its Plane", (In Ukranian), Prikl Mekh, Vol.6, No. 3, 1960.

13. Ellington,J.P. and McCallion, H.,"Blade Frequency of Turbines, Effect of Disc Elasticity", Engineering, Vol. 187, No. 4862, May 15, 1959.

14. Sohngen, H.,"Vibrational Behaviour of Blade Ring in Vacuum",(In German), Dtsch. Versuchsanstalt Luftabart E.V. Report 1, Aug. 1955.

15. Wagner, J.T.,"Coupling of Turbomachine Blade Vibrations Through the Rotor", ASME Paper No. 66-WA/GT-5, p966.

16. Ewins, D.J., "The Effects of Detuning Upon the Forced Vibrations of Bladed Disks" Journal of Sound and Vibrations, Vol. 9, No. 1, 1969.

17. Dye, R.C.F. and Henry, T.A., "Vibration Amplitudes of Compressor Blades Resulting From Scatter in Blade

Natural Frequencies", ASME Trans., Journal of Engineering for Power, july 1969.

18. Anderson, R.G., Irons, B.M and Zienkiewicz, O.C., "Vibration and Stability of Plates Using Finite Elements", Int. J. of Solids and Structures, 4, 1968.

19. Hurty, W.C., "Vibrations of Structural Systems by Component Mode Synthesis", Proceedings of ASCE, 85, EM4, 1960.

20. Hurty, W.C., "Dynamic Analysis of Structural Systems Using Component Modes", AIAA Journal, Vol. 3, 1965.

21. Craig, A., and Bampton, C., "Coupling of Substructures for Dynamic Analysis", AIAA Journal, Vol. 6, No. 7, July 1968.

22. Goldman, R.L., "Vibration Analysis by Dynamic Partioning", AIAA Journal, Vol. 7, 1969.

23. Gladwell, G., "Branch Modes Analysis of Vibrating Systems", Journal of Sound and Vibration, 1, 1964.

24. Uhrig, R., "The transfer Matrix Method Seen as One Method of Structural Analysis Among Others", J. of Sound and Vibration, 4, 2, 1966.

25. Pestel, C. and Leckie, A., "Matrix Methods in Elastomechanics", McGraw-Hill Book Company, Inc., 1963.

26. Fuhrke, H., "Bistimmung Von Balkenschwingungen mit Hilfe des Matrizenkalküls", Ing. Archiv, 24, 1955.

27. Leckie, F. and Pestel, E., "Transfer-Matrix Fundamentals", Int. J. Mech. Sci., Vol. 2, 1960.

28. Pestel, E., "Rectangular Transfer Matrices", Int. J. Mech.

Sci., Vol. 5, 1963.

29. Whitehead,D.S., "A Symmetry Property of Transfer Matrices", The Aeronautical Journal of the Royal Aero. Society, Aug., 1969.

30. Bergmann, H.W. and Pestel, E., "Die Anwendung von Übertragungsmatrizen auf die Untersuchung von Deltafliigen", Zeitschrift Für Flugwissenschaften, March, 1962.

31. Gradowezyk, M.H., "The Exact Theory of Bending of Prismatic Shells - An Application of Transfer Matrices", Ingenieur-Archiv, 1963.

32. Ramaih, M., "Computer Analysis of Folded Plates by the Method of Transfer Matrices", Journal of the Institution of Engineers, India, 1964.

33. Dokainish, M.A., "A New Approach for Plate Vibrations: Combination of Transfer Matrix and Finite-Element Technique", ASME Trans., Journal of Engineering for Industry, 94, 2, 1972.

34. Leckie, F.A., "The Application of Transfer Matrices to Plate Vibrations", Ingenieur-Archiv, XXXII, 1963.

35. Hrennikoff, A., "Solution of Problems of Elasticity by the Framework Method", J. of Applied Mechanics, ASME Trans., 8, 1941.

36. Geradin, M., "The Computational Efficiency of a New Minimization Algorithm for Eigenvalue Analysis", Journal of Sound and Vibration, 19, 13, 1971.

37. Fried, I., "Optimal Gradient Minimization Scheme for Finite Element Eigenproblems", Journal of Sound and Vibration, 20, 3, 1972.

38. Ergatoudis, I., Irons, B.M., and Zienkiewicz, O.C., "Curved Isoparametric Quadrilatiral Elements for Finite Element Analysis", Int. Journal of Solids and Structures, Vol. 4, Jan. 1968.

39. Olsen, M.D., Lindberg, G.M., and Tulloch, H.A., "Finite Plate - Bending Elements in Polar Co - Ordinates", National Research Council of Canada, Aero. Rep. LR-512, Oct. 1968.

40. Wang, C.T., "Applied Elasticity", McGraw Hill Book Company, Inc., 1953.

41. Sawko, F. and Merriman, P.A., "An Annular Segement Finite Element for Plates Bending", Int. J. for Numerical Methods in Engineering, Vol. 3, 1971.

42. Timoshenko, S., and Goodier, J.N., "Theory of Elasticity", McGraw - Hill Book Company, Inc., Second Edition, 1951.

43. Grafton, P., and Strome, D., "Analysis of Axisymmetric Shells by the Direct Stiffness Method", AIAA J., Vol. 1, No. 10, 1963.

44. Gallegher, R.H., "The Development and Evaluation of Matrix Methods for Thin Shells Structural Analysis", Ph. D. Thesis, State University of New York, Buffalo, N.Y., 1966.

45. Cantin, R. and Clough, R., "A Curved Cylindrical Shell

Discrete Element", AIAA Journal, Vol. 6, No. 6, 1968.

46. Conner, J. and Brebbia, C., "Stiffness Matrix for Shallow Rectangular Shell Element", Proc. ASCE,Journal of the Engg. Mech. Div., No. EN2, April 1968.

47. Bogner, F.K., Fox, R.L. and Schmit, L.A., "A Cylindrical Shell Discrete Element", AIAA Journal, Vol. 5, No. 4, 1967.

48. Olsen, M.D. and Lindberg, G.M., "A Finite Cylindrical Shell Element and the Vibrations of a Curved Fan Blade", National Research Council of Canada, Aero. Rep. LR-497, 1968.

49. Rawtani, S. and Dokainish, M.A., "Bending of Pretwisted Cantilever Plates", Canadian Aeronautical Space Inst. Trans., 2, 2, 1969.

50. Rawtani, S. and Dokainish, M.A., "Vibration Analysis of Pretwisted Cantilever Plates", Canadian Aeronautical Space Inst. Trans., 2, 2, 1969.

51. Young, D., "Vibration of Rectangular Plates by the Ritz Method", J. Applied Mechanics, Trans. ASME, 7, 4, 1950.

52. Volterra, E. and Zachmanoglou, E.C., "Dynamics of Vibrations", Merrill Books, Inc., Columbus, Ohio, 1965.

53. Sharma, C. and Johns, D.J., "Vibration Characteristics of a Clamped - Free and Clamped - Ring - Stiffened Circular Cylindrical Shell", J. Sound Vib., 14, 4, 1971.

APPENDIX I

TRANSFORMATION MATRIX BETWEEN CORNER DISPLACEMENTS AND POLYNOMIAL COEFFICIENTS FOR IN-PLANE ANNULAR SECTOR FINITE ELEMENT

IF R1 IS THE INNER RADIUS ,
BETA IS THE INCLUDED ANGLE ,
R2 IS THE OUTER RADIUS ,
D IS THE PLATE FLEXURAL RIGIDITY ,
RO IS THE DINSITY ,
H IS THE THICKNESS , AND
ANEW IS THE POISSON,S RATIO ,
THEN, THE NON-ZERO ELEMENTS OF THE MATRIX ARE GIVEN BY.

```
T(1,1)=1.
T(1,2)=R1
T(2,5)=1.
T(2,6)=R1
T(3,1)=1.
T(3,2)=R2
T(4,5)=1.
T(4,6)=R2
T(5,1)=1.
T(5,2)=R2
T(5,3)=BETA
T(5,4)=R2*BETA
T(6,5)=1.
T(6,6)=R2
T(6,7)=BETA
T(6,8)=R2*BETA
T(7,1)=1.
T(7,2)=R1
T(7,3)=BETA
T(7,4)=R1*BETA
T(8,5)=1.
T(8,6)=R1
T(8,7)=BETA
T(8,8)=R1*BETA
```

APPENDIX II

IN-PLANE STIFFNESS MATRIX K FOR ANNULAR SECTOR FINITE ELEMENT

USING THE DEFINITIONS OF APPENDIX I , ALSO ASSUMING THAT

BBETA=BETA*BETA ,
BBBETA=BETA*BBETA ,
G1=R2-R1 ,
G2=R2*R2-R1*R1 ,
AL=ALOG(R2/R1) ,
TEK=1.+ANEW , AND
TEM=1.-ANEW ,
THEN, THE NON-ZERO ELEMENTS OF THE MATRIX ARE GIVEN BY.
(NOTING THAT IT IS A SYMMETRIC MATRIX)

```
AA(1,1)=BETA*AL
AA(2,1)=TEK*BETA*G1
AA(2,2)=TEK*BETA*G2
AA(3,1)=AL*BBETA/2.
AA(3,2)=TEK*BBETA*G1/2.
AA(3,3)=AL*(BBBETA/3.+TEM*BETA/2.)
AA(4,1)=TEK*BBETA*G1/2.
AA(4,2)=TEK*BBETA*G2/2.
AA(4,3)=TEK*BBBETA*G1/3.+TEM*BETA*G1/2.
AA(4,4)=TEK*BBBETA*G2/3.+TEM*BETA*G2/4.
AA(5,3)=-TEM*BETA*AL/2.
AA(5,4)=-TEM*BETA*G1/2.
AA(5,5)=TEM*BETA*AL/2.
AA(7,1)=BETA*AL
AA(7,2)=TEK*BETA*G1
AA(7,3)=TEK*BBETA*AL/4.
AA(7,4)=(3.*ANEW+1.)*BBETA*G1/4.
AA(7,5)=TEM*BBETA*AL/4.
AA(7,7)=AL*(BETA+TEM*BBBETA/6.)
AA(8,1)=BETA*G1
AA(8,2)=TEK*BETA*G2/2.
AA(8,3)=BBETA*G1/2.
AA(8,4)=TEK*BBETA*G2/4.
AA(8,7)=BETA*G1
AA(8,8)=BETA*G2/2.
```

APPENDIX III

IN-PLANE MASS MATRIX (M/RO*H*BETA) FOR ANNULAR SECTOR FINITE ELEMENT

USING THE DEFINITIONS OF APPENDIX I , ALSO ASSUMING THAT

G1=R2-R1 ,
G2=R2*R2-R1*R1 ,
G3=R2*R2*R2-R1*R1*R1 , AND
G4=R2*R2*R2*R2-R1*R1*R1*R1 ,

THEN, THE NON-ZERO ELEMENTS OF THE MATRIX ARE GIVEN BY. (NOTING THAT IT IS A SYMMETRIC MATRIX)

```
AA(1,1)=G2/2.
AA(2,1)=G3/3.
AA(2,2)=G4/4.
AA(3,1)=BETA*G2/4.
AA(3,2)=BETA*G3/6.
AA(3,3)=BETA*BETA*G2/6.
AA(4,1)=BETA*G3/6.
AA(4,2)=BETA*G4/8.
AA(4,3)=BETA*BETA*G3/9.
AA(4,4)=BETA*BETA*G4/12.
AA(5,5)=AA(1,1)
AA(6,5)=AA(2,1)
AA(6,6)=AA(2,2)
AA(7,5)=AA(3,1)
AA(7,6)=AA(3,2)
AA(7,7)=AA(3,3)
AA(8,5)=AA(4,1)
AA(8,6)=AA(4,2)
AA(8,7)=AA(4,3)
AA(8,8)=AA(4,4)
```

APPENDIX IV

TRANSFORMATION MATRIX BETWEEN CORNER DISPLACEMENTS AND POLYNOMIAL COEFFICIENTS FOR BENDING ANNULAR SECTOR FINITE ELEMENT

USING THE DEFINITIONS OF APPENDIX I , ALSO ASSUMING THAT

RR1=R1*R1 ,
RRR1=R1*R1*R1 ,
RR2=R2*R2 ,
RRR2=R2*R2*R2 ,
BBETA=BETA*BETA , AND
BBBETA=BETA*BBETA ,
THEN, THE NON-ZERO ELEMENTS OF THE MATRIX ARE GIVEN BY.

```
T(1,2)=1.
T(1,5)=2.*R1
T(1,9)=3.*RR1
T(2,3)=1.
T(2,4)=R1
T(2,7)=RR1
T(2,11)=RRR1
T(3,1)=1.
T(3,2)=R1
T(3,5)=RR1
T(3,9)=RRR1
T(4,2)=1.
T(4,5)=2.*R2
T(4,9)=3.*RR2
T(5,3)=1.
T(5,4)=R2
T(5,7)=RR2
T(5,11)=RRR2
T(6,1)=1.
T(6,2)=R2
T(6,5)=RR2
T(6,9)=RRR2
T(7,2)=1.
T(7,4)=BETA
T(7,5)=T(4,5)
T(7,7)=2.*BETA*R2
T(7,8)=BBETA
T(7,9)=T(4,9)
T(7,11)=3.*BETA*RR2
T(7,12)=BBBETA
```

```
T(8,3)=1.
T(8,4)=R2
T(8,6)=2.*BETA
T(8,7)=RR2
T(8,8)=T(7,7)
T(8,10)=3.*BBETA
T(8,11)=RRR2
T(8,12)=3.*BBETA*R2
T(9,1)=1.
T(9,2)=R2
T(9,3)=BETA
T(9,4)=BETA*R2
T(9,5)=RR2
T(9,6)=BBETA
T(9,7)=BETA*RR2
T(9,8)=BBETA*R2
T(9,9)=RRR2
T(9,10)=BBBETA
T(9,11)=BETA*RRR2
T(9,12)=BBBETA*R2
T(10,2)=1.
T(10,4)=BETA
T(10,5)=2.*R1
T(10,7)=2.*BETA*R1
T(10,8)=BBETA
T(10,9)=T(1,9)
T(10,11)=3.*BETA*RR1
T(10,12)=BBBETA
T(11,3)=1.
T(11,4)=R1
T(11,6)=2.*BETA
T(11,7)=RR1
T(11,8)=T(10,7)
T(11,10)=T(8,10).
T(11,11)=RRR1
T(11,12)=3.*BBETA*R1
T(12,1)=1.
T(12,2)=R1
T(12,3)=BETA
T(12,4)=BETA*R1
T(12,5)=RR1
T(12,6)=BBETA
T(12,7)=BETA*RR1
T(12,8)=BBETA*R1
T(12,9)=RRR1
T(12,10)=BBBETA
T(12,11)=BETA*RRR1
T(12,12)=BBBETA*R1
```

APPENDIX V

BENDING STIFFNESS MATRIX (K/D) FOR ANNULAR SECTOR FINITE ELEMENT

USING THE DEFINITIONS OF APPENDIX I , ALSO ASSUMING THAT

RR1=R1*R1 ,
RRR1=R1*R1*R1 ,
RR2=R2*R2 ,
RRR2=R2*R2*R2 ,
BBETA=BETA*BETA ,
BBBETA=BETA*BBETA ,
AL=ALOG(R2/R1) ,
TEK=1.+ANEW , AND
TEM=1.-ANEW ,
THEN, THE NON-ZERO ELEMENTS OF THE MATRIX ARE GIVEN BY.
(NOTING THAT IT IS A SYMMETRIC MATRIX)

```
AA(2,2)=BETA*AL
AA(3,3)=TEM*BETA*(1./RR1-1./RR2)
AA(4,2)=0.5*BETA*AA(2,2)
AA(4,4)=BBETA*AA(2,2)/3.
AA(5,2)=2.*TEK*BETA*G1
AA(5,4)=BETA*AA(5,2)/2.
AA(5,5)=4.*TEK*BETA*G2
AA(6,2)=2.*BETA*(1./R1-1./R2)
AA(6,3)=BETA*AA(3,3)
AA(6,4)=BETA*AA(6,2)/2.
AA(6,5)=4.*TEK*AA(2,2)
AA(6,6)=2.*(1.+2.*TEM*BBETA/3.)*AA(3,3)/TEM
AA(7,2)=AA(5,4)
AA(7,3)=-2.*TEM*AA(2,2)
AA(7,4)=2.*BETA*AA(5,4)/3.
AA(7,5)=BETA*AA(5,5)/2.
AA(7,6)=4.*ANEW*BETA*AA(2,2)
AA(7,7)=(0.5*TEM+2.*TEK*BBETA/3.)*2.*BETA*G2
AA(8,2)=0.5*(4.+(2./3.)*BBETA)*AA(2,2)
AA(8,4)=0.5*BETA*(2.+0.5*BBETA)*AA(2,2)
AA(8,5)=2.*TEK*BETA*(2.+BBETA/3.)*G1
AA(8,6)=(4.+2.*BBETA/3.)*AA(6,2)/2.
AA(8,7)=0.5*TEK*BBETA*(4.+BBETA)*G1
AA(8,8)=(4.+4.*BBETA/3.+0.2*BBETA*BBETA)*AA(2,2)
AA(9,2)=2.*BETA*(0.5+ANEW)*G2
AA(9,4)=BETA*AA(9,2)/2.
AA(9,5)=6.*TEK*BETA*G3
AA(9,6)=6.*(1.+2.*ANEW)*BETA*G1
```

```
      AA(9,8)=(6.+BBETA)*AA(9,4)/(1.5*BETA)
      AA(9,9)=(9./4.)*(5.+4.*ANEW)*BETA*G4
      AA(10,2)=3.*BETA*AA(6,2)/2.
      AA(10,3)=BBETA*AA(3,3)
      AA(10,4)=BBETA*AA(6,2)
      AA(10,5)=6.*TEK*BETA*AA(2,2)
      AA(10,6)=3.*(1.+0.5*TEM*BBETA)*AA(6,3)/TEM
      AA(10,7)=2.*(1.+3.*ANEW)*BBETA*AA(2,2)
      AA(10,8)=1.5*BETA*(4.+BBETA)*AA(6,2)/2.
      AA(10,9)=9.*(1.+2.*ANEW)*BBETA*G1
      AA(10,10)=2.*BBETA*(3.+0.9*TEM*BBETA)*AA(3,3)/TEM
      AA(11,2)=BETA*AA(9,2)/2.
      AA(11,3)=-4.*TEM*BETA*G1
      AA(11,4)=BBETA*AA(9,2)/3.
      AA(11,5)=AA(9,7)
      AA(11,6)=(10.*ANEW-1.)*BBETA*G1
      AA(11,7)=(4.*TEM/3.+2.*TEK*BBETA)*BETA*G3
      AA(11,8)=(3./8.)*(1.+2.*ANEW)*BBETA*(4.+BBETA)*G2
      AA(11,9)=BETA*AA(9,9)/2.
      AA(11,10)=2.*(1.+8.*ANEW)*BBBETA*G1
      AA(11,11)=2.*((3./8.)*(5.+4.*ANEW)*BBETA+TEM)*BETA*G4
      AA(12,2)=(6.+0.5*BBETA)*AA(4,2)
      AA(12,4)=(2.+0.2*BBETA)*3.*AA(4,4)
      AA(12,5)=0.5*TEK*BBETA*(12.+BBETA)*G1
      AA(12,6)=0.5*(12.+BBETA)*AA(10,2)/3.
      AA(12,7)=2.*TEK*BBBETA*(2.+0.2*BBETA)*G1
      AA(12,8)=0.5*(12.+4.*BBETA+BBETA*BBETA/3.)*BETA*AA(2,2)
      AA(12,9)=(4.5*(1.+2.*ANEW)+(3./8.)*(1.+2.*ANEW)*BBETA)*BBETA*
     1G2
      AA(12,10)=3.*(2.+0.2*BBETA)*AA(10,4)
      AA(12,11)=3.*(2.+0.2*BBETA)*AA(11,4)
      AA(12,12)=(12.+BBETA*(12./5.+BBETA/7.))*BBETA*AA(2,2)
```

APPENDIX VI

BENDING MASS MATRIX (M/RO*H*BETA) FOR ANNULAR SECTOR FINITE ELEMENT

USING THE DEFINITIONS OF APPENDIX I , ALSO ASSUMING THAT

G1=R2-R1 ,
G2=R2*R2-R1*R1 ,
G3=R2*R2*R2-R1*R1*R1 , AND
G4=R2*R2*R2*R2-R1*R1*R1*R1 ,
THEN, THE NON-ZERO ELEMENTS OF THE MATRIX ARE GIVEN BY.
(NOTING THAT IT IS A SYMMETRIC MATRIX)

```
AA(1,1)=G2/2.
AA(2,1)=G3/3.
AA(2,2)=G4/4.
AA(3,1)=BETA*AA(1,1)/2.
AA(3,2)=BETA*AA(2,1)/2.
AA(3,3)=BETA*AA(3,1)*(4./6.)
AA(4,1)=AA(3,2)
AA(4,2)=BETA*AA(2,2)/2.
AA(4,3)=BETA*AA(4,1)*(6./9.)
AA(4,4)=BETA*AA(4,2)*(8./12.)
AA(5,1)=AA(2,2)
AA(5,2)=(R2**5-R1**5)/5.
AA(5,3)=AA(4,2)
AA(5,4)=BETA*AA(5,2)/2.
AA(5,5)=(R2**6-R1**6)/6.
AA(6,1)=AA(3,3)
AA(6,2)=AA(4,3)
AA(6,3)=BETA*AA(6,1)*(6./8.)
AA(6,4)=BETA*AA(6,2)*(9./12.)
AA(6,5)=AA(4,4)
AA(6,6)=BBETA*AA(3,3)*0.6
AA(7,1)=AA(4,2)
AA(7,2)=AA(5,4)
AA(7,3)=AA(6,5)
AA(7,4)=BETA*AA(5,4)*(10./15.)
AA(7,5)=BETA*(R2**6-R1**6)/12.
AA(7,6)=BETA*AA(7,3)*(12./16.)
AA(7,7)=BETA*AA(7,5)*(12./18.)
AA(8,1)=AA(4,3)
AA(8,2)=AA(7,3)
AA(8,3)=AA(6,4)
AA(8,4)=AA(7,6)
AA(8,5)=AA(7,4)
```

```
AA(8,6)=BETA*AA(6,4)*0.8
AA(8,7)=BETA*AA(8,5)*0.75
AA(8,8)=BETA*AA(8,4)*0.8
AA(9,1)=AA(5,2)
AA(9,2)=AA(5,5)
AA(9,3)=AA(5,4)
AA(9,4)=AA(7,5)
AA(9,5)=(P2**7-R1**7)/7.
AA(9,6)=BETA*AA(9,3)*(10./15.)
AA(9,7)=BETA*AA(9,5)*0.5
AA(9,8)=BETA*AA(9,4)*(12./18.)
AA(9,9)=(R2**8-R1**8)/8.
AA(10,1)=AA(6,3)
AA(10,2)=AA(6,4)
AA(10,3)=AA(6,6)
AA(10,4)=AA(8,6)
AA(10,5)=AA(8,4)
AA(10,6)=BETA*AA(10,3)*(10./12.)
AA(10,7)=BETA*AA(10,5)*0.8
AA(10,8)=BETA*AA(10,4)*(15./18.)
AA(10,9)=BETA*AA(9,6)*0.75
AA(10,10)=BETA*AA(10,6)*(12./14.)
AA(11,1)=AA(5,4)
AA(11,2)=AA(7,5)
AA(11,3)=AA(7,4)
AA(11,4)=AA(7,7)
AA(11,5)=AA(9,7)
AA(11,6)=AA(8,7)
AA(11,7)=BETA*AA(11,5)*(14./21.)
AA(11,8)=BETA*AA(11,4)*(18./24.)
AA(11,9)=BETA*AA(9,9)*0.5
AA(11,10)=BETA*AA(11,6)*0.8
AA(11,11)=BETA*AA(11,9)*(16./24.)
AA(12,1)=AA(6,4)
AA(12,2)=AA(7,6)
AA(12,3)=AA(8,6)
AA(12,4)=AA(8,8)
AA(12,5)=AA(8,7)
AA(12,6)=AA(10,8)
AA(12,7)=AA(11,10)
AA(12,8)=BETA*AA(12,4)*(20./24.)
AA(12,9)=AA(11,8)
AA(12,10)=BETA*AA(12,6)*(18./21.)
AA(12,11)=BETA*AA(12,9)*0.8
AA(12,12)=BETA*AA(12,8)*(24./28.)
```

APPENDIX VII

(20*20)
TRANSFORMATION MATRIX BETWEEN CORNER DISPLACEMENTS AND POLYNOMIAL COEFFICIENTS FOR CYLINDRICAL SHELL ELEMENT

IF A IS THE STRAIGHT SIDE ,
B IS THE CURVED SIDE ,
ANEW IS THE POISSON,S RATIO ,
R IS THE RADIUS OF THE SHELL ,
D IS THE FLEXURAL RIGIDITY ,
H IS THE THICKNESS , AND
RO IS THE DENSITY ,

AND ASSUMING THAT

A2=A**2 ,
A3=A**3 ,
A4=A**4 ,
A5=A**5 ,
A6=A**6 ,
A7=A**7 ,
B2=B**2 ,
B3=B**3 ,
B4=B**4 ,
B5=B**5 ,
B6=B**6 ,
B7=B**7 ,
H2=H**2 ,
H3=H**3 ,
H4=H**4 ,
AB=A*B ,
AB12=A*B2 ,
AB13=A*B3 ,
AB14=A*B4 ,
AB21=A2*B ,
AB22=A2*B2 ,
AB23=A2*B3 ,
AB24=A2*B4 ,
AB31=A3*B ,
AB32=A3*B2 ,
AB33=A3*B3 ,
AB34=A3*B4 ,
AB41=A4*B ,
AB42=A4*B2 ,
AB43=A4*B3 , AND
AB44=A4*B4 ,

THEN, THE NON-ZERO ELEMENTS OF THE MATRIX ARE GIVEN BY.

```
T(1,10)=1.
T(2,11)=1.
T(3,9)=1.
T(4,1)=1.
T(5,5)=1.
T(6,10)=1.
T(6,13)=2.*A
T(6,17)=3.*A2
T(7,11)=1.
T(7,12)=A
T(7,15)=A2
T(7,19)=A3
T(8,9)=1.
T(8,10)=A
T(8,13)=A2
T(8,17)=A3
T(9,1)=1.
T(9,2)=A
T(10,5)=1.
T(10,6)=A
T(11,10)=1.
T(11,12)=B
T(11,13)=2.*A
T(11,15)=2.*AB
T(11,16)=B2
T(11,17)=3.*A2
T(11,19)=3.*AB21
T(11,20)=B3
T(12,11)=1.
T(12,12)=A
T(12,14)=2.*B
T(12,15)=A2
T(12,16)=2.*AB
T(12,18)=3.*B2
T(12,19)=A3
T(12,20)=3.*AB12
T(13,9)=1.
T(13,10)=A
T(13,11)=B
T(13,12)=AB
T(13,13)=A2
T(13,14)=B2
T(13,15)=AB21
T(13,16)=AB12
T(13,17)=A3
T(13,18)=B3
T(13,19)=AB31
T(13,20)=AB13
T(14,1)=1.
T(14,2)=A
T(14,3)=B
```

```
T(14,4)=AB
T(15,5)=1.
T(15,6)=A
T(15,7)=B
T(15,8)=AB
T(16,10)=1.
T(16,12)=B
T(16,16)=B2
T(16,20)=B3
T(17,11)=1.
T(17,14)=2.*B
T(17,18)=3.*B2
T(18,9)=1.
T(18,11)=B
T(18,14)=B2
T(18,18)=B3
T(19,1)=1.
T(19,3)=B
T(20,5)=1.
T(20,7)=B
```

APPENDIX VIII

(20*20)
STIFFNESS MATRIX (K/D)
FOR CYLINDRICAL SHELL ELEMENT

USING THE DEFINITIONS OF APPENDIX VII , ALSO ASSUMING THAT

```
V=1./R
VV=1./R**2
TEM=(1.-ANEW)/2.
HV=H*V
HV2=H2*V
HVV2=H2*VV
HVV=H*VV
BV=B*V
BVV=B*VV
BVV2=B2*VV
AV=A*V
AVV=A*VV
AVV2=A2*VV
AH=A*H
BH=B*H
TEK=1.+HV/2.
TET=1.+HV
```

THEN, THE NON-ZERO ELEMENTS OF THE MATRIX ARE GIVEN BY.
(NOTING THAT IT IS A SYMMETRIC MATRIX)

```
AA(2,2)=1.
AA(3,3)=TEM
AA(4,2)=B/2.
AA(4,3)=TEM*A/2.
AA(4,4)=B2/3.+TEM*A2/3.
AA(6,3)=TEM*TET
AA(6,4)=AA(6,3)*A/2.
AA(6,6)=TEM*(1.+2.*HV+4.*HVV2/3.)
AA(7,2)=ANEW*TEK
AA(7,4)=AA(7,2)*B/2.
AA(7,7)=TET+HVV2/3.
AA(8,2)=ANEW*TEK*A/2.
AA(8,3)=TEM*TET*B/2.
AA(8,4)=ANEW*TEK*AB/4.+TEM*TET*AB/4.
AA(8,6)=AA(6,6)*B/2.
AA(8,7)=AA(7,7)*A/2.
AA(8,8)=(A2/3.)*(TET+HVV2/3.)+TEM*(B2/3.)*(1.+2.*HV+4.*HVV2/3
1.)
AA(9,2)=ANEW*V
AA(9,4)=AA(9,2)*B/2.
AA(9,7)=V*TEK
```

```
AA(9,8)=AA(9,7)*A/2.
AA(9,9)=VV
AA(10,2)=ANEW*AV/2.
AA(10,4)=AA(10,2)*B/2.
AA(10,7)=TEK*AV/2.
AA(10,8)=AA(10,7)*A*(2./3.)
AA(10,9)=AVV/2.
AA(10,10)=AA(10,9)*A*(2./3.)
AA(11,2)=ANEW*BV/2.
AA(11,4)=AA(11,2)*B*(2./3.)
AA(11,7)=TEK*BV/2.
AA(11,8)=AA(11,7)*A/2.
AA(11,9)=BVV/2.
AA(11,10)=AA(11,9)*A/2.
AA(11,11)=BVV2/3.
AA(12,2)=ANEW*A*BV/4.
AA(12,3)=-TEM*H
AA(12,4)=ANEW*(AB12*V/6.)-TEM*AH/2.
AA(12,6)=-TEM*(H/2.+2.*HV2/3.)*2.
AA(12,7)=TEK*AB*V/4.
AA(12,8)=AA(12,7)*A*2./3.-TEM*(BH/2.+2.*B*HV2/3.)
AA(12,9)=AB*VV/4.
AA(12,10)=A2*BVV/6.
AA(12,11)=AB12*VV/6.
AA(12,12)=A2*BVV2/9.+4.*TEM*H2/3.
AA(13,2)=-H+ANEW*A2*V/3.
AA(13,4)=-BH/2.+ANEW*A2*BV/6.
AA(13,7)=-ANEW*H-2.*ANEW*HV2/3.+TEK*A2*V/3.
AA(13,8)=-ANEW*AH/2.+TEK*A3*V/4.-ANEW*A*H2*V/3.
AA(13,9)=-ANEW*HV+A2*VV/3.
AA(13,10)=-ANEW*A*HV/2.+A3*VV/4.
AA(13,11)=AA(13,9)*B/2.
AA(13,12)=AA(13,10)*B/2.
AA(13,13)=4.*H2/3.-4.*ANEW*A2*H*V/6.+A4*VV/5.
AA(14,2)=ANEW*(B2*V/3.-H)
AA(14,4)=ANEW*(B3*V/4.-B*H/2.)
AA(14,7)=TEK*B2*V/3.-H-2.*HV2/3.
AA(14,8)=AA(14,7)*A/2.
AA(14,9)=B2*VV/3.-HV
AA(14,10)=AA(14,9)*A/2.
AA(14,11)=B3*VV/4.-B*HV/2.
AA(14,12)=AA(14,11)*A/2.
AA(14,13)=-2.*ANEW*(B2*HV/6.-2.*H2/3.)+AB22*VV/9.-A2*HV/3.
AA(14,14)=B4*VV/5.-4.*B2*HV/6.+4.*H2/3.
AA(15,2)=-BH/2.+ANEW*A2*BV/6.
AA(15,3)=-TEM*AH
AA(15,4)=-B2*H/3.+ANEW*AB22*V/9.-4.*TEM*A2*H/6.
AA(15,6)=-2.*TEM*(AH/2.+4.*A*HV2/6.)
AA(15,7)=-ANEW*BH/2.+A2*BV*TEK/6.-ANEW*B*H2*V/3.
AA(15,8)=(-2.*ANEW-4.*TEM)*AB*H/9.+(-2.*ANEW-8.*TEM)*AB*HV2/1
12.+TEK*AB31*V/8.
```

```
AA(15,9)=-ANEW*B*HV/2.+A2*BVV/6.
AA(15,10)=-ANEW*AB*HV/4.+A3*BVV/8.
AA(15,11)=AA(15,9)*B*2./3.
AA(15,12)=AA(15,10)*B*2./3.+8.*TEM*A*H2/6.
AA(15,13)=4.*B*H2/6.-ANEW*AB21*HV/3.+A4*BVV/10.
AA(15,14)=-ANEW*B3*HV/4.+AB23*VV/12.+4.*ANEW*B*H2/6.-AB21*HV/
16.
AA(15,15)=4.*B2*H2/9.-4.*ANEW*AB22*HV/18.+AB42*VV/15.+16.*TEM
1*A2*H2/9.
AA(16,2)=ANEW*(AB12*V/6.-AH/2.)
AA(16,3)=-TEM*BH
AA(16,4)=ANEW*(AB13*V/8.-AB*H/4.)-TEM*AB*H/2.
AA(16,6)=-4.*TEM*(BH/4.+B*H2*V/3.)
AA(16,7)=TEK*AB12*V/6.-AH*(0.5+HV/3.)
AA(16,8)=TEK*AB22*V/9.-A2*H/3.-2.*A2*HV2/9.-4.*TEM*(B2*H/6.+B
12*HV/4.5)
AX=A*B2*VV
BX=A*HV
AA(16,9)=AX/6.-BX/2.
AA(16,10)=A*(AX/9.-BX/3.)
AA(16,11)=B*(AX/8.-BX/4.)
AA(16,12)=AB*(AX/12.-BX/6.)+8.*TEM*B*H2/6.
AA(16,13)=-2.*ANEW*(AB12*HV/12.-A*H2/3.)+AB32*VV/12.-A3*HV/4.
AA(16,14)=A*B4*VV/10.-AB12*HV/2.+4.*A*H2/6.
AA(16,15)=-2.*ANEW*(AB13*HV/16.-AB*H2/6.)+AB33*VV/16.-AB31*HV
1/8.+16.*TEM*AB*H2/12.
AA(16,16)=AB24*VV/15.-4.*A2*B2*HV/18.+4.*A2*H2/9.+16.*B2*H2*T
1EM/9.
AA(17,2)=-6.*AH/4.+ANEW*A3*V/4.
AA(17,4)=AA(17,2)*B/2.
AA(17,7)=-6.*ANEW*AH/4.-ANEW*A*HV2+TEK*A3*V/4.
AA(17,8)=-ANEW*A2*H-6.*ANEW*A2*HV2/9.+TEK*A4*V/5.
AX=-6.*ANEW*A*HV/4.
BX=A3*VV/4.
AA(17,9)=AX+BX
AA(17,10)=AX*A*2./3.+BX*A*4./5.
AA(17,11)=AA(17,9)*B/2.
AA(17,12)=-ANEW*A2*B*HV/2.+A4*B*VV/10.
AA(17,13)=2.*A*H2-ANEW*A3*HV+A5*VV/6.
AA(17,14)=-ANEW*AB12*HV/2.+AB32*VV/12.+2.*ANEW*A*H2-A3*HV/4.
AA(17,15)=AB*H2-ANEW*AB31*HV/2.+A5*B*VV/12.
AA(17,16)=-ANEW*AB22*HV/3.+AB42*VV/15.+12.*ANEW*A2*H2/9.-A4*H
1V/5.
AA(17,17)=4.*A2*H2-12.*ANEW*A4*HV/10.+A6*VV/7.
AA(18,2)=ANEW*(B3*V/4.-6.*BH/4.)
AA(18,4)=ANEW*(B4*V/5.-B2*H)
AA(18,7)=-6.*BH/4.+TEK*B3*V/4.-B*HV2
AA(18,8)=AA(18,7)*A/2.
AA(18,9)=B3*VV/4.-6.*B*HV/4.
AA(18,10)=AA(18,9)*A/2.
AA(18,11)=B4*VV/5.-B2*HV
```

```
 AA(18,12)=AA(18,11)*A/2.
 AA(18,13)=-2.*ANEW*(B3*HV/8.-B*H2)+AB23*VV/12.-AB21*HV/2.
 AA(18,14)=B5*VV/6.-B3*HV+2.*B*H2
 AA(18,15)=-2.*ANEW*(B4*HV/10.-6.*B2*H2/9.)+AB24*VV/15.-AB22*H
1V/3.
 AA(18,16)=A*B5*VV/12.-AB13*HV/2.+AB*H2
 AA(18,17)=-6.*ANEW*(AB13*HV/16.-AB*H2/2.)+AB33*VV/16.-6.*AB31
1*HV/16.
 AA(18,18)=B6*VV/7.-12.*B4*HV/10.+4.*B2*H2
 AA(19,2)=(-6.*AB*H+ANEW*AB31*V)/8.
 AA(19,3)=-TEM*A2*H
 AA(19,4)=-AB12*H/2.+ANEW*AB32*V/12.-6.*TEM*A3*H/8.
 AA(19,6)=-6.*TEM*(A2*H/6.+2.*A2*H2*V/9.)
 AX=-6.*ANEW*A*BH/8.-6.*ANEW*AB*H2*V/12.
 BX=TEK*AB31*V/8.
 AA(19,7)=AX+BX
 AA(19,8)=AX*A*2./3.+BX*A*4./5.-6.*TEM*(A2*BH/12.+AB21*HV2/9.)
 AX=-6.*ANEW*AB*HV/8.
 BX=AB31*VV/8.
 AA(19,9)=AX+BX
 AA(19,10)=AX*A*2./3.+BX*A*4./5.
 AA(19,11)=AX*B*2./3.+BX*B*2./3.
 AA(19,12)=AX*AB*4./9.+BX*AB*8./15.+12.*TEM*A2*H2/9.
 AA(19,13)=AB*H2-ANEW*AB31*HV/2.+A5*BVV/12.
 AA(19,14)=-6.*ANEW*AB13*HV/16.+AB33*VV/16.+ANEW*AB*H2-AB31*HV
1/8.
 AA(19,15)=12.*AB12*H2/18.-ANEW*AB32*HV/3.+A5*B2*VV/18.+2.*TEM
1*A3*H2
 AA(19,16)=-ANEW*AB23*HV/4.+AB43*VV/20.-2.*(-ANEW*AB21*H2/3.+A
1B4)*HV/20.)+24.*TEM*AB21*H2/18.
 AA(19,17)=2.*AB21*H2-ANEW*AB41*HV*0.6+A6*B*VV/14.
 AA(19,18)=-6.*ANEW*AB14*HV/20.+AB34*VV/20.+2.*ANEW*AB12*H2-AB
132*HV/4.
 AA(19,19)=36.*AB22*H2/27.-12.*ANEW*AB42*HV/20.+A6*B2*VV/21.+3
16.*TEM*A4*H2/15.
 AA(20,2)=ANEW*(AB13*V-6.*AB*H)/8.
 AA(20,3)=-TEM*B2*H
 AA(20,4)=ANEW*AB14*V/10.+AB12*H*(-ANEW-TEM)/2.
 AA(20,6)=-6.*TEM*(B2*H/6.+2.*B2*H2*V/9.)
 AA(20,7)=-6.*AB*H/8.+TEK*AB13*V/8.-AB*HV2/2.
 AA(20,8)=-A2*BH/2.+TEK*AB23*V/12.-AB21*HV2/3.-6.*TEM*(B3*H/8.
1+B3*HV2/6.)
 AX=AB13*VV/8.
 BX=-6.*AB*HV/8.
 AA(20,9)=AX+BX
 AA(20,10)=AX*A*2./3.+BX*A*2./3.
 AA(20,11)=AX*B*4./5.+BX*B*2./3.
 AA(20,12)=AX*AB*8./15.+BX*AB*4./9.+12.*TEM*B2*H2/9.
 AA(20,13)=-2.*ANEW*(AB13*HV/16.-AB*H2/2.)+AB33*VV/16.-6.*AB31
1*HV/16.
 AA(20,14)=A*B5*VV/12.-AB13*HV/2.+AB*H2
```

```
 AA(20,15)=-2.*ANEW*(AB14*HV/20.-AB12*H2/3.)+AB34*VV/20.
1+24.*TEM*AB12*H2/18.-AB32*HV/4.
 AA(20,16)=AA(20,14)*A*2./3.+2.*TEM*B3*H2
 AX=-ANEW*AB23*HV/4.+AB43*VV/20.
 BX=2.*ANEW*AB21*H2-0.3*AB41*HV
 AA(20,17)=AX+BX
 AA(20,18)=A*B6*VV/14.-12.*AB14*HV/20.+2.*AB12*H2
 AA(20,19)=AX*B*4./5.+BX*B*2./3.+36.*TEM*AB22*H2/27.
 AA(20,20)=A2*B6*VV/21.-12.*A2*B4*HV/30.+36.*AB22*H2/27.+36.*T
1EM*B4*H2/15.
```

APPENDIX IX

(20*20)
MASS MATRIX (M/RO*H)
FOR CYLINDRICAL SHELL ELEMENT

USING THE DEFINITIONS OF APPENDIX VII , ALSO ASSUMING ZERO ELEMENTS OF THE MATRIX ARE GIVEN BY .
(NOTING THAT IT IS A SYMMETRIC MATRIX)

```
AA(1,1)=AB
AA(2,1)=AB21/2.
AA(2,2)=AB31/3.
AA(3,1)=AB12/2.
AA(3,2)=AB22/4.
AA(3,3)=AB13/3.
AA(4,1)=AB22/4.
AA(4,2)=AB32/6.
AA(4,3)=AB23/6.
AA(4,4)=AB33/9.
AA(5,5)=AA(1,1)
AA(6,5)=AA(2,1)
AA(6,6)=AA(2,2)
AA(7,5)=AA(3,1)
AA(7,6)=AA(3,2)
AA(7,7)=AA(3,3)
AA(8,5)=AA(4,1)
AA(8,6)=AA(4,2)
AA(8,7)=AA(4,3)
AA(8,8)=AA(4,4)
AA(9,9)=AA(1,1)
AA(10,9)=AA(2,1)
AA(10,10)=AA(2,2)
AA(11,9)=AA(3,1)
AA(11,10)=AA(3,2)
AA(11,11)=AA(3,3)
AA(12,9)=AA(4,1)
AA(12,10)=AA(4,2)
AA(12,11)=AA(4,3)
AA(12,12)=AA(4,4)
AA(13,9)=AB31/3.
AA(13,10)=AB41/4.
AA(13,11)=AB32/6.
AA(13,12)=AB42/8.
AA(13,13)=A5*B/5.
AA(14,9)=AB13/3.
AA(14,10)=AB23/6.
AA(14,11)=AB14/4.
```

```
AA(14,12)=AB24/8.
AA(14,13)=AB33/9.
AA(14,14)=A*B5/5.
AA(15,9)=AB32/6.
AA(15,10)=AB42/8.
AA(15,11)=AB33/9.
AA(15,12)=AB43/12.
AA(15,13)=A5*B2/10.
AA(15,14)=AB34/12.
AA(15,15)=A5*B3/15.
AA(16,9)=AB23/6.
AA(16,10)=AB33/9.
AA(16,11)=AB24/8.
AA(16,12)=AB34/12.
AA(16,13)=AB43/12.
AA(16,14)=A2*B5/10.
AA(16,15)=AB44/16.
AA(16,16)=A3*B5/15.
AA(17,9)=AB41/4.
AA(17,10)=A5*B/5.
AA(17,11)=AB42/8.
AA(17,12)=A5*B2/10.
AA(17,13)=A6*B/6.
AA(17,14)=AB43/12.
AA(17,15)=A6*B2/12.
AA(17,16)=A5*B3/15.
AA(17,17)=A7*B/7.
AA(18,9)=AB14/4.
AA(18,10)=AB24/8.
AA(18,11)=A*B5/5.
AA(18,12)=A2*B5/10.
AA(18,13)=AB34/12.
AA(18,14)=A*B6/6.
AA(18,15)=A3*B5/15.
AA(18,16)=A2*B6/12.
AA(18,17)=AB44/16.
AA(18,18)=A*B7/7.
AA(19,9)=AB42/8.
AA(19,10)=A5*B2/10.
AA(19,11)=AB43/12.
AA(19,12)=A5*B3/15.
AA(19,13)=A6*B2/12.
AA(19,14)=AB44/16.
AA(19,15)=A6*B3/18.
AA(19,16)=A5*B4/20.
AA(19,17)=A7*B2/14.
AA(19,18)=A4*B5/20.
AA(19,19)=A7*B3/21.
AA(20,9)=AB24/8.
AA(20,10)=AB34/12.
AA(20,11)=A2*B5/10.
```

```
AA(20,12)=A3*B5/15.
AA(20,13)=AB44/16.
AA(20,14)=A2*B6/12.
AA(20,15)=A4*B5/20.
AA(20,16)=A3*B6/18.
AA(20,17)=A5*B4/20.
AA(20,18)=A2*B7/14.
AA(20,19)=A5*B5/25.
AA(20,20)=A3*B7/21.
```

APPENDIX X

(28*28)
TRANSFORMATION MATRIX BETWEEN CORNER DISPLACEMENTS AND POLYNOMIAL COEFFICIENTS FOR CYLINDRICAL SHELL ELEMENT

IF STRL IS THE STRAIGHT SIDE ,
CURVL IS THE CURVED SIDE ,
A IS THE POISSON'S RATIO , AND
RAD IS THE RADIUS ,
THEN, THE NON-ZERO ELEMENTS OF THE MATRIX ARE GIVEN BY.

```
T(1,13)=1.
T(2,21)=1.
T(3,1)=1.
T(4,3)=1.
T(5,2)=-1.
T(5,15)=1.
T(7,23)=1.
T(8,13)=1.
T(8,14)=STRL
T(9,21)=1.
T(9,22)=STRL
T(10,1)=1.
T(10,2)=STRL
T(10,5)=STRL**2
T(10,9)=STRL**3
T(11,3)=1.
T(11,4)=STRL
T(11,7)=STRL**2
T(11,11)=STRL**3
T(12,2)=-1.
T(12,5)=-2.*STRL
T(12,9)=-3.*STRL**2
T(13,15)=1.
T(13,16)=STRL
T(14,23)=1.
T(14,24)=STRL
T(15,13)=1.
T(15,14)=STRL
T(15,15)=CURVL
T(15,16)=STRL*CURVL
T(15,17)=CURVL**2
T(15,18)=STRL*CURVL**2
T(15,19)=CURVL**3
T(15,20)=STRL*CURVL**3
T(16,21)=1.
```

```
T(16,22)=STRL
T(16,23)=CURVL
T(16,24)=STRL*CURVL
T(16,25)=CURVL**2
T(16,26)=STRL*CURVL**2
T(16,27)=CURVL**3
T(16,28)=STRL*CURVL**3
T(17,1)=1.
T(17,2)=STRL
T(17,3)=CURVL
T(17,4)=STRL*CURVL
T(17,5)=STRL**2
T(17,6)=CURVL**2
T(17,7)=STRL**2*CURVL
T(17,8)=STRL*CURVL**2
T(17,9)=STRL**3
T(17,10)=CURVL**3
T(17,11)=STRL**3*CURVL
T(17,12)=STRL*CURVL**3
T(18,3)=1.
T(18,4)=STRL
T(18,6)=2.*CURVL
T(18,7)=STRL**2
T(18,8)=2.*STRL*CURVL
T(18,10)=3.*CURVL**2
T(18,11)=STRL**3
T(18,12)=3.*STRL*CURVL**2
T(19,2)=-1.
T(19,4)=-CURVL
T(19,5)=-2.*STRL
T(19,7)=-2.*STRL*CURVL
T(19,8)=-CURVL**2
T(19,9)=-3.*STRL**2
T(19,11)=-3.*STRL**2*CURVL
T(19,12)=-CURVL**3
T(20,15)=1.
T(20,16)=STRL
T(20,17)=2.*CURVL
T(20,18)=2.*STRL*CURVL
T(20,19)=3.*CURVL**2
T(20,20)=3.*STRL*CURVL**2
T(21,23)=1.
T(21,24)=STRL
T(21,25)=2.*CURVL
T(21,26)=2.*STRL*CURVL
T(21,27)=3.*CURVL**2
T(21,28)=3.*STRL*CURVL**2
T(22,13)=1.
T(22,15)=CURVL
T(22,17)=CURVL**2
T(22,19)=CURVL**3
```

```
T(23,21)=1.
T(23,23)=CURVL
T(23,25)=CURVL**2
T(23,27)=CURVL**3
T(24,1)=1.
T(24,3)=CURVL
T(24,6)=CURVL**2
T(24,10)=CURVL**3
T(25,3)=1.
T(25,6)=2.*CURVL
T(25,10)=3.*CURVL**2
T(26,2)=-1.
T(26,4)=-CURVL
T(26,8)=-CURVL**2
T(26,12)=-CURVL**3
T(27,15)=1.
T(27,17)=2.*CURVL
T(27,19)=3.*CURVL**2
T(28,23)=1.
T(28,25)=2.*CURVL
T(28,27)=3.*CURVL**2
```

APPENDIX XI

(28*28)
STIFFNESS MATRIX (K/D)
FOR CYLINDRICAL SHELL ELEMENT

USING THE DEFINITIONS OF APPENDIX X , ALSO ASSUMING THAT
G=(1.-A)/2. ,
R=1./RAD ,
RR=R*R , AND
QA(I,J,K)=STRL**(I+1)*CURVL**(J+1)*H**(K+1)/((I+1)*(J+1)*(K+1)) ,
THEN, THE NON-ZERO ELEMENTS OF THE MATRIX ARE GIVEN BY.
(NOTING THAT IT IS A SYMMETRIC MATRIX)

```
AA(1,1)=QA(0,0,0)*RR
AA(2,1)=QA(1,0,0)*RR
AA(2,2)=QA(2,0,0)*RR
AA(3,1)=QA(0,1,0)*RR
AA(3,2)=QA(1,1,0)*RR
AA(3,3)=QA(0,2,0)*RR
AA(4,1)=QA(1,1,0)*RR
AA(4,2)=QA(2,1,0)*RR
AA(4,3)=QA(1,2,0)*RR
AA(4,4)=QA(2,2,0)*RR+4.*G*QA(0,0,2)
AA(5,1)=-2.*A*QA(0,0,1)*R+QA(2,0,0)*RR
AA(5,2)=-2.*A*QA(1,0,1)*R+QA(3,0,0)*RR
AA(5,3)=-2.*A*QA(0,1,1)*R+QA(2,1,0)*RR
AA(5,4)=-2.*A*QA(1,1,1)*R+QA(3,1,0)*RR
AA(5,5)=4.*QA(0,0,2)-4.*A*QA(2,0,1)*R+QA(4,0,0)*RR
AA(6,1)=QA(0,2,0)*RR-2.*QA(0,0,1)*R
AA(6,2)=QA(1,2,0)*RR-2.*QA(1,0,1)*R
AA(6,3)=QA(0,3,0)*RR-2.*QA(0,1,1)*R
AA(6,4)=QA(1,3,0)*RR-2.*QA(1,1,1)*R
AA(6,5)=-2.*A*QA(0,2,1)*R+4.*A*QA(0,0,2)+QA(2,2,0)*RR-2.*QA(2
1,0,1)*R
AA(6,6)=QA(0,4,0)*RR-4.*QA(0,2,1)*R+4.*QA(0,0,2)
AA(7,1)=-2.*A*QA(0,1,1)*R+QA(2,1,0)*RR
AA(7,2)=-2.*A*QA(1,1,1)*R+QA(3,1,0)*RR
AA(7,3)=-2.*A*QA(0,2,1)*R+QA(2,2,0)*RR
AA(7,4)=-2.*A*QA(1,2,1)*R+QA(3,2,0)*RR+8.*G*QA(1,0,2)
AA(7,5)=4.*QA(0,1,2)-4.*A*QA(2,1,1)*R+QA(4,1,0)*RR
AA(7,6)=-2.*A*QA(0,3,1)*R+QA(2,3,0)*RR+4.*A*QA(0,1,2)-2.*QA(2
1,1,1)*R
AA(7,7)=4.*QA(0,2,2)-4.*A*QA(2,2,1)*R+QA(4,2,0)*RR+16.*G*QA(2
1,0,2)
AA(8,1)=QA(1,2,0)*RR-2.*QA(1,0,1)*R
AA(8,2)=QA(2,2,0)*RR-2.*QA(2,0,1)*R
```

```
      AA(8,3)=QA(1,3,0)*RR-2.*QA(1,1,1)*R
      AA(8,4)=QA(2,3,0)*RR-2.*QA(2,1,1)*R+8.*G*QA(0,1,2)
      AA(8,5)=-2.*A*QA(1,2,1)*R+4.*A*QA(1,0,2)+QA(3,2,0)*RR-2.*QA(3
     1,0,1)*R
      AA(8,6)=QA(1,4,0)*RR-4.*QA(1,2,1)*R+4.*QA(1,0,2)
      AA(8,7)=-2.*A*QA(1,3,1)*R+4.*A*QA(1,1,2)+QA(3,3,0)*RR
     1   +16.*G*QA(1,1,2)-2.*QA(3,1,1)*R
      AA(8,8)=QA(2,4,0)*RR-4.*QA(2,2,1)*R+4.*QA(2,0,2)+16.*G*QA(0,2
     1,2)
      AA(9,1)=-6.*A*QA(1,0,1)*R+QA(3,0,0)*RR
      AA(9,2)=-6.*A*QA(2,0,1)*R+QA(4,0,0)*RR
      AA(9,3)=-6.*A*QA(1,1,1)*R+QA(3,1,0)*RR
      AA(9,4)=-6.*A*QA(2,1,1)*R+QA(4,1,0)*RR
      AA(9,5)=12.*QA(1,0,2)-8.*A*QA(3,0,1)*R+QA(5,0,0)*RR
      AA(9,6)=-6.*A*QA(1,2,1)*R+QA(3,2,0)*RR+12.*A*QA(1,0,2)-2.*QA(
     13,0,1)*R
      AA(9,7)=12.*QA(1,1,2)-8.*A*QA(3,1,1)*R+QA(5,1,0)*RR
      AA(9,8)=-6.*A*QA(2,2,1)*R+QA(4,2,0)*RR+12.*A*QA(2,0,2)-2.*QA(
     14,0,1)*R
      AA(9,9)=36.*QA(2,0,2)-12.*A*QA(4,0,1)*R+QA(6,0,0)*RR
      AA(10,1)=QA(0,3,0)*RR-6.*QA(0,1,1)*R
      AA(10,2)=QA(1,3,0)*RR-6.*QA(1,1,1)*R
      AA(10,3)=QA(0,4,0)*RR-6.*QA(0,2,1)*R
      AA(10,4)=QA(1,4,0)*RR-6.*QA(1,2,1)*R
      AA(10,5)=-2.*A*QA(0,3,1)*R+12.*A*QA(0,1,2)+QA(2,3,0)*RR-6.*QA
     1(2,1,1)*R
      AA(10,6)=QA(0,5,0)*RR-8.*QA(0,3,1)*R+12.*QA(0,1,2)
      AA(10,7)=-2.*A*QA(0,4,1)*R+12.*A*QA(0,2,2)+QA(2,4,0)*RR-6.*QA
     1(2,2,1)*R
      AA(10,8)=QA(1,5,0)*RR-8.*QA(1,3,1)*R+12.*QA(1,1,2)
      AA(10,9)=-6.*A*QA(1,3,1)*R+36.*A*QA(1,1,2)+QA(3,3,0)*RR-6.*QA
     1(3,1,1)*R
      AA(10,10)=QA(0,6,0)*RR-12.*QA(0,4,1)*R+36.*QA(0,2,2)
      AA(11,1)=-6.*A*QA(1,1,1)*R+QA(3,1,0)*RR
      AA(11,2)=-6.*A*QA(2,1,1)*R+QA(4,1,0)*RR
      AA(11,3)=-6.*A*QA(1,2,1)*R+QA(3,2,0)*RR
      AA(11,4)=-6.*A*QA(2,2,1)*R+QA(4,2,0)*RR+12.*G*QA(2,0,2)
      AA(11,5)=12.*QA(1,1,2)-8.*A*QA(3,1,1)*R+QA(5,1,0)*RR
      AA(11,6)=-6.*A*QA(1,3,1)*R+QA(3,3,0)*RR+12.*A*QA(1,1,2)-2.*QA
     1(3,1,1)*R
      AA(11,7)=12.*QA(1,2,2)-8.*A*QA(3,2,1)*R+QA(5,2,0)*RR+24.*G*QA
     1(3,0,2)
      AA(11,8)=-6.*A*QA(2,3,1)*R+QA(4,3,0)*RR+12.*A*QA(2,1,2)-2.*QA
     1(4,1,1)*R+24.*G*QA(2,1,2)
      AA(11,9)=36.*QA(2,1,2)-12.*A*QA(4,1,1)*R+QA(6,1,0)*RR
      AA(11,10)=-6.*A*QA(1,4,1)*R+QA(3,4,0)*RR+36.*A*QA(1,2,2)-6.*Q
     1A(3,2,1)*R
      AA(11,11)=36.*QA(2,2,2)-12.*A*QA(4,2,1)*R+QA(6,2,0)*RR+36.*G*
     1QA(4,0,2)
      AA(12,1)=QA(1,3,0)*RR-6.*QA(1,1,1)*R
      AA(12,2)=QA(2,3,0)*RR-6.*QA(2,1,1)*R
```

```
 AA(12,3)=QA(1,4,0)*RR-6.*QA(1,2,1)*R
 AA(12,4)=QA(2,4,0)*RR-6.*QA(2,2,1)*R+12.*G*QA(0,2,2)
 AA(12,5)=-2.*A*QA(1,3,1)*R+12.*A*QA(1,1,2)+QA(3,3,0)*RR-6.*QA
1(3,1,1)*R
 AA(12,6)=QA(1,5,0)*RR-8.*QA(1,3,1)*R+12.*QA(1,1,2)
 AA(12,7)=12.*A*QA(1,2,2)+QA(3,4,0)*RR-6.*QA(3,2,1)*R+24.*G*QA
1(1,2,2)-2.*A*QA(1,4,1)
 AA(12,8)=QA(2,5,0)*RR-8.*QA(2,3,1)*R+12.*QA(2,1,2)+24.*G*QA(0
1,3,2)
 AA(12,9)=-6.*A*QA(2,3,1)*R+36.*A*QA(2,1,2)+QA(4,3,0)*RR-6.*QA
1(4,1,1)*R
 AA(12,10)=QA(1,6,0)*RR-12.*QA(1,4,1)*R+36.*QA(1,2,2)
 AA(12,11)=-6.*A*QA(2,4,1)*R+36.*A*QA(2,2,2)+QA(4,4,0)*RR-6.*Q
1A(4,2,1)*R+36.*QA(2,2,2)*G
 AA(12,12)=QA(2,6,0)*RR-12.*QA(2,4,1)*R+36.*QA(2,2,2)+36.*G*QA
1(0,4,2)
 AA(14,1)=A*QA(0,0,0)*R
 AA(14,2)=A*QA(1,0,0)*R
 AA(14,3)=A*QA(0,1,0)*R
 AA(14,4)=A*QA(1,1,0)*R
 AA(14,5)=-2.*QA(0,0,1)+A*QA(2,0,0)*R
 AA(14,6)=A*QA(0,2,0)*R-2.*A*QA(0,0,1)
 AA(14,7)=-2.*QA(0,1,1)+A*QA(2,1,0)*R
 AA(14,8)=A*QA(1,2,0)*R-2.*A*QA(1,0,1)
 AA(14,9)=-6.*QA(1,0,1)+A*QA(3,0,0)*R
 AA(14,10)=A*QA(0,3,0)*R-6.*A*QA(0,1,1)
 AA(14,11)=-6.*QA(1,1,1)+A*QA(3,1,0)*R
 AA(14,12)=A*QA(1,3,0)*R-6.*A*QA(1,1,1)
 AA(14,14)=QA(0,0,0)
 AA(15,4)=-2.*G*QA(0,0,1)
 AA(15,7)=-4.*G*QA(1,0,1)
 AA(15,8)=-4.*G*QA(0,1,1)
 AA(15,11)=-6.*G*QA(2,0,1)
 AA(15,12)=-6.*G*QA(0,2,1)
 AA(15,15)=G*QA(0,0,0)
 AA(16,1)=A*QA(0,1,0)*R
 AA(16,2)=A*QA(1,1,0)*R
 AA(16,3)=A*QA(0,2,0)*R
 AA(16,4)=A*QA(1,2,0)*R-2.*G*QA(1,0,1)
 AA(16,5)=-2.*QA(0,1,1)+A*QA(2,1,0)*R
 AA(16,6)=A*QA(0,3,0)*R-2.*A*QA(0,1,1)
 AA(16,7)=-2.*QA(0,2,1)+A*QA(2,2,0)*R-4.*G*QA(2,0,1)
 AA(16,8)=A*QA(1,3,0)*R-2.*A*QA(1,1,1)-4.*G*QA(1,1,1)
 AA(16,9)=-6.*QA(1,1,1)+A*QA(3,1,0)*R
 AA(16,10)=A*QA(0,4,0)*R-6.*A*QA(0,2,1)
 AA(16,11)=-6.*QA(1,2,1)+A*QA(3,2,0)*R-6.*G*QA(3,0,1)
 AA(16,12)=A*QA(1,4,0)*R-6.*A*QA(1,2,1)-6.*G*QA(1,2,1)
 AA(16,14)=QA(0,1,0)
 AA(16,15)=G*QA(1,0,0)
 AA(16,16)=QA(0,2,0)+G*QA(2,0,0)
 AA(17,4)=-4.*G*QA(0,1,1)
```

```
AA(17,7)=-8.*G*QA(1,1,1)
AA(17,8)=-8.*G*QA(0,2,1)
AA(17,11)=-12.*G*QA(2,1,1)
AA(17,12)=-12.*G*QA(0,3,1)
AA(17,15)=2.*G*QA(0,1,0)
AA(17,16)=2.*G*QA(1,1,0)
AA(17,17)=4.*G*QA(0,2,0)
AA(18,1)=A*QA(0,2,0)*R
AA(18,2)=A*QA(1,2,0)*R
AA(18,3)=A*QA(0,3,0)*R
AA(18,4)=A*QA(1,3,0)*R-4.*G*QA(1,1,1)
AA(18,5)=-2.*QA(0,2,1)+A*QA(2,2,0)*R
AA(18,6)=A*QA(0,4,0)*R-2.*A*QA(0,2,1)
AA(18,7)=-2.*QA(0,3,1)+A*QA(2,3,0)*R-8.*G*QA(2,1,1)
AA(18,8)=A*QA(1,4,0)*R-2.*A*QA(1,2,1)-8.*G*QA(1,2,1)
AA(18,9)=-6.*QA(1,2,1)+A*QA(3,2,0)*R
AA(18,10)=A*QA(0,5,0)*R-6.*A*QA(0,3,1)
AA(18,11)=-6.*QA(1,3,1)+A*QA(3,3,0)*R+12.*G*QA(3,1,1)
AA(18,12)=A*QA(1,5,0)*R-6.*A*QA(1,3,1)-12.*G*QA(1,3,1)
AA(18,14)=QA(0,2,0)
AA(18,15)=2.*G*QA(1,1,0)
AA(18,16)=QA(0,3,0)+2.*G*QA(2,1,0)
AA(18,17)=4.*G*QA(1,2,0)
AA(18,18)=QA(0,4,0)+4.*G*QA(2,2,0)
AA(19,4)=-6.*G*QA(0,2,1)
AA(19,7)=-12.*G*QA(1,2,1)
AA(19,8)=-12.*G*QA(0,3,1)
AA(19,11)=-18.*G*QA(2,2,1)
AA(19,12)=-18.*G*QA(0,4,1)
AA(19,15)=3.*G*QA(0,2,0)
AA(19,16)=3.*G*QA(1,2,0)
AA(19,17)=6.*G*QA(0,3,0)
AA(19,18)=6.*G*QA(1,3,0)
AA(19,19)=9.*G*QA(0,4,0)
AA(20,1)=A*QA(0,3,0)*R
AA(20,2)=A*QA(1,3,0)*R
AA(20,3)=A*QA(0,4,0)*R
AA(20,4)=A*QA(1,4,0)*R-6.*G*QA(1,2,1)
AA(20,5)=-2.*QA(0,3,1)+A*QA(2,3,0)*R
AA(20,6)=A*QA(0,5,0)*R-2.*A*QA(0,3,1)
AA(20,7)=-2.*QA(0,4,1)+A*QA(2,4,0)*R-12.*G*QA(2,2,1)
AA(20,8)=A*QA(1,5,0)*R-2.*A*QA(1,3,1)-12.*G*QA(1,3,1)
AA(20,9)=-6.*QA(1,3,1)+A*QA(3,3,0)*R
AA(20,10)=A*QA(0,6,0)*R-6.*A*QA(0,4,1)
AA(20,11)=-6.*QA(1,4,1)+A*QA(3,4,0)*R-18.*G*QA(3,2,1)
AA(20,12)=A*QA(1,6,0)*R-6.*A*QA(1,4,1)-18.*G*QA(1,4,1)
AA(20,14)=QA(0,3,0)
AA(20,15)=3.*G*QA(1,2,0)
AA(20,16)=QA(0,4,0)+3.*G*QA(2,2,0)
AA(20,17)=6.*G*QA(1,3,0)
AA(20,18)=QA(0,5,0)+6.*G*QA(2,3,0)
```

```
AA(20,19)=9.*G*QA(1,4,0)
AA(20,20)=QA(0,6,0)+9.*G*QA(2,4,0)
AA(22,4)=-2.*G*QA(0,0,1)-4.*G*QA(0,0,2)*R
AA(22,7)=-4.*G*QA(1,0,1)-8.*G*QA(1,0,2)*R
AA(22,8)=-4.*G*QA(0,1,1)-8.*G*QA(0,1,2)*R
AA(22,11)=-6.*G*QA(2,0, )-12.*G*QA(2,0,2)*R
AA(22,12)=-6.*G*QA(0,2,1)-12.*G*QA(0,2,2)*R
AA(22,15)=G*QA(0,0,0)+2.*G*QA(0,0,1)*R
AA(22,16)=G*QA(1,0,0)+2.*G*QA(1,0,1)*R
AA(22,17)=2.*G*QA(0,1,0)+4.*G*QA(0,1,1)*R
AA(22,18)=2.*G*QA(1,1,0)+4.*G*QA(1,1,1)*R
AA(22,19)=3.*G*QA(0,2,0)+6.*G*QA(0,2,1)*R
AA(22,20)=3.*G*QA(1,2,0)+6.*G*QA(1,2,1)*R
AA(22,22)=G*QA(0,0,0)+2.*G*QA(0,0,1)*R+2.*G*QA(0,0,1)*R+4.*G*
1QA(0,0,2)*RR
AA(23,1)=QA(0,0,0)*R+QA(0,0,1)*RR
AA(23,2)=QA(1,0,0)*R+QA(1,0,1)*RR
AA(23,3)=QA(0,1,0)*R+QA(0,1,1)*RR
AA(23,4)=QA(1,1,0)*R+QA(1,1,1)*RR
AA(23,5)=QA(2,0,0)*R+QA(2,0,1)*RR-2.*A*QA(0,0,1)-2.*A*QA(0,0,
12)*R
AA(23,6)=QA(0,2,0)*R+QA(0,2,1)*RR-2.*QA(0,0,1)-2.*QA(0,0,2)*R
AA(23,7)=QA(2,1,0)*R+QA(2,1,1)*RR-2.*A*QA(0,1,1)-2.*A*QA(0,1,
12)*R
AA(23,8)=QA(1,2,0)*R+QA(1,2,1)*RR-2.*QA(1,0,1)-2.*QA(1,0,2)*R
AA(23,9)=-6.*A*QA(1,0,1)-6.*A*QA(1,0,2)*R+QA(3,0,0)*R+QA(3,0,
11)*RR
AA(23,10)=QA(0,3,0)*R+QA(0,3,1)*RR-6.*QA(0,1,1)-6.*QA(0,1,2)*
1R
AA(23,11)=-6.*A*QA(1,1,1)-6.*A*QA(1,1,2)*R+QA(3,1,0)*R+QA(3,1
1,1)*RR
AA(23,12)=QA(1,3,0)*R+QA(1,3,1)*RR-6.*QA(1,1,1)-6.*QA(1,1,2)*
1R
AA(23,14)=A*QA(0,0,0)+A*QA(0,0,1)*R
AA(23,16)=A*QA(0,1,0)+A*QA(0,1,1)*R
AA(23,18)=A*QA(0,2,0)+A*QA(0,2,1)*R
AA(23,20)=A*QA(0,3,0)+A*QA(0,3,1)*R
AA(23,23)=QA(0,0,0)+2.*QA(0,0,1)*R+QA(0,0,2)*RR
AA(24,1)=QA(1,0,0)*R+QA(1,0,1)*RR
AA(24,2)=QA(2,0,0)*R+QA(2,0,1)*RR
AA(24,3)=QA(1,1,0)*R+QA(1,1,1)*RR
AA(24,4)=QA(2,1,0)*R+QA(2,1,1)*RR-2.*G*QA(0,1,1)-4.*G*QA(0,1,
12)*R
AA(24,5)=QA(3,0,0)*R+QA(3,0,1)*RR-2.*A*QA(1,0,1)-2.*A*QA(1,0,
12)*R
AA(24,6)=QA(1,2,0)*R+QA(1,2,1)*RR-2.*QA(1,0,1)-2.*QA(1,0,2)*R
AA(24,7)=QA(3,1,0)*R+QA(3,1,1)*RR-2.*A*QA(1,1,1)-
14.*G*QA(1,1,1)-8.*G*QA(1,1,2)*R-2.*A*QA(1,1,2)*R
AA(24,8)=QA(2,2,0)*R+QA(2,2,1)*RR-2.*QA(2,0,1)-2.*QA(2,0,2)*R
1-4.*G*QA(0,2,1)-8.*G*QA(0,2,2)*R
AA(24,9)=-6.*A*QA(2,0,1)-6.*A*QA(2,0,2)*R+QA(4,0,0)*R+QA(4,0,
11)*RR
```

```
 AA(24,10)=QA(1,3,0)*R+QA(1,3,1)*RR-6.*QA(1,1,1)-6.*QA(1,1,2)*
1R
 AA(24,11)=-6.*A*QA(2,1,1)-6.*A*QA(2,1,2)*R+QA(4,1,0)*R
1 -6.*G*QA(2,1,1)-12.*G*QA(2,1,2)*R+QA(4,1,1)*RR
 AA(24,12)=QA(2,3,0)*R+QA(2,3,1)*RR-6.*QA(2,1,1)-6.*QA(2,1,2)*
1R-6.*G*QA(0,3,1)-12.*G*QA(0,3,2)*R
 AA(24,14)=A*QA(1,0,0)+A*QA(1,0,1)*R
 AA(24,15)=G*QA(0,1,0)+2.*G*QA(0,1,1)*R
 AA(24,16)=A*QA(1,1,0)+A*QA(1,1,1)*R+G*QA(1,1,0)+2.*G*QA(1,1,1
1)*R
 AA(24,17)=2.*G*QA(0,2,0)+4.*G*QA(0,2,1)*R
 AA(24,18)=A*QA(1,2,0)+A*QA(1,2,1)*R+2.*G*QA(1,2,0)+4.*G*QA(1,
12,1)*R
 AA(24,19)=3.*G*QA(0,3,0)+6.*G*QA(0,3,1)*R
 AA(24,20)=A*QA(1,3,0)+A*QA(1,3,1)*R+3.*G*QA(1,3,0)+6.*G*QA(1,
13,1)*R
 AA(24,22)=G*QA(0,1,0)+4.*G*QA(0,1,1)*R+4.*G*QA(0,1,2)*RR
 AA(24,23)=QA(1,0,0)+2.*QA(1,0,1)*R+QA(1,0,2)*RR
 AA(24,24)=QA(2,0,0)+2.*QA(2,0,1)*R+QA(2,0,2)*RR+G*QA(0,2,0)
1          +4.*G*QA(0,2,2)*RR+4.*G*QA(0,2,1)*R
 AA(25,1)=2.*QA(0,1,0)*R+2.*QA(0,1,1)*RR
 AA(25,2)=2.*QA(1,1,0)*R+2.*QA(1,1,1)*RR
 AA(25,3)=2.*QA(0,2,0)*R+2.*QA(0,2,1)*RR
 AA(25,4)=2.*QA(1,2,0)*R+2.*QA(1,2,1)*RR
 AA(25,5)=2.*QA(2,1,0)*R+2.*QA(2,1,1)*RR-4.*A*QA(0,1,1)-4.*A*Q
1A(0,1,2)*R
 AA(25,6)=2.*QA(0,3,0)*R+2.*QA(0,3,1)*RR-4.*QA(0,1,1)-4.*QA(0,
11,2)*R
 AA(25,7)=-4.*A*QA(0,2,1)-4.*A*QA(0,2,2)*R+2.*QA(2,2,0)*R+2.*Q
1A(2,2,1)*RR
 AA(25,8)=2.*QA(1,3,0)*R+2.*QA(1,3,1)*RR-4.*QA(1,1,1)-4.*QA(1,
11,2)*R
 AA(25,9)=-12.*A*QA(1,1,1)-12.*A*QA(1,1,2)*R+2.*QA(3,1,0)*R+2.
1*QA(3,1,1)*RR
 AA(25,10)=2.*QA(0,4,0)*R+2.*QA(0,4,1)*RR-12.*QA(0,2,1)-12.*QA
1(0,2,2)*R
 AA(25,11)=-12.*A*QA(1,2,1)-12.*A*QA(1,2,2)*R+2.*QA(3,2,0)*R+2
1.*QA(3,2,1)*RR
 AA(25,12)=2.*QA(1,4,0)*R+2.*QA(1,4,1)*RR-12.*QA(1,2,1)-12.*QA
1(1,2,2)*R
 AA(25,14)=2.*A*QA(0,1,0)+2.*A*QA(0,1,1)*R
 AA(25,16)=2.*A*QA(0,2,0)+2.*A*QA(0,2,1)*R
 AA(25,18)=2.*A*QA(0,3,0)+2.*A*QA(0,3,1)*R
 AA(25,20)=2.*A*QA(0,4,0)+2.*A*QA(0,4,1)*R
 AA(25,23)=2.*QA(0,1,0)+4.*QA(0,1,1)*R+2.*QA(0,1,2)*RR
 AA(25,24)=2.*QA(1,1,0)+4.*QA(1,1,1)*R+2.*QA(1,1,2)*RR
 AA(25,25)=4.*QA(0,2,0)+8.*QA(0,2,1)*R+4.*QA(0,2,2)*RR
 AA(26,1)=2.*QA(1,1,0)*R+2.*QA(1,1,1)*RR
 AA(26,2)=2.*QA(2,1,0)*R+2.*QA(2,1,1)*RR
 AA(26,3)=2.*QA(1,2,0)*R+2.*QA(1,2,1)*RR
 AA(26,4)=2.*QA(2,2,0)*R+2.*QA(2,2,1)*RR-2.*G*QA(0,2,1)-4.*G*Q
1A(0,2,2)*R
```

```
      AA(26,5)=-4.*A*QA(1,1,1)-4.*A*QA(1,1,2)*R+2.*QA(3,1,0)*R+2.*Q
     1A(3,1,1)*RR
      AA(26,6)=2.*QA(1,3,0)*R+2.*QA(1,3,1)*RR-4.*QA(1,1,1)-4.*QA(1,
     11,2)*R
      AA(26,7)=-4.*A*QA(1,2,1)-4.*A*QA(1,2,2)*R+2.*QA(3,2,0)*R
     1      -4.*G*QA(1,2,1)-8.*G*QA(1,2,2)*R+2.*QA(3,2,1)*RR
      AA(26,8)=2.*QA(2,3,0)*R+2.*QA(2,3,1)*RR-4.*QA(2,1,1)
     1 -4.*G*QA(0,3,1)-8.*G*QA(0,3,2)*R-4.*QA(2,1,2)*R
      AA(26,9)=-12.*A*QA(2,1,1)-12.*A*QA(2,1,2)*R+2.*QA(4,1,0)*R+2.
     1*QA(4,1,1)*RR
      AA(26,10)=2.*QA(1,4,0)*R+2.*QA(1,4,1)*RR-12.*QA(1,2,1)-12.*QA
     1(1,2,2)*R
      AA(26,11)=-12.*A*QA(2,2,1)-12.*A*QA(2,2,2)*R+2.*QA(4,2,0)*R
     1      -6.*G*QA(2,2,1)-12.*G*QA(2,2,2)*R+2.*QA(4,2,1)*RR
      AA(26,12)=2.*QA(2,4,0)*R+2.*QA(2,4,1)*RR-12.*QA(2,2,1)
     1   -6.*G*QA(0,4,1)-12.*G*QA(0,4,2)*R-12.*QA(2,2,2)*R
      AA(26,14)=2.*A*QA(1,1,0)+2.*A*QA(1,1,1)*R
      AA(26,15)=G*QA(0,2,0)+2.*G*QA(0,2,1)*R
      AA(26,16)=G*QA(1,2,0)+2.*G*QA(1,2,1)*R+2.*A*QA(1,2,0)+2.*A*QA
     1(1,2,1)*R
      AA(26,17)=2.*G*QA(0,3,0)+4.*G*QA(0,3,1)*R
      AA(26,18)=2.*G*QA(1,3,0)+4.*G*QA(1,3,1)*R+2.*A*QA(1,3,0)+2.*A
     1*QA(1,3,1)*R
      AA(26,19)=3.*G*QA(0,4,0)+6.*G*QA(0,4,1)*R
      AA(26,20)=3.*G*QA(1,4,0)+6.*G*QA(1,4,1)*R+2.*A*QA(1,4,0)+2.*A
     1*QA(1,4,1)*R
      AA(26,22)=G*QA(0,2,0)+4.*G*QA(0,2,1)*R+4.*G*QA(0,2,2)*RR
      AA(26,23)=2.*QA(1,1,0)+4.*QA(1,1,1)*R+2.*QA(1,1,2)*RR
      AA(26,24)=2.*QA(2,1,0)+4.*QA(2,1,1)*R+2.*QA(2,1,2)*RR+
     14.*G*QA(0,2,1)*R+4.*G*QA(0,2,2)*RR+G*QA(0,3,0)
      AA(26,25)=4.*QA(1,2,0)+8.*QA(1,2,1)*R+4.*QA(1,2,2)*RR
      AA(26,26)=4.*QA(2,2,0)+8.*QA(2,2,1)*R+4.*QA(2,2,2)*RR+
     14.*G*QA(0,4,1)*R+4.*G*QA(0,4,2)*RR+G*QA(0,4,0)
      AA(27,1)=3.*QA(0,2,0)*R+3.*QA(0,2,1)*RR
      AA(27,2)=3.*QA(1,2,0)*R+3.*QA(1,2,1)*RR
      AA(27,3)=3.*QA(0,3,0)*R+3.*QA(0,3,1)*RR
      AA(27,4)=3.*QA(1,3,0)*R+3.*QA(1,3,1)*RR
      AA(27,5)=3.*QA(2,2,0)*R+3.*QA(2,2,1)*RR-6.*A*QA(0,2,1)-6.*A*Q
     1A(0,2,2)*R
      AA(27,6)=3.*QA(0,4,0)*R+3.*QA(0,4,1)*RR-6.*QA(0,2,1)-6.*QA(0,
     12,2)*R
      AA(27,7)=-6.*A*QA(0,3,1)-6.*A*QA(0,3,2)*R+3.*QA(2,3,0)*R+3.*Q
     1A(2,3,1)*R
      AA(27,8)=3.*QA(1,4,0)*R+3.*QA(1,4,1)*RR-6.*QA(1,2,1)-6.*QA(1,
     12,2)*R
      AA(27,9)=-18.*A*QA(1,2,1)-18.*A*QA(1,2,2)*R+3.*QA(3,2,0)*R+3.
     1*QA(3,2,1)*RR
      AA(27,10)=3.*QA(0,5,0)*R+3.*QA(0,5,1)*RR-18.*QA(0,3,1)-18.*QA
     1(0,3,2)*R
      AA(27,11)=-18.*A*QA(1,3,1)-18.*A*QA(1,3,2)*R+3.*QA(3,3,0)*R+3
     1.*QA(3,3,1)*RR
```

```
      AA(27,12)=3.*QA(1,5,1)*RR-18.*QA(1,3,1)-18.*QA(1,3,2)*R+3.*QA
     1(1,5,0)*R
      AA(27,14)=3.*A*QA(0,2,0)+3.*A*QA(0,2,1)*R
      AA(27,16)=3.*A*QA(0,3,0)+3.*A*QA(0,3,1)*R
      AA(27,18)=3.*A*QA(0,4,0)+3.*A*QA(0,4,1)*R
      AA(27,20)=3.*A*QA(0,5,0)+3.*A*QA(0,5,1)*R
      AA(27,22)=3.*QA(0,2,0)+6.*QA(0,2,1)*R+3.*QA(0,2,2)*RR
      AA(27,24)=3.*QA(1,2,0)+6.*QA(1,2,1)*R+3.*QA(1,2,2)*RR
      AA(27,25)=6.*QA(0,3,0)+12.*QA(0,3,1)*R+6.*QA(0,3,2)*RR
      AA(27,26)=6.*QA(1,3,0)+12.*QA(1,3,1)*R+6.*QA(1,3,2)*RR
      AA(27,27)=9.*QA(0,4,0)+18.*QA(0,4,1)*R+9.*QA(0,4,2)*RR
      AA(28,1)=3.*QA(1,2,0)*R+3.*QA(1,2,1)*RR
      AA(28,2)=3.*QA(2,2,0)*R+3.*QA(2,2,1)*RR
      AA(28,3)=3.*QA(1,3,0)*R+3.*QA(1,3,1)*RR
      AA(28,4)=3.*QA(2,3,0)*R+3.*QA(2,3,1)*RR-2.*G*QA(0,3,1)-4.*G*Q
     1A(0,3,2)*R
      AA(28,5)=-6.*A*QA(1,2,1)-6.*A*QA(1,2,2)*R+3.*QA(3,2,0)*R+3.*Q
     1A(3,2,1)*RR
      AA(28,6)=3.*QA(1,4,0)*R+3.*QA(1,4,1)*RR-6.*QA(1,2,1)-6.*QA(1,
     12,2)*R
      AA(28,7)=-6.*A*QA(1,3,1)-6.*A*QA(1,3,2)*R+3.*QA(3,3,0)*R
     1       -4.*G*QA(1,3,1)-8.*G*QA(1,3,2)*R+3.*QA(3,3,1)*RR
      AA(28,8)=3.*QA(2,4,0)*R+3.*QA(2,4,1)*RR-6.*QA(2,2,1)-
     1   4.*G*QA(0,4,1)-8.*G*QA(0,4,2)*R-6.*QA(2,2,2)*R
      AA(28,9)=-18.*A*QA(2,2,1)-18.*A*QA(2,2,2)*R+3.*QA(4,2,0)*R+3.
     1*QA(4,2,1)*RR
      AA(28,10)=3.*QA(1,5,0)*R+3.*QA(1,5,1)*RR-18.*QA(1,3,1)-18.*QA.
     1(1,3,2)*R
      AA(28,11)=-18.*A*QA(2,3,1)-18.*A*QA(2,3,2)*R+3.*QA(4,3,0)*R
     1       -6.*G*QA(2,3,1)-12.*G*QA(2,3,2)*R+3.*QA(4,3,1)*RR
      AA(28,12)=3.*QA(2,5,0)*R+3.*QA(2,5,1)*RR-18.*QA(2,3,1)-
     1    6.*G*QA(0,5,1)-12.*G*QA(0,5,2)*R-18.*QA(2,3,2)*R
      AA(28,14)=3.*A*QA(1,2,0)+3.*A*QA(1,2,1)*R
      AA(28,15)=G*QA(0,3,0)+2.*G*QA(0,3,1)*R
      AA(28,16)=G*QA(1,3,0)+2.*G*QA(1,3,1)*R+3.*A*QA(1,3,0)+3.*A*QA
     1(1,3,1)*R
      AA(28,17)=2.*G*QA(0,4,0)+4.*G*QA(0,4,1)*R
      AA(28,18)=2.*G*QA(1,4,0)+4.*G*QA(1,4,1)*R+3.*A*QA(1,4,0)+3.*A
     1*QA(1,4,1)*R
      AA(28,19)=3.*G*QA(0,5,0)+6.*G*QA(0,5,1)*R
      AA(28,20)=3.*G*QA(1,5,0)+6.*G*QA(1,5,1)*R+3.*A*QA(1,5,0)+3.*A
     1*QA(1,5,1)*R
      AA(28,22)=G*QA(0,3,0)+4.*G*QA(0,3,1)*R+4.*G*QA(0,3,2)*RR
      AA(28,23)=3.*QA(1,2,0)+6.*QA(1,2,1)*R+3.*QA(1,2,2)*RR
      AA(28,24)=3.*QA(2,2,0)+6.*QA(2,2,1)*R+3.*QA(2,2,2)*RR+
     14.*G*QA(0,4,1)*R+4.*G*QA(0,4,2)*RRG*QA(0,4,0)
      AA(28,25)=6.*QA(1,3,0)+12.*QA(1,3,1)*R+6.*QA(1,3,2)*RR
      AA(28,26)=6.*QA(2,3,0)+12.*QA(2,3,1)*R+6.*QA(2,3,2)*RR
     1+4.*G*QA(0,5,1)*R+4.*G*QA(0,5,2)*RR+G*QA(0,5,0)
      AA(28,27)=9.*QA(1,4,0)+18.*QA(1,4,1)*R+9.*QA(1,4,2)*RR
      AA(28,28)=9.*QA(2,4,0)+18.*QA(2,4,1)*R+18.*QA(2,4,2)*RR+
     1   4.*G*QA(0,6,1)*R+4.*G*QA(0,6,2)*RR+G*QA(0,6,0)
```

APPENDIX XII

(28*28)
MASS MATRIX (M/RO*H)
FOR CYLINDRICAL SHELL ELEMENT

USING THE DEFINITIONS OF APPENDIX X , ALSO ASSUMING THAT
ZA(STRL,CURVL,I,J)=STRL**(I+1)*CURVL**(J+1)/((I+1)*(J+1))
THEN, THE NON-ZERO ELEMENTS OF THE MATRIX ARE GIVEN BY.
(NOTING THAT IT IS A SYMMETRIC MATRIX)

```
AA(1,1)=ZA(STRL,CURVL,0,0)
AA(2,1)=ZA(STRL,CURVL,1,0)
AA(2,2)=ZA(STRL,CURVL,2,0)
AA(3,1)=ZA(STRL,CURVL,0,1)
AA(3,2)=ZA(STRL,CURVL,1,1)
AA(3,3)=ZA(STRL,CURVL,0,2)
AA(4,1)=ZA(STRL,CURVL,1,1)
AA(4,2)=ZA(STRL,CURVL,2,1)
AA(4,3)=ZA(STRL,CURVL,1,2)
AA(4,4)=ZA(STRL,CURVL,2,2)
AA(5,1)=ZA(STRL,CURVL,2,0)
AA(5,2)=ZA(STRL,CURVL,3,0)
AA(5,3)=ZA(STRL,CURVL,2,1)
AA(5,4)=ZA(STRL,CURVL,3,1)
AA(5,5)=ZA(STRL,CURVL,4,0)
AA(6,1)=ZA(STRL,CURVL,0,2)
AA(6,2)=ZA(STRL,CURVL,1,2)
AA(6,3)=ZA(STRL,CURVL,0,3)
AA(6,4)=ZA(STRL,CURVL,1,3)
AA(6,5)=ZA(STRL,CURVL,2,2)
AA(6,6)=ZA(STRL,CURVL,0,4)
AA(7,1)=ZA(STRL,CURVL,2,1)
AA(7,2)=ZA(STRL,CURVL,3,1)
AA(7,3)=ZA(STRL,CURVL,2,2)
AA(7,4)=ZA(STRL,CURVL,3,2)
AA(7,5)=ZA(STRL,CURVL,4,1)
AA(7,6)=ZA(STRL,CURVL,2,3)
AA(8,1)=ZA(STRL,CURVL,1,2)
AA(8,2)=ZA(STRL,CURVL,2,2)
AA(8,3)=ZA(STRL,CURVL,1,3)
AA(8,4)=ZA(STRL,CURVL,2,3)
AA(8,5)=ZA(STRL,CURVL,3,2)
AA(8,6)=ZA(STRL,CURVL,1,4)
AA(9,1)=ZA(STRL,CURVL,3,0)
AA(9,2)=ZA(STRL,CURVL,4,0)
AA(9,3)=ZA(STRL,CURVL,3,1)
```

```
AA(9,4)=ZA(STRL,CURVL,4,1)
AA(9,5)=ZA(STRL,CURVL,5,0)
AA(9,6)=ZA(STRL,CURVL,3,2)
AA(10,1)=ZA(STRL,CURVL,0,3)
AA(10,2)=ZA(STRL,CURVL,1,3)
AA(10,3)=ZA(STRL,CURVL,0,4)
AA(10,4)=ZA(STRL,CURVL,1,4)
AA(10,5)=ZA(STRL,CURVL,2,3)
AA(10,6)=ZA(STRL,CURVL,0,5)
AA(11,1)=ZA(STRL,CURVL,3,1)
AA(11,2)=ZA(STRL,CURVL,4,1)
AA(11,3)=ZA(STRL,CURVL,3,2)
AA(11,4)=ZA(STRL,CURVL,4,2)
AA(11,5)=ZA(STRL,CURVL,5,1)
AA(11,6)=ZA(STRL,CURVL,3,3)
AA(12,1)=ZA(STRL,CURVL,1,3)
AA(12,2)=ZA(STRL,CURVL,2,3)
AA(12,3)=ZA(STRL,CURVL,1,4)
AA(12,4)=ZA(STRL,CURVL,2,4)
AA(12,5)=ZA(STRL,CURVL,3,3)
AA(12,6)=ZA(STRL,CURVL,1,5)
AA(7,7)=ZA(STRL,CURVL,4,2)
AA(8,7)=ZA(STRL,CURVL,3,3)
AA(8,8)=ZA(STRL,CURVL,2,4)
AA(9,7)=ZA(STRL,CURVL,5,1)
AA(9,8)=ZA(STRL,CURVL,4,2)
AA(9,9)=ZA(STRL,CURVL,6,0)
AA(10,7)=ZA(STRL,CURVL,2,4)
AA(10,8)=ZA(STRL,CURVL,1,5)
AA(10,9)=ZA(STRL,CURVL,3,3)
AA(10,10)=ZA(STRL,CURVL,0,6)
AA(11,7)=ZA(STRL,CURVL,5,2)
AA(11,8)=ZA(STRL,CURVL,4,3)
AA(11,9)=ZA(STRL,CURVL,6,1)
AA(11,10)=ZA(STRL,CURVL,3,4)
AA(11,11)=ZA(STRL,CURVL,6,2)
AA(12,7)=ZA(STRL,CURVL,3,4)
AA(12,8)=ZA(STRL,CURVL,2,5)
AA(12,9)=ZA(STRL,CURVL,4,3)
AA(12,10)=ZA(STRL,CURVL,1,6)
AA(12,11)=ZA(STRL,CURVL,4,4)
AA(12,12)=ZA(STRL,CURVL,2,6)
AA(13,13)=ZA(STRL,CURVL,0,0)
AA(13,14)=ZA(STRL,CURVL,1,0)
AA(14,14)=ZA(STRL,CURVL,2,0)
AA(14,13)=ZA(STRL,CURVL,1,0)
AA(15,13)=ZA(STRL,CURVL,0,1)
AA(15,14)=ZA(STRL,CURVL,1,1)
AA(16,13)=ZA(STRL,CURVL,1,1)
AA(16,14)=ZA(STRL,CURVL,2,1)
AA(17,13)=ZA(STRL,CURVL,0,2)
```

```
AA(17,14)=ZA(STRL,CURVL,1,2)
AA(18,13)=ZA(STRL,CURVL,1,2)
AA(18,14)=ZA(STRL,CURVL,2,2)
AA(19,13)=ZA(STRL,CURVL,0,3)
AA(19,14)=ZA(STRL,CURVL,1,3)
AA(20,13)=ZA(STRL,CURVL,1,3)
AA(20,14)=ZA(STRL,CURVL,2,3)
AA(15,15)=ZA(STRL,CURVL,0,2)
AA(16,15)=ZA(STRL,CURVL,1,2)
AA(16,16)=ZA(STRL,CURVL,2,2)
AA(17,15)=ZA(STRL,CURVL,0,3)
AA(17,16)=ZA(STRL,CURVL,1,3)
AA(17,17)=ZA(STRL,CURVL,0,4)
AA(18,15)=ZA(STRL,CURVL,1,3)
AA(18,16)=ZA(STRL,CURVL,2,3)
AA(18,17)=ZA(STRL,CURVL,1,4)
AA(18,18)=ZA(STRL,CURVL,2,4)
AA(19,15)=ZA(STRL,CURVL,0,4)
AA(19,16)=ZA(STRL,CURVL,1,4)
AA(19,17)=ZA(STRL,CURVL,0,5)
AA(19,18)=ZA(STRL,CURVL,1,5)
AA(19,19)=ZA(STRL,CURVL,0,6)
AA(20,15)=ZA(STRL,CURVL,1,4)
AA(20,16)=ZA(STRL,CURVL,2,4)
AA(20,17)=ZA(STRL,CURVL,1,5)
AA(20,18)=ZA(STRL,CURVL,2,5)
AA(20,19)=ZA(STRL,CURVL,1,6)
AA(20,20)=ZA(STRL,CURVL,2,6)
AA(21,21)=ZA(STRL,CURVL,0,0)
AA(22,21)=ZA(STRL,CURVL,1,0)
AA(22,22)=ZA(STRL,CURVL,2,0)
AA(23,21)=ZA(STRL,CURVL,0,1)
AA(23,22)=ZA(STRL,CURVL,1,1)
AA(23,23)=ZA(STRL,CURVL,0,2)
AA(24,21)=ZA(STRL,CURVL,1,1)
AA(24,22)=ZA(STRL,CURVL,2,1)
AA(24,23)=ZA(STRL,CURVL,1,2)
AA(24,24)=ZA(STRL,CURVL,2,2)
AA(25,21)=ZA(STRL,CURVL,0,2)
AA(25,22)=ZA(STRL,CURVL,1,2)
AA(25,23)=ZA(STRL,CURVL,0,3)
AA(25,24)=ZA(STRL,CURVL,1,3)
AA(25,25)=ZA(STRL,CURVL,0,4)
AA(26,21)=ZA(STRL,CURVL,1,2)
AA(26,22)=ZA(STRL,CURVL,2,2)
AA(26,23)=ZA(STRL,CURVL,1,3)
AA(26,24)=ZA(STRL,CURVL,2,3)
AA(26,25)=ZA(STRL,CURVL,1,4)
AA(26,26)=ZA(STRL,CURVL,2,4)
AA(27,21)=ZA(STRL,CURVL,0,3)
AA(27,22)=ZA(STRL,CURVL,1,3)
```

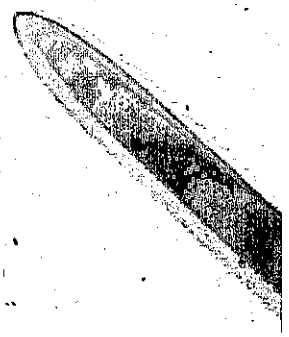

```
AA(27,23)=ZA(STRL,CURVL,0,4)
AA(27,24)=ZA(STRL,CURVL,1,4)
AA(27,25)=ZA(STRL,CURVL,0,5)
AA(27,26)=ZA(STRL,CURVL,1,5)
AA(27,27)=ZA(STRL,CURVL,0,6)
AA(28,21)=ZA(STRL,CURVL,1,3)
AA(28,22)=ZA(STRL,CURVL,2,3)
AA(28,23)=ZA(STRL,CURVL,1,4)
AA(28,24)=ZA(STRL,CURVL,2,4)
AA(28,25)=ZA(STRL,CURVL,1,5)
AA(28,26)=ZA(STRL,CURVL,2,5)
AA(28,27)=ZA(STRL,CURVL,1,6)
AA(28,28)=ZA(STRL,CURVL,2,6)
```
